


5-2017

CHARACTERIZATION AND REVERSAL OF DOXORUBICIN- MEDIATED CHANGES IN SENSORY NEURONS

Brittany L. Coughlin

Follow this and additional works at: https://digitalcommons.library.tmc.edu/utgsbs_dissertations

 Part of the [Chemicals and Drugs Commons](#), and the [Molecular and Cellular Neuroscience Commons](#)

Recommended Citation

Coughlin, Brittany L., "CHARACTERIZATION AND REVERSAL OF DOXORUBICIN-MEDIATED CHANGES IN SENSORY NEURONS" (2017). *The University of Texas MD Anderson Cancer Center UTHealth Graduate School of Biomedical Sciences Dissertations and Theses (Open Access)*. 755.
https://digitalcommons.library.tmc.edu/utgsbs_dissertations/755

This Dissertation (PhD) is brought to you for free and open access by the The University of Texas MD Anderson Cancer Center UTHealth Graduate School of Biomedical Sciences at DigitalCommons@TMC. It has been accepted for inclusion in The University of Texas MD Anderson Cancer Center UTHealth Graduate School of Biomedical Sciences Dissertations and Theses (Open Access) by an authorized administrator of DigitalCommons@TMC. For more information, please contact digitalcommons@library.tmc.edu.

CHARACTERIZATION AND REVERSAL OF DOXORUBICIN-MEDIATED
CHANGES IN SENSORY NEURONS

by

Brittany Louise Coughlin, B.S., M.A.T.

APPROVED:

John H. Byrne, Ph.D.
Advisory Professor

Michael Beierlein, Ph.D.

Rebecca Berdeaux, Ph.D.

Ruth Heidelberg, M.D., Ph.D.

M. Neal Waxham, Ph.D.

APPROVED:

Dean, The University of Texas MD Anderson Cancer Center UTHealth Graduate
School of Biomedical Sciences

CHARACTERIZATION AND REVERSAL OF DOXORUBICIN-MEDIATED
CHANGES IN SENSORY NEURONS

A

DISSERTATION

Presented to the Faculty of

The University of Texas

MD Anderson Cancer Center UTHealth

Graduate School of Biomedical Sciences

in Partial Fulfillment

of the Requirements

for the Degree of

DOCTOR OF PHILOSOPHY

by

Brittany Louise Coughlin, B.S., M.A.T.

Houston, Texas

May, 2017

Dedication

This work is dedicated to my husband and our wonderful kids.

Acknowledgments

I would first like to communicate my sincere appreciation to my advisor, Dr. Jack Byrne, for his guidance throughout the years. Dr. Byrne is adept at providing a structured learning environment and fostering the development of independent scientists. His attention to detail and ability to maintain sight on the big picture has been a major source of motivation. Dr. Byrne has been highly supportive of the various research directions I have pursued while in the lab, regardless of their relative success or failure. I thank Dr. Byrne for significantly aiding in my professional development and for supporting my career goals.

I also would like to thank my close collaborator Dr. Harini Lakshminarasimhan, a recent post-doctoral fellow in the Byrne lab. Dr. Lakshminarasimhan is not only a collaborator but a mentor. Because of her, I have an enhanced understanding of the types of behaviors that foster productive teamwork. She played a major role in shaping my ability to reach goals regardless of time constraints. I learned to multi-task more efficiently and to tackle tasks one day at a time. In the future, I hope to be able to help others the way she has helped me.

I also wish to express great appreciation for my committee members, past and present: Dr. Beierlein, Dr. Heidelberger, Dr. Waxham, Dr. Berdeaux, and Dr. Dubinsky. I thank them for their accessibility, advice, willingness to write letters of recommendation for various endeavors, and their overall support. I admire their professionalism and fully appreciate the kind attention they have provided over the years.

I would also like to thank other current members of the Byrne lab. I thank Dr. Doug Baxter for his honest and direct feedback in lab meetings. He has a knack for provoking novel thinking through highly pertinent questions. I truly have benefited from interactions with him. I would also like to thank Dr. Paul Smolen for his feedback during lab meetings and I would like to acknowledge his influence on my way of thinking about scientific problems. I would also like to thank Dr. Len Cleary for his attention and feedback during lab meetings and also for career advice. I thank Endang Kartikaningrum for the enormous amount of help with providing cultures for many of my experiments and for her role in teaching me how to culture for myself. I also thank Dr. Rongyu Liu and Dr. Yili Zhang for their mentorship throughout my graduate training. Dr. Liu introduced me to electrophysiology, and Drs. Liu and Zhang were collaborators on early investigations. I also thank Curtis Neveu for his excellent troubleshooting skills and patience throughout the years, especially when I was setting up my electrophysiology rig. I would also like to acknowledge Renan Costa for his friendliness and his modeling of professionalism through his ability to approach problems with a rare level of calmness.

Several previous members of the Byrne lab have also played major roles in my graduate training. I thank Jing Liu who was always very gracious and provided many cultures for experiments. I also would like to thank Dr. Hsin-Mei Chen who mentored me at the beginning of my graduate training. She was instrumental in sparking my curiosity and teaching me how to think critically about certain scientific topics. I would also like to acknowledge Dr. Anne Hart for her mentorship, friendship and for her

modeling of professionalism and altruism. I also thank Dr. Lian Zhou for his kind feedback during lab meetings.

I would like to thank Dr. Andrey Tsvetkov and Dr. Jose Felix Moruno Manchon for making the cortical neuron experiments described in this dissertation possible. I also would like to thank the following people for their help in numerous ways throughout the years: Soraya Thompson, Donna Wood, Amanda Williamson, Sharon Gordon, Raquel Cornell, Tammy Dawson, Diana Parker, John Concha and Ismael Perez, to name a few.

I must also express sincere appreciation to the Graduate School for all their support and the Zilkha Family for providing the Discovery Fellowship that funded my research for three years. And I also thank the Worsham family for acknowledgement of my research through their Scholarship in Behavior or Neurosciences.

And finally, I cannot thank my family enough for all the support, guidance, and motivation that was necessary to be successful. I thank my parents for allowing me to find my own path. I thank my mother for teaching me compassion and empathy and to appreciate the unique. And I thank my dad for his work ethic, sense of humor and overall support. I would also like to acknowledge my brother for his caring and helpful nature. Most importantly, I thank my husband, Mike, for his support and motivation. He always had full faith in my abilities to achieve my goals and provided unwavering support along the way making the pursuit of a doctoral degree possible while raising two young children.

CHARACTERIZATION AND REVERSAL OF DOXORUBICIN-MEDIATED CHANGES IN SENSORY NEURONS

Brittany Louise Coughlin, M.A.T.

Advisory Professor: John H. Byrne, Ph.D.

Chemotherapeutic agents impair memory in humans as well as in animal models. Such memory impairments can be persistent, lasting years after exposure to chemotherapy. Doxorubicin (DOX), a common chemotherapeutic agent, has been associated with memory impairments in humans and induces memory deficits in rodent models. DOX also impairs serotonin (5-HT)-induced long-term synaptic facilitation (LTF) in *Aplysia* sensorimotor co-cultures, a cellular analog of long-term memory formation. In addition, DOX leads to dynamic activation of extracellular signal-regulated kinase (ERK), consisting of an immediate and a delayed phase of activation, and to transient activation of p38 mitogen-activated protein kinase (p38 MAPK) in *Aplysia* sensory neurons. These two MAPKs have competing roles in the induction of LTF, with ERK promoting LTF and p38 MAPK opposing it. Further characterization of the effects of DOX on the basal state of neurons may aid the understanding of how DOX interferes with memory processes. Using isolated *Aplysia* sensory neurons in culture, we characterized the persistent effects of a single, brief exposure to DOX to understand how such exposure may be producing complex ERK activation and to determine whether DOX modulates the basal biophysical properties of these neurons and whether any changes can be reversed. We also sought to determine how DOX

affects a cellular analog of memory formation complimentary to LTF, 5-HT-induced long-term enhanced excitability (LTEE). The two phases of ERK activation appeared to have distinct induction mechanisms, with the early phase likely depending upon a transient decrease in MAPK phosphatase-1 (MKP-1) protein, and thus reduced dephosphorylation rates, and the late phase of ERK activation depending upon delayed ERK kinase (MEK) activation. Early MEK activation also contributed to the late ERK activity, seemingly indirectly through its influence on late MKP-1 expression. DOX also produced a persistent increase in sensory neuron excitability that coincided with impaired 5-HT-induced LTEE, similar to the LTF deficit. The DOX-induced increase in basal excitability was reversed by blocking early MEK activity and was negatively correlated with the late phase of ERK activation. These findings show that acute exposure to DOX can produce complex, persistent effects that may interfere with processes important for memory induction.

Table of Contents

Approval Sheet	i
Title Page.....	ii
Dedication.....	iii
Acknowledgments.....	iv
Abstract.....	vii
Table of Contents.....	ix
List of Figures	xii
List of Tables	xiv
Abbreviations	xv
Chapter 1: Background and Significance	1
Introduction	2
Studying learning and memory in <i>Aplysia</i> : Physiological correlates and <i>in vitro</i> analogs	3
Neuronal excitability and memory formation	8
Molecular mechanisms of LTS, LTF and LTEE: An overview	9
A closer look at the role of the MAPK pathways in learning and memory	11
Doxorubicin-induced impairment of memory.....	15
Significance	22
Chapter 2: Materials and Methods	24
Preparation of sensory neuronal cultures	25
Preparation of cortical neuronal cultures.....	25
Pharmacological treatments	26

Immunofluorescence.....	28
Electrophysiology	31
Correlation	34
Statistical analyses	35
Chapter 3: Doxorubicin-induced biphasic regulation of the ERK pathway is accompanied by dynamic regulation of MKP-1	36
Introduction	37
Results.....	40
Conclusion	54
Chapter 4: Doxorubicin induces persistent changes in the biophysical properties of sensory neurons similar to serotonin and prevents serotonin-mediated long-term enhanced excitability.....	57
Introduction	58
Results.....	59
Conclusion	76
Chapter 5: Doxorubicin-induced persistent changes in basal excitability depend on early ERK activity, but not p38 MAPK activity	80
Introduction	81
Results.....	85
Conclusion	93
Chapter 6: Doxorubicin-induced persistent changes in excitability and input resistance of sensory neurons are negatively correlated with late ERK activity.....	95
Introduction	96

Results	96
Conclusion	106
Chapter 7: Discussion	108
Bibliography	120
Vita.....	142

List of Figures

Figure 1. Long-term enhanced excitability of SNs is a cellular correlate of a form of long-term memory, LTS	6
Figure 2. <i>In vitro</i> analog of a cellular correlate of LTS, LTEE	7
Figure 3. DOX leads to increased levels of phosphorylated ERK and p38 MAPK .	18
Figure 4. Activation levels of ERK and p38 MAPK show complex temporal dynamics after DOX treatment.....	20
Figure 5. Confocal image of a cultured <i>Aplysia</i> SN.....	30
Figure 6. Measurement of biophysical properties of isolated SNs	33
Figure 7. Potential mechanisms for DOX-induced increase in ERK activation.....	39
Figure 8. DOX caused a transient decrease in expression of MKP-1	42
Figure 9. MEK inhibition during DOX treatment does not block the early phase of ERK activation but potentiates the late phase of ERK activation	44
Figure 10. MEK inhibition during DOX treatment did not affect the initial decrease in MKP-1 protein.....	48
Figure 11. MEK inhibition during DOX treatment caused a late decrease in MKP-1 protein.....	49
Figure 12. ERK activation was enhanced in DOX-treated cortical neurons from rat both immediately and 24 h after treatment.....	52
Figure 13. DOX produced persistent changes in the biophysical properties of SNs	61
Figure 14. The standard 5-HT protocol produced persistent changes in the biophysical properties of SNs	68

Figure 15. 5-HT does not potentiate the DOX-induced basal increase in excitability	73
Figure 16. A single brief application of the MKP-3 inhibitor NSC 295642 induced a persistent increase in excitability of SNs.....	82
Figure 17. MEK inhibition during DOX treatment blocked the increase in basal excitability at 24 h	86
Figure 18. p38 MAPK inhibition during DOX treatment did not affect the persistent increase in basal excitability	91
Figure 19. The DOX-induced increase in excitability and the late phase of ERK activation were negatively correlated	98
Figure 20. The DOX-induced increase in input resistance and the late phase of ERK activation were negatively correlated	101
Figure 21. The DOX-induced decrease in firing threshold and the late phase of ERK activation were not correlated	104
Figure 22. Summary diagram.....	115

List of Tables

Table 1. Pre-test measures of biophysical properties for groups in Fig. 13	64
Table 2. Pre-test measures of biophysical properties for groups in Fig. 14	70
Table 3. Pre-test measures of biophysical properties for groups in Fig. 15	75
Table 4. Pre-test measures of biophysical properties for groups in Fig. 17	87
Table 5. Effects of the MEK inhibitor U0126 (20 μ M) on DOX-induced changes in biophysical properties of SNs	89
Table 6. Pre-test measures of biophysical properties for groups in Fig. 18	92

Abbreviations

5-HT	serotonin (5-hydroxytryptamine)
ATF4	activating transcription factor 4
BDNF	brain-derived neurotrophic factor
DOX	doxorubicin
cAMP	cyclic adenosine monophosphate
C/EBP	CCAAT enhancer-binding protein
CICD	chemotherapy-induced cognitive dysfunction
CREB1	cAMP responsive element-binding protein 1
CREB2	cAMP responsive element-binding protein 2
EPSP	excitatory postsynaptic potential
ERK	extracellular signal-regulated kinase
FGFR	fibroblast growth factor receptor
IF	immunofluorescence
ITM	intermediate-term memory
JNK	c-Jun N-terminal protein kinase
LTD	long-term depression
LTEE	long-term enhanced excitability
LTF	long-term facilitation
LTM	long-term memory
LTP	long-term potentiation
LTS	long-term sensitization
MAPK	mitogen-activated protein kinase

MAPKK	MAPK kinase
MAPKKK	MAPK kinase kinase
MEK	mitogen-activated protein kinase kinase/ERK kinase
MKP-1	mitogen-activated protein kinase phosphatase-1
MKP-3	mitogen-activated protein kinase phosphatase-3
MN	motor neuron
pERK	phosphorylated ERK
PKA	protein kinase A (cAMP-dependent protein kinase)
PKC	protein kinase C
p38 MAPK	p38 mitogen-activated protein kinase
p-p38 MAPK	phosphorylated p38 MAPK
SN	sensory neuron
STF	short-term facilitation
STM	short-term memory
TGF- β 1	transforming growth factor beta 1
TGF- β r-II	transforming growth factor beta receptor 2
TrkB	tropomyosin-related kinase B
Veh	vehicle (control)

Chapter 1: Background and Significance

Introduction

Chemotherapy-induced cognitive dysfunction (CICD) is gaining recognition for its role in hindering patients and cancer survivors from returning to their daily responsibilities with ease (Myers 2009). The majority of investigations into CICD, both cross-sectional and longitudinal, over the past couple of decades have provided evidence for a link between chemotherapy and impairment of cognition (Wefel and Schagen 2012). While estimates range greatly for the occurrence rate of CICD, it is thought that approximately one-third of patients that receive chemotherapy experience cognitive impairment, which may occur during and/or long after treatment (O'Farrell, MacKenzie and Collins 2013). Chemotherapy can affect many aspects of cognition including processing speed, working memory and other forms of memory (O'Farrell et al. 2013). The mechanism of CICD has been investigated mostly from the perspective that chemotherapeutic agents are toxic species that promote oxidative stress, DNA damage, inflammation, and cell death, among other damaging effects (Ahles and Saykin 2007). An alternative, although not mutually exclusive explanation for CICD is that chemotherapeutic drugs modulate molecular pathways implicated in memory formation. The lack of penetration of many chemotherapeutic drugs through the blood-brain barrier has likely deterred such investigations. For example, doxorubicin (DOX), a common chemotherapeutic agent, does not accumulate in the brain at concentrations sufficient for antitumor action following intraperitoneal injection into rats, based on measurements from cerebral hemispheres, but is detected at low concentrations (Sardi et al. 2013). Recent studies, including one from our lab, have suggested that the greatly reduced concentrations of DOX that likely accumulate in

the brain (Sardi et al. 2013) are sufficient to modulate molecular pathways important for memory formation (Alhowail, Suppiramaniam and Arnold 2016; Liu et al. 2014; Salas-Ramirez et al. 2015). In addition, Liu et al. (2014) found that a single treatment with DOX impairs strengthening of synapses using the invertebrate model system *Aplysia californica in vitro*, and that this effect could be prevented by interfering with DOX-induced changes to a protein implicated in modulating synaptic strength. A subsequent study using rat hippocampal slices showed deficits in long-term potentiation (LTP) following DOX treatment (Alhowail, Suppiramaniam and Arnold 2016). A closer inspection of the effects of this common chemotherapeutic agent regarding its ability to modulate neural pathways tied to memory as well as influence physiological correlates of memory formation is necessary to begin to understand the full range of potential causes of CICD.

Studying Learning and Memory in *Aplysia*: Physiological correlates and *in vitro* analogs

The concept of memory as a tangible event associated with measurable physiological changes was introduced in large part by two seminal studies published back-to-back in *Science* in 1970. Kandel and colleagues demonstrated that habituation, a simple form of nonassociative learning characterized by a decrement in response to repetitive weak to mild stimulation, is associated with a decrease in synaptic strength (Castellucci et al. 1970; Pinsker et al. 1970). These studies utilized the relatively simple organization of the nervous system of *Aplysia*. Studies in *Aplysia* have been central to the discovery of principles fundamental to memory formation (for

review, see Sweatt 2016). For example, such studies have provided an understanding of the mechanistic underpinnings of different types of memory: memory can be divided into short-term memory (STM, persisting for minutes), intermediate-term memory (ITM, persisting for minutes to hours), and long-term memory (LTM, persisting for days). These different forms of memory are not only characterized by their duration but also by their mechanisms, with STM requiring post-translational modifications to preexisting proteins but not new translation or transcription, ITM requiring translation but not transcription, and LTM requiring both translation and transcription (for review, see Byrne and Hawkins 2015).

Many of the investigations into the mechanisms of memory formation in *Aplysia* have focused on another form of nonassociative learning, sensitization, elicited by noxious stimulation resulting in the enhancement of a behavioral response. These studies have utilized several withdrawal reflexes of *Aplysia* including the tail-elicited tail and siphon withdrawal reflex (for review, see Cleary et al. 1995). Underlying this reflex are mechanosensory neurons (SNs) of the pleural ganglia that innervate the tail and form connections with motor neurons (MNs) of the pedal ganglia both monosynaptically and through interneurons. These MNs are responsible for withdrawal of the tail and siphon. Delivery of sensitizing stimuli (typically an electric shock to the body wall) facilitates the connections between the SNs and MNs (for review, see Byrne and Kandel 1996) and increases SN excitability (Klein, Hochner and Kandel 1986; Walters et al. 1983). Long-term sensitization (LTS) training (four spaced trains of electrical shock) induces a persistent facilitation of the excitatory postsynaptic potential (EPSP) elicited in the MNs in response to injection of current

into the SNs (Cleary et al. 1998; Frost et al. 1985; Montarolo et al. 1986; Pinsker et al. 1973; Wainwright et al. 2004), a reduction in the net outward current of tail SNs (Scholz and Byrne 1987) and enhanced excitability of the SNs (Fig. 1; Cleary et al. 1998) 24 h after training. These persistent physiological changes termed long-term facilitation (LTF) and long-term enhanced excitability (LTEE), respectively, coincide with the enhanced withdrawal response observed 24 h after LTS training and therefore, are correlates of LTS (Cleary et al. 1998). Enhancement of the reflex response induced by tail shock depends upon the release of the neurotransmitter serotonin (5-hydroxytryptamine, 5-HT) (Glanzman et al. 1989), which is released from modulatory interneurons (Hawkins 1989; Levenson, Byrne and Eskin 1999; Mackey, Kandel and Hawkins 1989; Marinesco and Carew 2002; Marinesco, Kolkman and Carew 2004; also see, Zhang et al. 2003). SNs can be isolated from the pleural ganglia and cultured with MNs so that they form synaptic contacts in order to study LTF. SNs can also be isolated and cultured to study LTEE without any confounding influences from the postsynaptic MNs (Fig. 2). Such an approach is desired when considering presynaptic excitability as a mechanism of memory formation intrinsic to the SNs (for review, see Mozzachiodi and Byrne 2010). To induce LTF and LTEE *in vitro*, 5-HT is applied in a pulsatile fashion (five, five-min pulses of 5-HT with 20-min interstimulus intervals (from start of 5-HT-pulse to the start of the next pulse)) (Dale et al. 1987; Montarolo et al. 1986). Such preparations have enabled meticulous analysis of cellular and molecular changes implicated in memory formation.

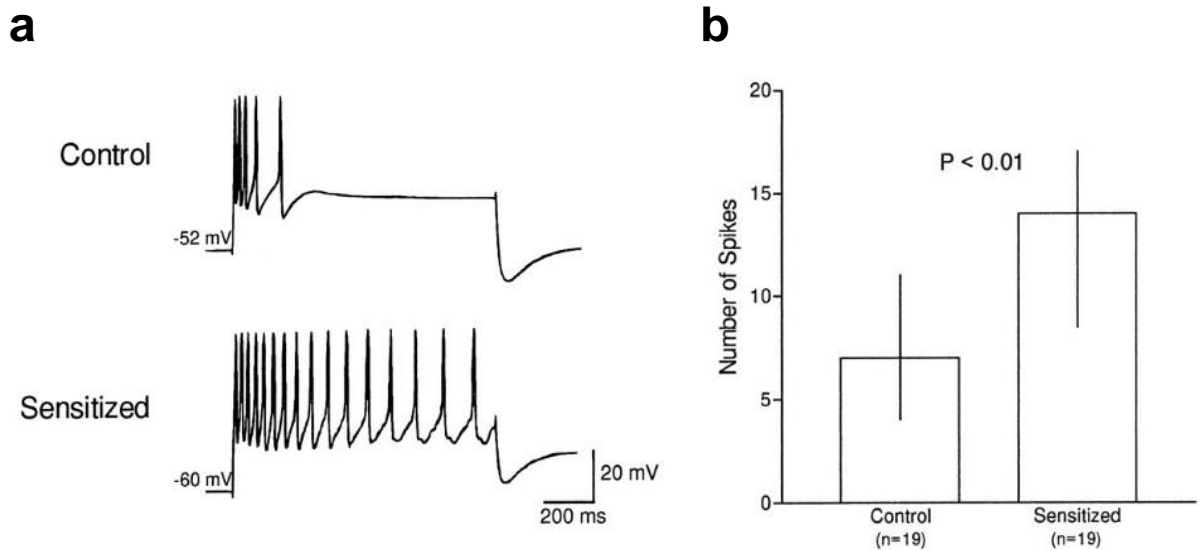


Figure 1. Long-term enhanced excitability of SNs is a cellular correlate of a form of long-term memory, LTS. These SNs compose a critical component of the circuit mediating the behavioral response that is enhanced following LTS training. (a) Representative action potentials from a SN from a control side of an *Aplysia* (top) and a SN from a sensitized side (bottom). Sensitization is lateralized, therefore a single animal has a sensitized side and a control side (Wainwright et al. 2004). (b) Summary data showing a significant increase in the number of action potentials produced by a depolarizing current injection (1 sec, 2 nA). Data are represented as median and interquartile range. The median number of spikes doubled for the sensitized SNs compared to the control SNs.

Figure adapted from: Cleary LJ, Lee WL, Byrne JH (1998). Cellular correlates of long-term sensitization in *Aplysia*. *J. Neurosci.* 18: 5988–5998.

Figure used with permission from *The Journal of Neuroscience*.

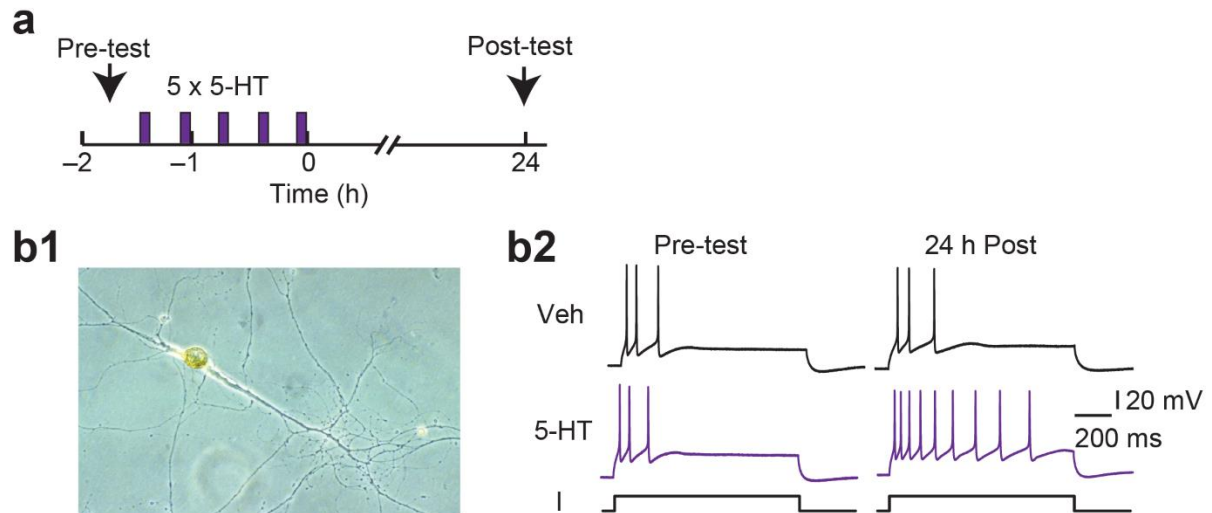


Figure 2. *In vitro* analog of a cellular correlate of LTS, LTEE. (a) Protocol for application of 5-HT (or Vehicle control (Veh)) relative to the pre- and post-test measurements of excitability. Arrows represent recording times. (b1) Cultured SN from the pleural ganglion of *Aplysia*. (b2) Representative action potentials elicited by a constant current injection (I) before (Pre-test) and after (24 h Post) Veh or 5-HT treatment. Image of SN in b1 taken by Dr. Jeannie Chin while a graduate student in the Byrne lab, but the traces in b2 are my recordings. Image of SN used with permission from Dr. Jeannie Chin and Dr. Jack Byrne.

Neuronal excitability and memory formation

Changes in neuronal excitability concurrent with memory induction have been repeatedly documented in both vertebrates and invertebrates (for review, see Mozzachiodi and Byrne 2010). The neuronal population activated during learning is both necessary and sufficient to express the memory formed from that particular learning experience (for review, see Kim et al. 2016). The mechanism by which altered neuronal excitability facilitates memory formation has been debated. The prevailing thought is that it can both facilitate changes in synaptic efficacy associated with memory formation and serve as an independent contributor to the memory trace (Mozzachiodi and Byrne 2010).

Early studies of classical conditioning in the invertebrate *Hermisenda* demonstrated that learning-related changes to the biophysical properties of sensory neurons involved in the circuit mediating the learned behavior include enhanced input resistance and excitability, and that these intrinsic changes (not synaptically driven) could be attributed, at least in part, to decreases in several K⁺ currents (Alkon, Shoukimas and Heldman 1982; Alkon et al. 1985; Crow and Alkon 1980; Farley 1988). Studies of operant conditioning of feeding behavior in *Aplysia* revealed that intrinsic excitability and related changes are capable of inducing circuit modifications known to mediate the learned behavior (Lorenzetti, Baxter and Byrne 2008; Mozzachiodi et al. 2008). Such studies suggest that excitability serves as a contributor to the memory trace in invertebrates (Mozzachiodi and Byrne 2010), as has been shown in vertebrates (Kim et al. 2016).

As mentioned previously, LTS in *Aplysia* coincides with LTEE (Fig. 1; Cleary et al. 1998), and such changes can be induced by repeated application of 5-HT to isolated SNs (Fig. 2), suggesting that the excitability changes that occur during LTS do not require influence from the postsynaptic MN (Dale et al. 1987; Liu, Cleary and Byrne 2011; Liu et al. 2014). A long-term decrease in net outward current in SNs occurs during LTS which would promote the excitability changes observed (Scholz and Byrne 1987). Such a decrease in net outward current, likely due to decreased K⁺ conductances (Baxter et al. 1999), would also prolong the duration of action potentials leading to more release of neurotransmitter and thus a larger postsynaptic potential. Indeed, repeated pulses of 5-HT (analogous to LTS training) produced LTF that coincided with enhanced transmitter release from the presynaptic SN in the absence of evidence for enhanced sensitivity or density of postsynaptic receptors (Dale et al. 1988). Therefore, LTF and LTEE are thought to occur together. While it is possible that LTEE has a unique role in memory formation, it also likely contributes to LTF through enhanced transmitter release (Mozzachiodi and Byrne 2010).

Molecular mechanisms of LTS, LTF and LTEE: An overview

While both LTF and LTEE are considered important to understanding LTS, most studies have focused on LTF. Importantly, many studies on the molecular mechanisms underlying LTF have focused on changes in the presynaptic SN, so they have implications for LTEE as well. From these studies, investigators have made significant contributions to the understanding of molecular events responsible for LTS. Repeated pulses of 5-HT lead to a sustained increase in the level of cyclic adenosine

monophosphate (cAMP) (Sweatt and Kandel 1989), which leads to enhanced activity of cAMP-dependent protein kinase A (PKA) (Müller and Carew 1998) and translocation of its catalytic subunit to the nucleus of the SN (Bacskai et al. 1993). After nuclear translocation, PKA phosphorylates and thereby activates cAMP response element-binding protein 1 (CREB1) (Dash, Hochner and Kandel 1990; Kaang, Kandel and Grant 1993; Lee et al. 2007). CREB1-mediated transcription is required for LTF (Bartsch et al. 1998; Dash et al. 1990; Liu et al. 2008, 2011; Zhou et al. 2015; for reviews, see Alberini 2009; Barco, Bailey and Kandel 2006; Benito and Barco 2010; Kandel 2001, 2012) and LTEE (Liu et al. 2011). The importance of CREB1-mediated transcription in LTM has also been reported in numerous studies in *Drosophila* and rodents (for review, see Alberini 2009). Repeated pulses of 5-HT also lead to activation of extracellular signal-regulated kinase (ERK) (Michael et al. 1998; Sharma, Sherff et al. 2003) and its translocation to the nucleus (Martin et al. 1997), where it phosphorylates and thereby inactivates the transcriptional repressor CREB2, thus allowing for CREB1-mediated transcription (Bartsch et al. 1995). CREB2 (*Aplysia* homolog of mouse activating transcription factor 4 (ATF4)) has been recognized for its roles in the negative regulation of synaptic strength and memory in mice (Chen et al. 2003).

In addition, 5-HT is known to modulate p38 mitogen-activated protein kinase (p38 MAPK). Activation of p38 MAPK promotes long-term synaptic depression (LTD) via phosphorylation of CREB2 at a site distinct from the ERK phosphorylation site resulting in activation of CREB2. 5-HT suppresses p38 MAPK activation immediately after treatment (Guan et al. 2003; Zhang et al. 2017). Therefore, it appears that the

balance between ERK and p38 MAPK activation is an important factor in determining the direction of synaptic plasticity.

While the focus of many *Aplysia* studies has been on the role of the presynaptic SN in LTF, the importance of postsynaptic changes such as postsynaptic protein synthesis and increased postsynaptic Ca^{2+} must be acknowledged (Glanzman 2008, 2013). LTS training produces long-term changes in the biophysical properties of MNs (Cleary et al. 1998). In addition, retrograde signaling from the postsynaptic MN is thought to influence presynaptic changes associated with LTM (Glanzman 2008). The studies outlined in this dissertation focus on isolated presynaptic SNs, so contributions from the postsynaptic MNs will not be examined but should be considered in future studies.

A closer look at the role of MAPK pathways in learning and memory

MAPKs are widely recognized for their roles in memory formation (for reviews, see Adams and Sweatt 2002; Giese and Mizuno 2013; Roth and Sweatt 2008; Sharma and Carew 2004; Sweatt 2001, 2004). There are four conventional MAPKs: ERK, p38 MAPK, c-Jun N-terminal protein kinase (JNK), and ERK5 (Cargnello and Roux 2011). MAPKs are activated as a result of serial phosphorylation of three core kinases: MAPK kinase kinase (MAPKKK) phosphorylates MAPK kinase (MAPKK) which then phosphorylates both a threonine residue and a tyrosine residue on MAPK resulting in its activation. The majority of investigations into the role of MAPKs in memory and its physiological correlates have focused on the ERK pathway, but the roles of p38 MAPK and JNK are gaining recognition (Mirisic et al. 2016; Thomas and

Huganar 2004). ERK is well known for its role in synaptic plasticity, excitability and memory in both vertebrates and invertebrates (Adams and Sweatt 2002; Chin et al. 2006; Cohen-Matsliah et al. 2007; Rosenkranz, Frick & Johnston 2009; Stambouliau et al. 2010; Sung, Povelones & Ambron 2001; Sweatt 2004). Many different extracellular stimuli lead to activation of small G proteins which in turn leads to activation of the ERK cascade and the translocation of ERK to the nucleus where it can initiate activation of gene transcription (Martin et al. 1997; Mirisis et al. 2016). ERK can activate numerous substrates via phosphorylation of either a serine or a threonine residue (for review, see Sweatt 2001). Specific biological outcomes are likely achieved by variations in extracellular signal duration and strength, the abundance of cell surface receptors for activating stimuli (such as growth factors), the presence of phosphatases that target and inactivate phosphorylated ERK, and scaffolding proteins. These factors, among others, shape the temporal and spatial aspects of the ERK signal, likely promoting a specific biological outcome (Murphy and Blenis 2006).

ERK in *Aplysia*

ERK is the most studied MAPK in *Aplysia*. Activation of ERK is required for LTF and LTS, but not for their short-term counterparts (short-term facilitation (STF) and short-term sensitization) (Martin et al. 1997; Ormond et al. 2004; Purcell et al. 2003; Sharma, Sherff et al. 2003). ERK promotes and is also required for certain forms of long-term excitability in *Aplysia* (Chin et al. 2006; Sung et al. 2001). In addition, ERK has been implicated as a requirement for the growth of new synapses (Bailey et al. 1997; Michael et al. 1998) and is involved in the movement of synaptic vesicles after 5-HT treatment in SNs (Angers et al. 2002). Five pulses of 5-HT leads to activation of

ERK (Michael et al. 1998), and mounting evidence suggests this activation occurs through growth factor-mediated stimulation of tropomyosin-related kinase B (TrkB), transforming growth factor β receptor II (TGF- β -II), and fibroblast growth factor receptors (FGFRs) (Chin et al. 2002, 2006; Kassabov et al. 2013; Kopec and Carew 2013; Kopec, Philips and Carew 2015; Ormond et al. 2004; Pollak et al. 2014; Pu et al. 2014; Purcell et al. 2003; Sharma et al. 2006; Zhang et al. 1997). In addition, 5-HT leads to PKA-dependent synthesis of the neuropeptide sensorin which binds to autoreceptors on SNs to activate ERK (Hu et al. 2004). Active ERK translocates to the nucleus of the presynaptic SN but not the postsynaptic MN (Martin et al. 1997), and activation is sustained nearly 3 h following 5, 5-min pulses of 5-HT delivered in 20-min interstimulus intervals (Sharma, Sherff et al. 2003). In the nucleus, active ERK is believed to phosphorylate CREB2, a repressor of CREB1-mediated transcription and of LTF (Bartsch et al. 1995; Lee et al. 2003), based on the presence of a consensus sequence for ERK on *Aplysia* CREB2 (Bartsch et al. 1995), and the ability of ERK from *Aplysia* CNS extracts to phosphorylate CREB2 *in vitro* (Michael et al. 1998). In addition, the transcription factor CCAAT enhancer-binding protein (C/EBP) contains a consensus site for ERK and is required for LTF (Alberini et al. 1994; Lee et al. 2012). ERK phosphorylates C/EBP *in vitro* (Michael et al. 1998) and enhances binding of C/EBP to DNA (Yamamoto et al. 1999).

p38 MAPK in *Aplysia*

p38 MAPK counteracts induction of LTF through its activation of CREB2 (for review, see Sharma and Carew 2004), resulting in repression of gene transcription necessary for LTF (Guan et al. 2002, 2003). When p38 MAPK activity is blocked, a

single pulse of 5-HT, which is normally only capable of inducing STF, is now capable of inducing LTF (Guan et al. 2003; Lee et al. 2003). Furthermore, overexpression of p38 MAPK or injection of active p38 MAPK into SNs prevents 5-HT-induced LTF (5 pulses of 5-HT), and p38 MAPK activity mediates LTD (Guan et al. 2003; Lee et al. 2003). Blocking activation of CREB2 (a substrate of p38 MAPK) prevents LTD (Guan et al. 2002, 2003).

Phosphatases in *Aplysia*

Activation levels of MAPKs are dependent upon phosphorylation by MAPKKs and dephosphorylation by phosphatases (Zhou et al. 2002). It is recognized that multiple phosphatases can target a single MAPK whereas only one MAPKK targets each MAPK, suggesting that the specificity of a biological outcome may be largely controlled by phosphatase expression (Zhou et al. 2002). Inactivation of ERK occurs through dephosphorylation of either its tyrosine or threonine residue required for activation (Camps et al. 2000). In *Aplysia*, phosphatases have been implicated in the modulation of ERK phosphorylation levels (Michael et al. 1998; Sharma, Bagnall et al. 2003) and the regulation of memory formation (Esdin, Pearce and Glanzman 2010; Ezzeddine and Glanzman 2003; Michel et al. 2013; Sharma, Bagnall et al. 2003). For example, MAPK phosphatase-1 (MKP-1) dephosphorylates ERK in *Aplysia* SN extracts (Michael et al. 1998). Another example is the inhibitory effect of the phosphatase calcineurin on ERK activation and LTF (Sharma, Bagnall et al. 2003).

Interaction between ERK and p38 MAPK

The ability of a p38 MAPK inhibitor to enhance phosphorylation of ERK is evidence for crosstalk between MAPK pathways in *Aplysia* SNs (Fioravante, Smolen

and Byrne 2006; Zhang et al. 2017). In mammalian cells, activation of p38 MAPK leads to inhibition of ERK kinase (MEK) and ERK activity through activation of phosphatases that target MEK (Westermarck et al. 2001). The mechanism for p38 MAPK-mediated inhibition of ERK activity in *Aplysia* is also likely indirect, although detailed mechanistic studies of this effect have not been conducted.

Doxorubicin-induced impairment of memory

CICD has been reported in cancer patients for decades with evidence of persistent effects years after the end of treatment (Ahles and Saykin 2007). Decline in cognitive function associated with chemotherapy is not simply a result of cancer itself or confounding psychological conditions or states such as depression, anxiety or fatigue (Ahles and Saykin 2007; Tannock et al. 2004; Wang et al. 2015). It appears that chemotherapeutic agents themselves can impair cognitive abilities including learning and memory (Ahles and Saykin 2007). It is difficult to assess the effects of individual drugs due to the common use of combined pharmacotherapy in treating cancer. Furthermore, detailed mechanistic studies of the underlying factors inducing memory impairment require animal studies. The mechanisms underlying CICD are in the early stages and very few investigations focus on individual drugs. Such studies are necessary to understand how to prevent or treat CICD.

DOX, an anthracycline antibiotic derived from *Streptomyces* also known by the brand names Adriamycin and Rubex, is a common chemotherapeutic agent that has many well-documented side effects including memory deficits, myelosuppression, nausea, emesis, hair loss, and cardiotoxicity (Aluise et al. 2010). DOX has several

modes of action that may contribute to its ability to destroy tumor cells (and healthy cells). These are: 1) DNA intercalation, by which DOX interferes with replication and subsequent tumor growth; 2) Inhibition of topoisomerase II activity, which prevents the relaxation of DNA, thus preventing replication and gene transcription; and 3) production of cytokines and reactive oxygen/nitrogen species, promoting diffuse cellular damage and cellular death. The chemical structure of DOX allows it to participate in redox cycling which produces a large amount of free radicals (Aluise et al. 2010).

Chemotherapy regimens that include DOX have been cited for their association with cognitive dysfunction in humans. For example, breast cancer patients who received DOX in combination with cyclophosphamide showed impairment of memory (Jansen et al. 2011; Ramalho et al. 2017). DOX also impairs memory in rodent models. Specifically, a single injection of DOX impairs inhibitory avoidance memory 1 and 7 d after training (Liedke et al. 2009) as well as novel location recognition and novel object recognition memory (Seigers et al. 2015). In addition, repeated injections of DOX impair memory for novel object recognition and decrease metabolism in the prefrontal cortex (Barry et al. 2017), as well as impair memory for contextual fear conditioning (Christie et al. 2012). Furthermore, treatment regimens involving a combination of DOX and some other chemotherapeutic agent also impair memory in rodents (For examples, see Konat et al. 2008; Macleod et al. 2007; Philpot, Ficken and Wecker 2016; Salas-Ramirez et al. 2015). While it is becoming clear that DOX impairs performance on memory tasks in rodents, consistent with findings in humans, the mechanisms underlying such impairments are largely unknown.

It is highly likely that the ability of DOX to impair memory depends on numerous mechanisms as is hypothesized for its antitumor actions (Aluise et al. 2010). Such mechanisms may include suppression of hippocampal neurogenesis (Christie et al. 2012) and neuronal damage from generation of free radicals (Konat et al. 2008). Recent work from our lab has revealed another potential mechanism for DOX-induced memory impairment previously unexplored. Liu et al. (2014) found that a single application of DOX to SN-MN co-cultures impairs 5-HT-induced LTF and that this synaptic impairment can be prevented by application of the p38 MAPK inhibitor SB 203580 before and during DOX treatment. Therefore, DOX appeared to prevent 5-HT-induced LTF through enhancement of p38 MAPK activity, which counters the 5-HT-induced inhibition of p38 MAPK (Guan et al. 2003; Zhang et al. 2017), an effect thought to promote LTF (Fig. 3). In addition, this study showed that DOX treatment leads to increased levels of activation of ERK, p38 MAPK, and CREB2 as well as decreased levels of MKP-1 in *Aplysia* SNs 45 min after treatment. DOX also enhances levels of activated ERK and p38 MAPK in cultured cortical neurons from rats 45 min after treatment. While DOX has been shown to modulate ERK and p38 MAPK in various cell types (e.g., Guise et al. 2001; Poizat et al. 2005; Rojo et al. 2009; Small et al. 2003), Liu et al. (2014) was the first to report on the modulation of these molecules in neurons and furthermore, the first to provide a connection to synaptic plasticity. While it is not suggested that deficits in synaptic facilitation are the sole cause of DOX-induced memory impairment, it may be a significant contributing factor.

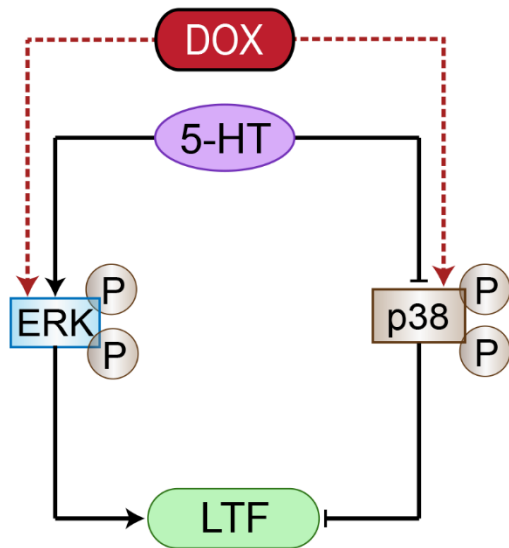


Figure 3. DOX leads to increased levels of phosphorylated ERK and p38 MAPK.

DOX-induced enhancement of p38 MAPK activity counters 5-HT-induced inhibition of p38 MAPK activity. This competition may explain the ability of a p38 MAPK inhibitor to rescue the DOX-induced impairment of LTF (Liu et al. 2014).

More recent work in our lab has shown that the DOX-induced activation of ERK and p38 MAPK occurs during a 2-h DOX treatment and persists for about 1 h after treatment in *Aplysia* SNs (Fig. 4). A delayed phase of ERK but not p38 MAPK activation is observed 24 h after treatment (Fig. 4b and Fig. 4c). Only phosphorylated levels of the proteins were measured, not total protein levels. Therefore, we do not know whether this increase in activity is a reflection of an overall increase in protein levels, but DOX has been shown to increase activity of ERK without any changes in total protein levels of ERK and p38 MAPK in breast cancer cells (Rojo et al. 2009). Complex patterns of ERK activation following DOX treatment in addition to impairment of synaptic plasticity due to activation of p38 MAPK suggest that modulations of MAPK pathways in SNs by DOX affect processes implicated in memory formation.

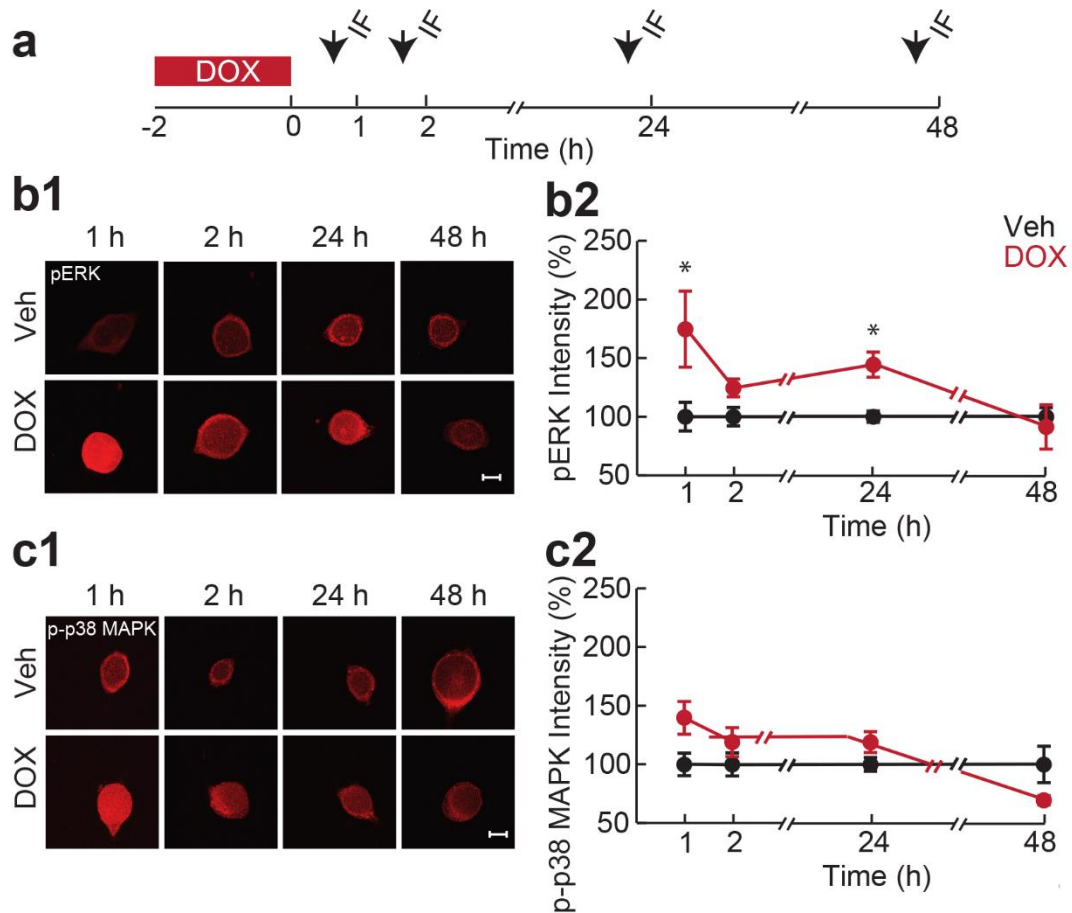


Figure 4: Activation levels of ERK and p38 MAPK show complex temporal dynamics after DOX treatment. (a) Isolated SNs were treated with DOX (2h, 2.5 μ M) or Veh and then fixed and stained with either phosphorylated ERK (pERK) or phosphorylated p38 MAPK (p-p38 MAPK) antibody at different times after treatment. pERK (b1 and b2) and p-p38 MAPK (c1 and c2) levels are elevated initially and return to baseline within two hours after the end of DOX treatment. ERK exhibits a second, delayed phase of activation 24 h later (b2) that is not sustained for 48 h. p38 MAPK does not show a second phase of activation (c2). * indicates $p \leq 0.05$ as determined by pairwise post hoc comparisons. n values ranged from 8 – 10 for both pERK (b2)

and p-p38 MAPK (c2). Each n represents an average of at least 4 cells that compose a single dish. Dishes were obtained from multiple animals.

Data collected and figure made by Dr. Harini Lakshminarasimhan.

Adapted and included in this dissertation with permission from Dr. H. Lakshminarasimhan.

Significance

The mechanism by which DOX causes a delayed phase of ERK activation (Fig. 4b) in SNs is unknown. ERK activation levels are controlled by the balance between MEK-mediated activation and phosphatase-mediated deactivation. DOX decreases MKP-1 protein levels shortly after treatment (Liu et al. 2014), therefore it is of interest to determine whether DOX causes a persistent or delayed decrease in MKP-1 levels, which may account for the late increase in levels of active ERK, or whether the persistent ERK activation is dependent upon late MEK activation, or both. In several human breast cancer cell lines, downregulation of MKP-1, not changes in MEK activity, appears to be responsible for DOX-induced activation of ERK (Small et al. 2003). When basal MKP-1 levels are decreased by small interfering RNA, DOX is unable to produce the enhancement of ERK phosphorylation, indicating that MKP-1 must be present initially and that subsequent DOX-induced downregulation of MKP-1 leads to the enhancement of pERK (Small et al. 2003). Given the short half-lives of MKP-1 mRNA (1 to 2 h) and MKP-1 protein (40 min to 2 h) (Boutros, Chevet and Metrakos 2008), it is possible that blockage of new transcription of MKP-1 by DOX would lead to reduced levels of MKP-1 protein following a 2-h DOX treatment.

Furthermore, it is of interest to determine whether there is a link between early and late ERK activation, possibly through MKP-1, given the ability of the MEK-ERK pathway to promote expression of MKP-1 through increased transcription and protein stabilization (Brondello et al. 1997; Caunt and Keyse 2013; Cook et al. 1997; Li et al. 2001; Small et al. 2003, 2004).

Finally, given that DOX enhances ERK activation in SNs, it is of interest to characterize the basal biophysical changes induced by DOX and compare them to the changes induced by a memory stimulus (i.e., 5-HT), and to determine whether DOX impairs 5-HT-induced LTEE. In addition, it is unknown how any biophysical changes induced by DOX may relate to different phases of ERK activation. These investigations may shed light on strategies to reverse any persistent biophysical changes. Reversal of basal changes induced by DOX may be advantageous given that DOX impairs synaptic plasticity (Liu et al. 2014), which would be predicted to have a negative impact on memory induction.

Chapter 2: Materials and Methods

Part of this chapter is based upon: Liu RY, Zhang Y, Coughlin BL, Cleary LJ, Byrne JH (2014). Doxorubicin attenuates serotonin-induced long-term synaptic facilitation by phosphorylation of p38 mitogen-activated protein kinase. *J. Neurosci.* 34: 13289-13300.

Permission policy of *The Journal of Neuroscience*: “If the request for permission is from an Original Author you DO NOT need to obtain permission for any non-commercial reuse of your own material.”

Preparation of sensory neuronal cultures

Aplysia californica (60-100 g) were purchased from the US National Institutes of Health *Aplysia* resource facility (University of Miami). Preparation of primary cultures followed established protocols (Chin et al. 1999, 2006; Schacher and Proshansky 1983). *Aplysia* were anesthetized with injection of isotonic $MgCl_2$ into their body cavity equal in volume to half their body weight in grams. The left and right pleural ganglia were removed and placed in a petri dish containing L15 medium. Ganglia were trimmed and placed in protease solution at 34.5°C for 3 h. Ganglia were moved to room temperature and rinsed three times with L15 medium and then pinned to a Sylgard-coated dish containing culture medium (50% L15, 50% hemolymph). The sheaths of the pleural ganglia were removed and SNs of the ventrocaudal cluster of each ganglion were pulled out with sharp electrodes and placed into poly-L-lysine-coated dishes filled with culture medium. SNs were allowed to rest undisturbed overnight at room temperature and were then moved to an incubator (18°C). Experiments were initiated 4–6 days after cultures were made.

Preparation of cortical neuronal cultures

Primary cortical neuronal cultures were prepared and provided by the laboratory of Dr. Andrey Tsvetkov. Briefly, cortical neurons were isolated from rat embryos (E17–18) and plated on poly-D-lysine-coated 24-well plates (650,000/well) as described (Mitra, Tsvetkov and Finkbeiner 2009; Moruno Manchon et al. 2015; Tsvetkov et al. 2010; Tsvetkov, Ando and Finkbeiner 2013; Tsvetkov et al. 2013). Neurons were incubated in modified neuronal growth medium (Neurobasal Medium (Life Technologies), B-27 supplement (Life Technologies) or SM1 supplement

(STEMCELL), GlutaMAX (Life Technologies), and penicillin-streptomycin (Life Technologies)) for 2 weeks.

Pharmacological treatments

To examine the effects of DOX on MKP-1 protein levels in SNs at various times after treatment, Veh solution containing 50% L15 medium and 50% artificial seawater (ASW, comprised of 450 mM NaCl, 10 mM KCl, 11 mM CaCl₂, 29 mM MgCl₂, 10 mM HEPES at pH 7.6) or DOX (2.5 μ M (final concentration in Veh solution), Sigma) was applied for 2 h. This concentration of DOX is higher than the concentration measured in rat cerebral hemispheres (0.25 μ M) following injection of DOX into the peritoneum (Sardi et al. 2013). However, in rat cortical neurons, both 2.5 μ M DOX and 0.25 μ M DOX activate ERK and p38 MAPK to a similar extent (Liu et al. 2014). SNs were fixed (see Immunofluorescence section for details) 0, 1, 2, and 24 h after treatment and processed for immunofluorescence (IF) analyses. For the 1- and 2-h time points, DOX was washed out at the end of treatment and replaced with Veh control medium until time of fixation. For the 24-h time point, DOX was washed out at the end of treatment and replaced with culture medium (to maintain the health of the cells over this longer incubation period) until time of fixation. Veh-treated groups were subjected to the same wash and incubation protocols. The mean intensity of each dish was normalized to the Veh average intensity. Therefore, in the summary graphs, Veh averages are always 100%.

To determine the effects of MEK inhibition on MKP-1 protein levels immediately and 24 h after DOX treatment, SNs were incubated with the MEK inhibitor U0126 (20 μ M in 0.2% DMSO, Promega) 30 min prior to and during DOX treatment (2.5 μ M, 2

h). For the 0-h time point, SNs were fixed immediately after treatment. For the 24-h time point, SNs were incubated in culture medium until time of fixation. DOX-treated SNs were normalized to Veh-treated SNs. U0126 (IC₅₀: 0.5 μ M, *in vitro*) is a non-competitive inhibitor of MEK1 and MEK2 and prevents MEK-dependent activation of ERK (Favata et al. 1998). U0126 (20 μ M) decreases pERK levels in *Aplysia* SNs (Chin et al. 2002).

To examine pERK levels in rat cortical neurons, DOX (0.25 μ M in 0.0025% DMSO, Selleckchem) or Veh was applied for 30 min. For the immediate time point, cortical neurons were fixed at the end of the 30-min treatment. For the 24-h time point, DOX was washed out and replaced with modified neuronal growth medium for 24 h and then fixed. DOX-treated neurons were normalized to Veh-treated neurons.

To determine whether MEK or p38 MAPK activation during DOX treatment contributes to the DOX-induced increase in basal excitability, SNs were incubated with U0126 (20 μ M) or SB 203580 (3 μ M in 0.2% DMSO, EMD Millipore), respectively, 30 min prior to and during DOX treatment (2.5 μ M, 2 h). SNs were subsequently incubated in culture medium and excitability was tested 24 h after the end of treatment. SB 203580 (IC₅₀: 34 nM, *in vitro*; 600 nM, cells) competitively inhibits the activity of the α and β isoforms of p38 MAPK (Bain et al. 2007), which are the only isoforms expressed in the brain of mice (Lee et al. 2000). SB 203580 also inhibits *Aplysia* p38 MAPK *in vitro*, which closely resembles the α and β isoforms (Guan et al. 2003). The concentration of SB 203580 chosen inhibits FMRFa-induced LTD in *Aplysia* SN-MN co-cultures but has no basal effects on synaptic strength (Guan et al. 2003).

To determine the effects of DOX or the standard 5-HT protocol (5, 5-min pulses of 5-HT separated by 20-min interstimulus intervals) on the biophysical properties of SNs, pre-test measures of biophysical properties were taken immediately prior to DOX (2.5 μ M, 2 h) or Veh treatment or 5-HT (50 μ M, Sigma) or Veh treatment and then 24 and 48 h after treatment. SNs were incubated in culture medium during the time between treatment and the 24-h post-test and then again until the 48-h post-test.

To determine whether DOX affects 5-HT-induced LTEE, a pre-test measure of SN excitability was performed, followed by treatment with DOX (2.5 μ M) or Veh beginning 30 min before and persisting throughout treatment with the standard 5-HT (1 μ M) protocol. Treatment solutions were washed out at the end of the standard protocol and replaced with culture medium until the 24-h post-test.

To determine the effects of NSC 295642 on the biophysical properties of SNs, pre-test measures of biophysical properties were obtained and then SNs were treated with NSC 295642 (0.01 μ M, Sigma) or Veh for 2 h and then solution was replaced with culture medium until the 24-h post-test.

Immunofluorescence

Aplysia SNs were processed for immunofluorescence as described (Chin et al. 1999). SNs were fixed using 4% paraformaldehyde (wt/vol) in phosphate-buffered saline (PBS) containing 30% sucrose for 20 min at 4°C and then rinsed twice with PBS. Subsequently, cells were exposed to blocking solution (Superblock buffer (Pierce), 0.2% Triton X-100, and 3% normal goat serum) for 30 min at room temperature and then probed with anti-MKP-1 antibody (1:500, Santa Cruz Biotechnology) or anti-pERK antibody (1:200, Cell Signaling Technology) at 4°C

overnight. Cells were rinsed twice with PBS and then incubated at room temperature with secondary antibody (goat anti-rabbit IgG conjugated to Cy-3; 1:200 dilution, Jackson Laboratory) for 1 h in the dark. Cells were rinsed, mounted in Mowiol 4-88 medium and optical sections obtained from the middle of the nucleus were imaged with a confocal microscope (Zeiss LSM510, 63x oil-immersion lens), as has been completed routinely in the laboratory (e.g., Chin et al. 2006; Fioravante et al. 2006; Liu et al. 2011, 2014; Zhang et al. 2012, 2017). To determine the location of the middle of the nucleus, the top and bottom of the SN were identified and the imaging software was directed to find the middle section. In *Aplysia* SNs, the nucleus composes a large proportion of the cell body (Fig. 5). The mean fluorescence intensity was determined with MetaMorph software (version 7.5, Molecular Devices). Mean fluorescence intensity of a SN cell body was determined by measurement of the total intensity of the SN cell body divided by its area. Measurements from at least four neurons on each coverslip were averaged. Therefore, n values reported in Results are individual dish averages. Multiple animals, at least two, were used for each experiment. The levels of MKP-1 in DOX-treated SNs were normalized to levels measured in Veh-treated SNs.

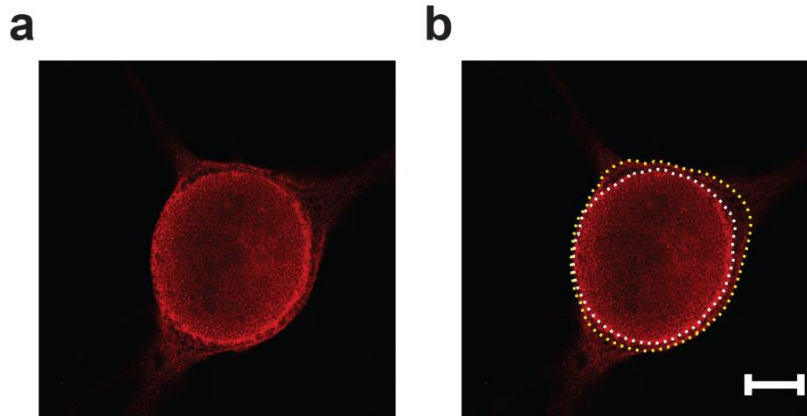


Figure 5. Confocal image of a cultured *Aplysia* SN. (a) Image of the middle section of a SN stained with MKP-1 antibody. (b) Same SN with cell body outlined in yellow and nucleus outlined in white. The nucleus composes a large area of the cell body. The intensity of staining within the entire cell body was measured for each immunofluorescence experiment. Scale bar, 20 μ m.

Rat cortical neurons were processed for immunofluorescence as described (Moruno Manchon et al. 2016). Briefly, neurons were fixed at room temperature using 4% paraformaldehyde in PBS (pH 7.4) for 15 min and then washed twice with PBS. Cells were permeabilized by a 10-min application of PBS containing 0.1% Triton X-100 and then washed three times with PBS. Cells were blocked at 4°C overnight with 10% fetal bovine serum in PBS. Cells were washed once in PBS followed by overnight incubation with anti-pERK antibody (1:200) diluted in 10% serum in PBS at 4°C. Cells were then rinsed three times with PBS and incubated in the dark with secondary antibody (goat anti-rabbit IgG conjugated to Cy-3; 1:200 dilution) at room temperature for 1 h. Again, cells were washed three times with PBS followed by nuclear staining with Hoechst or DAPI (0.1-1 µg/mL) in PBS and then rinsed with PBS. Images of fixed neurons were acquired with a 20x objective using the automated EVOS microscopy system (Life Technologies) and then analyzed using ImageJ software. n values reported in Results represent an average of 25-50 cells per well.

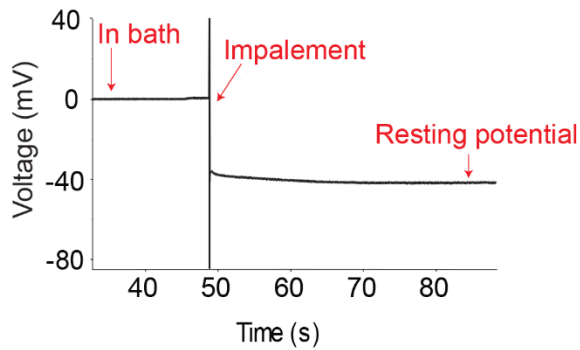
Experimenters were blind to the treatment group identities until the end of the analyses.

Electrophysiology

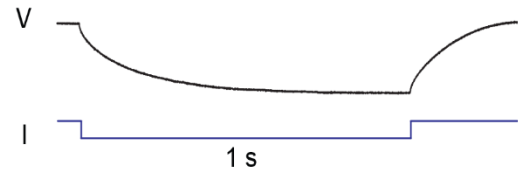
Biophysical properties of cultured *Aplysia* SNs were measured as previously described (Liu et al. 2014). Sharp microelectrodes (10 – 20 MΩ resistance) were filled with 3 M potassium acetate and attached to an Axoclamp 2-B amplifier (Molecular Devices). For each SN, a single microelectrode was inserted into its soma for purposes of current injection and voltage measurements. pClamp software (version 10.2, Molecular Devices) was employed for both the acquisition and analysis of data.

After impalement, SNs were allowed to stabilize and the resting potential was recorded (Fig. 6a). SNs were then current clamped at -45 mV (for several early experiments) or -55 mV (most experiments), and 1 s of hyperpolarizing current (0.3 nA) was injected to assess input resistance (Fig. 6b). A 1-s depolarizing current injection was then applied beginning with 0.1 nA and then additional current injections were provided in increasing 0.1-nA steps until an action potential was elicited. The minimal current required to elicit an action potential in a SN was recorded as its firing threshold (Fig. 6c). The firing threshold is stable for an individual SN avoiding the need to stimulate multiple times to obtain an average (personal observations). A 1-s depolarizing current was then injected, the magnitude of which depended upon the firing threshold, and the number of action potentials produced was recorded as a measure of excitability (Fig. 6d). If the firing threshold was between 0.1 and 0.4 nA, then 0.5 nA of depolarizing current was employed to evaluate excitability. If the firing threshold was between 0.5 and 0.9 nA, then a 1.0 nA depolarizing current was injected (Chin et al. 1999; Liu et al. 2011, 2014). The excitability measured on the post-test was calculated as percent of pre-test.

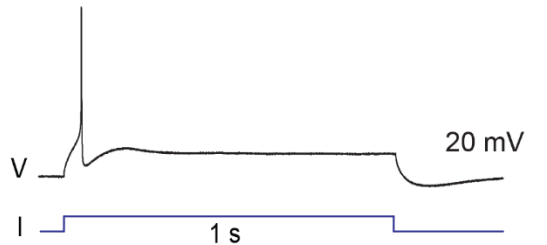
a Resting Potential



b Input Resistance



c Firing Threshold



d Excitability

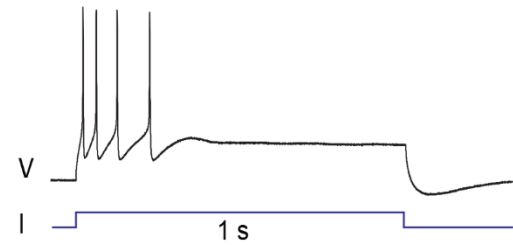


Figure 6. Measurement of biophysical properties of isolated SNs. (a) Resting potential was recorded as the stabilized voltage achieved shortly (~30 - 45 s) after impalement of each SN. (b) Input resistance was calculated using the voltage change measured upon injection of a 0.3 nA hyperpolarizing current for 1 s. (c) Firing threshold was recorded as the lowest current injection necessary to elicit an action potential. (d) Excitability was determined by the number of action potentials elicited by a set current injection. See Materials and Methods for more detailed descriptions of these biophysical measurements.

For all electrophysiology experiments, with the exception of the correlations, each data point represents a mean percent for all recorded SNs (2-5 SNs) in a single dish. If multiple dishes containing SNs from a single animal received the same treatment, the mean of the dish averages from that animal was calculated and represented a single n. Therefore, n values represent an average response from SNs from a single animal. For the correlation experiments, each data point represents a single SN. SNs were obtained from numerous animals/independent cultures. Individual SNs were excluded from use at pre-test if their firing threshold was less than or equal to 0.2 nA or if their resting membrane potential was more depolarized than -40 mV. Individual SNs were excluded from analyses if their input resistance decreased by 50% or more from the pre- to post-test or if their resting membrane potential was more depolarized than -30 mV on the post-test. For all electrophysiology experiments other than the correlations, only individual experiments containing a Veh-treated group that did not show a large increase in excitability (dish average of 50% or more) between the pre- and post-test were included for analysis. For the correlation, SNs were included regardless of the magnitude of the average response from all cells in the Veh dish, because we were interested in determining individual SN responses and their relation to pERK levels in response to both Veh and DOX treatment.

Experimenters were blind to the treatment group identities until the end of the analyses.

Correlation

To determine whether pERK levels and biophysical properties were correlated 24 h after DOX or Veh treatment, properties were measured before and 24 h after

DOX or Veh treatment as indicated previously. Immediately after the 24-h post-test, SNs were fixed and stained with anti-pERK antibody (1:200) and then processed for immunofluorescence analysis. Detailed maps and illustrations of the SNs were created during the electrophysiological measurements to ensure assessment of the same neurons during confocal imaging.

Experimenters were blind to the treatment group identities until the end of the analyses.

Statistical analyses

Excel (Microsoft Office Professional Plus 2013) and Matlab (version 8.3; Mathworks) were used to plot data. Sigmaplot (version 12; Systat Software) was used for statistical analyses. Two-way ANOVAs followed by Tukey's Honestly Significant Difference were used in experiments involving multiple comparisons unless otherwise indicated. Tukey's multiple-comparison procedure is very conservative and provides greater protection from type I errors (falsely detecting differences) than most other procedures (Dowdy, Wearden and Chilko 2004). Student's t-tests were used in experiments involving comparison between two groups unless otherwise indicated. Correlation coefficients were calculated as Pearson's. Exact sample sizes are included in the text. Some data were log (base 10)-transformed to achieve normality, as indicated in results. In those cases, statistical analysis was performed on the transformed data. Data are presented as mean \pm SEM or median (interquartile range) as indicated; $p \leq 0.05$ was set as the threshold for statistical significance.

Chapter 3: Doxorubicin-induced biphasic regulation of the ERK pathway is accompanied by dynamic regulation of MKP-1.

Introduction

DOX induces biphasic activation of ERK in SNs (Fig. 4). DOX also decreases levels of MKP-1 in breast cancer cell lines and in breast cancer tumor cells from patients (Rojo et al. 2009; Small et al. 2003). In several breast cancer cell lines, a basal level of MKP-1 expression must be present upon DOX exposure to induce ERK activation (Small et al. 2003). DOX-induced ERK activation in these cell lines does not depend on MEK, but likely depends on decreases in MKP-1 expression through transcriptional repression as DOX caused a decrease in MKP-1 mRNA transcript levels associated with a decrease in activity of the MKP-1 promoter region (Small et al. 2003). A caveat to this study is that Small et al. (2003) observed decreased levels of MKP-1 protein early with just a 2-h DOX treatment, but mRNA levels and promoter activity were assessed following longer treatment durations. Therefore, it is unclear if the early decrease in MKP-1 protein is a manifestation of the combination of repressed transcription of MKP-1 by DOX and the short half-lives of both MKP-1 mRNA and protein, or if it is due to enhanced degradation possibly through the ubiquitin-proteasome pathway (Boutros et al. 2008). Indeed, DOX enhances proteasome activity in leukemia cells (Ciftci et al. 2001). Rojo et al. (2009) also observed a decrease in transcript and protein levels of MKP-1 in breast cancer cell lines in response to DOX treatment. Therefore, DOX may induce ERK activation through decreased expression of MKP-1 rather than through upstream activation of the MEK-ERK pathway. In contrast, DOX-induced ERK activation is MEK-dependent in two hepatocellular cell lines (Choi et al. 2008). These examples show that DOX can lead to enhanced ERK activity through either upstream activation of the Raf-MEK-ERK

pathway or repression of phosphatase activity (Fig. 7). The mechanism by which DOX acts seems to vary with regard to cell type, but the mechanism may also vary within a cell type. DOX induces two phases of ERK activation in *Aplysia* SNs (Fig. 4b). It is possible that the early phase, occurring during and shortly after DOX treatment, and the late phase of ERK activation arise from different mechanisms.

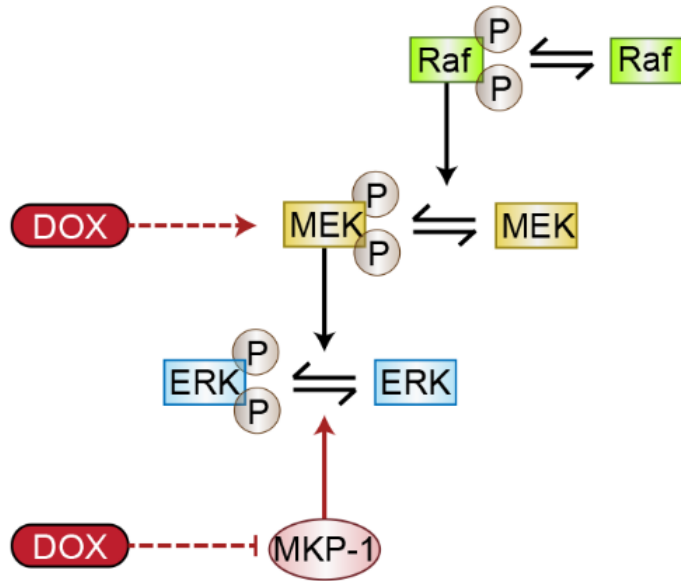


Figure 7. Potential mechanisms for DOX-induced increase in ERK activation.

DOX may enhance levels of phosphorylated ERK through upstream activation of MEK and/or a decrease in levels of phosphatases. For example, MKP-1 is a phosphatase that is modulated by DOX in *Aplysia* SNs (Liu et al. 2014).

One hypothesis is that DOX-induced activation of ERK may be due to a decrease in expression of MKP-1. Previous work in our lab showed that MKP-1 protein levels are decreased 45 min after a 2-h DOX treatment, although the decrease was very small (~12%) (Liu et al. 2014). It is important to determine whether decreased levels of MKP-1 protein could explain the dynamics of ERK activation. Therefore, similar to the time course measurements of ERK and p38 MAPK phosphorylation following DOX treatment (Fig. 4), the time course of MKP-1 protein levels was determined.

Results

To determine whether a decrease in MKP-1 expression could account for the DOX-mediated activation of ERK, we (Dr. H. Lakshminarasimhan, Amber Darr (a medical student), and myself) measured levels of MKP-1 protein at multiple time points after DOX (2h, 2.5 μ M) application to SNs (Fig. 8a). MKP-1 levels decreased to $52.8 \pm 8.9\%$ ($n = 4$) immediately after DOX treatment (0 h) compared to Veh ($100 \pm 10.5\%$, $n = 6$) and were depressed 1 h after the end of treatment ($82.4 \pm 4.7\%$, $n = 9$) compared to Veh ($100 \pm 7.2\%$, $n = 10$). By 2 h after the end of the treatment, MKP-1 levels returned to baseline ($109.4 \pm 12\%$, $n = 9$) compared to Veh ($100 \pm 8.6\%$, $n = 10$), and remained at baseline ($99.6 \pm 10.6\%$, $n = 10$) compared to Veh ($100 \pm 8.1\%$, $n = 11$) at 24 h post-treatment (Fig. 8b). A two-way ANOVA revealed a significant main effect of treatment ($F_{(1,60)} = 4.11$; $p = 0.047$), and strong trends towards a main effect of time ($F_{(3,60)} = 2.64$; $p = 0.057$) and interaction of treatment with time ($F_{(3,60)} = 2.64$; $p = 0.057$). Pairwise post-hoc comparisons revealed a significant difference between MKP-1 levels in DOX- and Veh-treated groups at 0 h ($p = 0.009$), but not at 1 h ($p =$

0.16), 2 h (0.46), or 24 h ($p = 0.97$). In summary, DOX led to a transient decrease in MKP-1 expression that returned to baseline within 2 h of removal of DOX and did not show any delayed modulation. The apparent higher intensity of MKP-1 staining in the cytosol (Fig. 8b1) was surprising. MKP-1 is thought to be active only in the nucleus (Boutros et al. 2008), but it is possible that while higher concentrations of MKP-1 protein are in the cytosol relative to the nucleus overall, there may still be an overall decrease in MKP-1 in the nucleus as well with DOX treatment. Furthermore, MKP-1 protein function has not been characterized in *Aplysia* SNs. Therefore, *Aplysia* MKP-1 may also be functional in the cytosol.

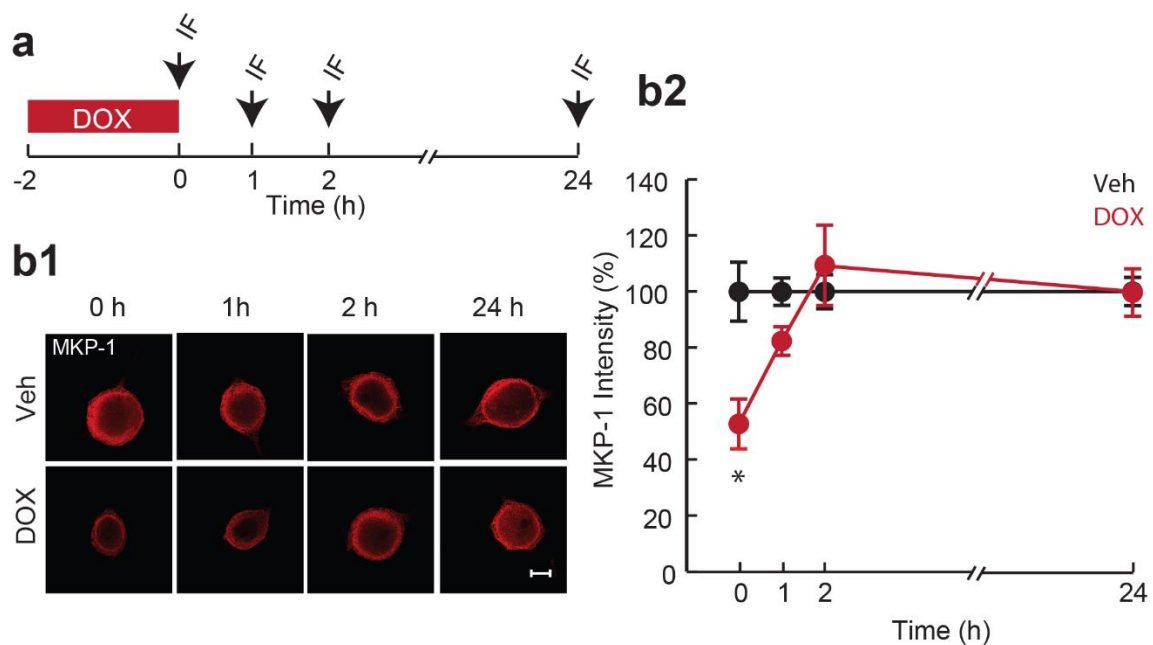


Figure 8. DOX caused a transient decrease in expression of MKP-1. (a) Protocol for DOX application and measurement of MKP-1 expression levels. Arrows represent fixation times and subsequent IF staining. (b1) Representative confocal images of MKP-1 staining in SNs 0, 1, 2, and 24 h after the end of DOX treatment. Scale bar, 20 μ m. (b2) Summary data. The decrease in levels of MKP-1 reversed within 2 h after the end of treatment. Data are plotted as mean \pm SEM; * represents $p \leq 0.05$. n values ranged from 4 – 11. Each n represents an average of at least 4 cells that compose a single dish. Dishes were obtained from multiple animals.

Data contributing to this time course were collected by myself, Dr. H. Lakshminarasimhan, and Amber Darr, a medical student who participated in the McGovern Medical School's summer research program. Appropriate data and aspects of figure used with permission from Dr. H. Lakshminarasimhan and A. Darr.

As part of our collaborative project, Dr. H. Lakshminarasimhan showed that application of a MEK inhibitor (U0126, 20 μ M) before and during DOX treatment did not block the early phase of ERK activation when measured immediately after DOX treatment (Fig. 9a). This finding in combination with results from the MKP-1 time course experiments (Fig. 8), led to the hypothesis that the early phase of ERK activation occurring immediately after DOX treatment is likely due to the decrease in MKP-1 protein (See also Fig. 7). Dr. H. Lakshminarasimhan also found that blocking MEK activity during DOX treatment potentiated the late phase of ERK activation occurring 24 h after treatment (Fig. 9b). This result was unexpected but it indicated that some initial level of DOX-induced MEK activity, possibly occurring early during DOX treatment, was influencing the level of delayed ERK activation. The finding that immediate ERK activation is not affected by application of the MEK inhibitor (Fig. 9a) suggests that DOX-induced activation of MEK is suppressed by the end of a 2-h treatment with DOX, possibly due to the accumulation of p38 MAPK (Fig. 4c) which can inhibit the MEK pathway (Fioravante et al. 2006; Zhang et al. 2017). The late phase of ERK activation was found to be, in part, dependent on late MEK activation, as application of a MEK inhibitor just prior to the 24-h fixation time point attenuated that late pERK (Fig. 9c, See also Fig. 7). Together, these findings (Fig. 8 and Fig. 9) suggest that the early and late phases of DOX-induced ERK activation (Fig. 4) depend on different mechanisms, but also that the late phase may depend on events occurring early during DOX treatment. This latter point was investigated further.

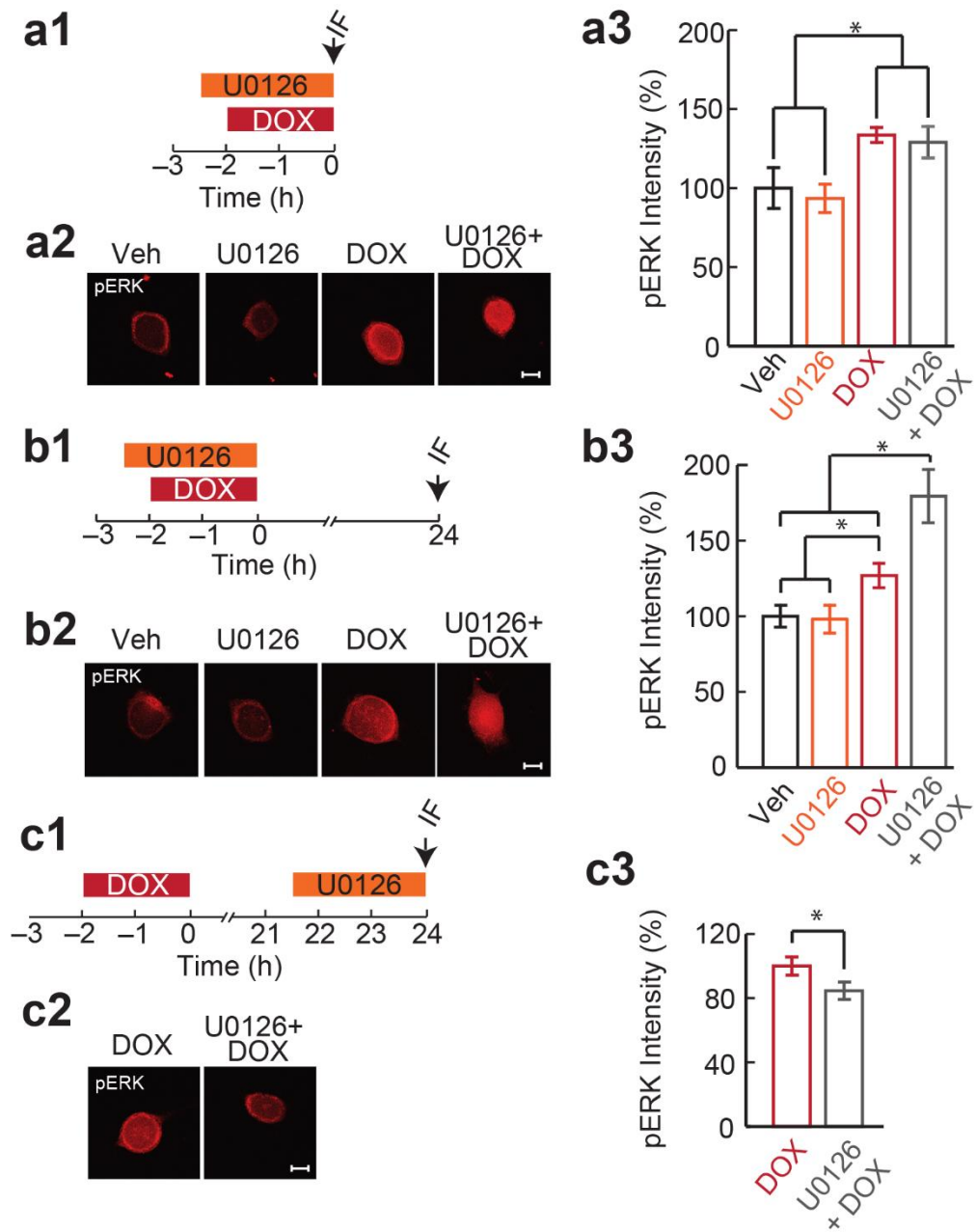


Figure 9. MEK inhibition during DOX treatment does not block the early phase of ERK activation but potentiates the late phase of ERK activation. (a1, b1, c1)

Protocols for DOX and U0126 (MEK inhibitor) application and measurement of pERK levels. Arrows represent fixation times and subsequent IF staining. (a2, b2, c2) Representative confocal images of pERK staining in SNs for each experiment. Scale bars, 20 μ m. (a3, b3, c3) Summary data. Data are plotted as mean \pm SEM; * represents $p \leq 0.05$. MEK inhibition during DOX treatment did not block the increase in early pERK (a3) but potentiated the late pERK (b3). MEK inhibition long after DOX treatment attenuated the late pERK (c3). n values ranged from 10 – 17. Each n represents an average of at least 4 cells that compose a single dish. Dishes were obtained from multiple animals.

Data shown in this figure were collected by and figure was made by Dr. H. Lakshminarasimhan. Figure and data used with permission from Dr. H. Lakshminarasimhan.

MEK inhibition during DOX treatment facilitates the late phase of ERK activation (Fig. 9b). It is possible that inhibition of MEK prolongs the decrease in MKP-1 expression (see Fig. 8), given the established role of the MEK-ERK pathway in inducing MKP-1, which can serve as a feedback inhibition mechanism to limit ERK activation (Brondello et al. 1997; Caunt and Keyse 2013; Cook et al. 1997; Li et al. 2001). To determine the feasibility of this hypothesis, we determined how MEK inhibition affects levels of MKP-1 after removal of DOX (Fig. 10 and Fig. 11). Inhibition of MEK during DOX treatment may induce a late or prolonged decrease in MKP-1 expression, and thereby contribute to the enhancement of DOX-induced late ERK activation.

To test whether MKP-1 protein levels may be a possible link between the early and late ERK activation, U0126 (20 μ M) was applied before and during DOX treatment and SNs were fixed either immediately or 24 h after treatment and MKP-1 levels were assessed using immunofluorescence (Fig. 10a and Fig. 11a). The immediate time point was included as a control to determine if MEK inhibition would further repress MKP-1 levels at a time (See Fig. 8 for MKP-1 time course) when MEK inhibition had no apparent effect on ERK activation levels (Fig. 9a). If DOX further repressed MKP-1 levels in the presence of a MEK inhibitor at a time when ERK activation levels were not changed, it would suggest that MKP-1 is not modulating ERK activity. Immediately after the end of treatment (0 h), at a time when MKP-1 levels were decreased by DOX alone (Fig. 8), both the DOX ($100 \pm 4.2\%$, $n = 8$) and U0126 + DOX groups ($95.7 \pm 8.2\%$, $n = 8$) showed comparable levels of MKP-1 protein ($t_{(7)} = 0.4$; $p = 0.35$) (Fig. 10b1 and Fig. 10b2), as expected. However, 24 h after the end of treatment, at a time

when DOX alone had no effect on MKP-1 (Fig. 8), the U0126 + DOX group ($86 \pm 4.6\%$, $n = 9$) showed a significant decrease in levels of MKP-1 protein ($t_{(8)} = 1.9$; $p = 0.05$) in comparison to DOX alone ($100 \pm 4.3\%$, $n = 9$) (Fig. 11b1 and Fig. 11b2). Thus, inhibition of MEK during DOX treatment prolongs downregulation of MKP-1, and this may explain the potentiation of the late DOX-induced ERK activation by early MEK inhibition (Fig. 9b).

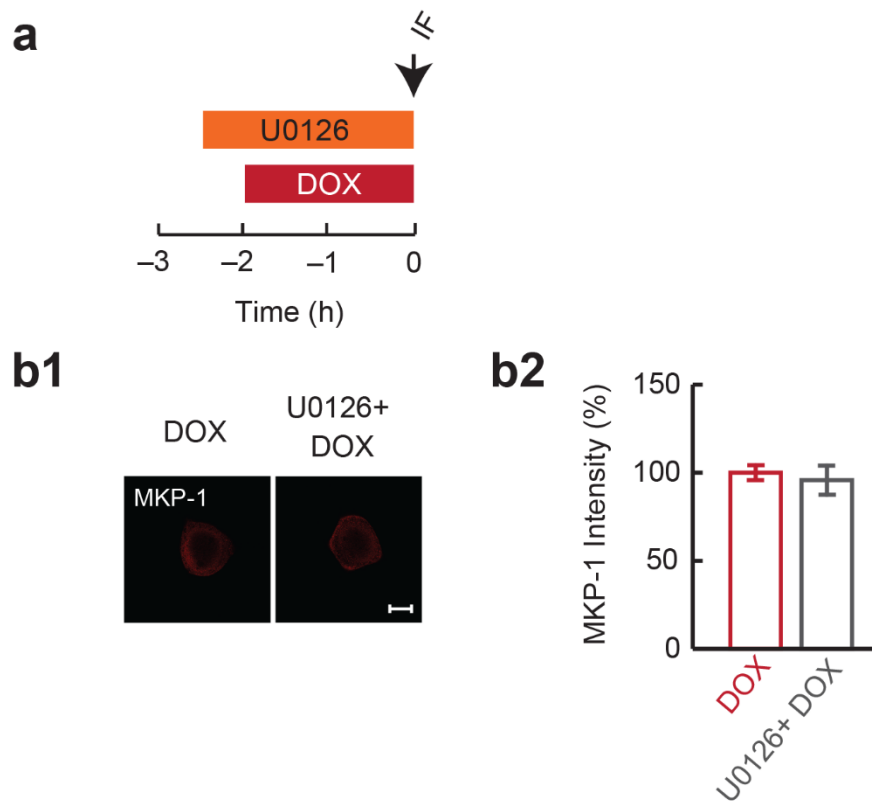


Figure 10. MEK inhibition during DOX treatment did not affect the initial decrease in MKP-1 protein. (a) Protocol for application of U0126 and DOX followed by measurement of MKP-1 expression immediately after the end of DOX treatment. Arrow represents fixation time and subsequent IF staining. (b1) Representative confocal images of MKP-1 staining in SNs immediately after the end of DOX and U0126 + DOX treatments. Scale bar, 20 μ m. (b2) Summary data. Application of U0126 did not affect MKP-1 levels immediately after DOX treatment. Data are plotted as mean \pm SEM. $n = 8$ for both groups. Each n represents an average of at least 4 cells that compose a single dish. Dishes were obtained from multiple animals.

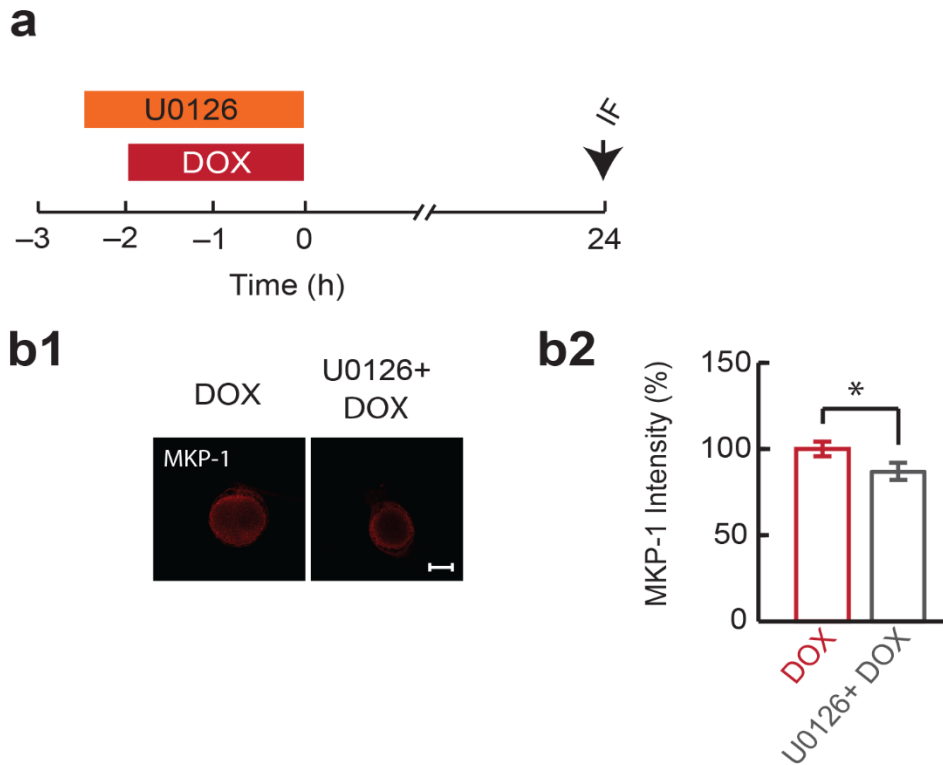


Figure 11. MEK inhibition during DOX treatment caused a late decrease in MKP-1 protein. (a) Protocol for application of U0126 and DOX followed by measurement of MKP-1 expression 24 h after the end of treatment. Arrow represents fixation time and subsequent IF staining. (b1) Representative confocal images of MKP-1 staining in SNs 24 h after the end of DOX and U0126 + DOX treatments. Scale bar, 20 μ m. (b2) Summary data. Application of U0126 caused a decrease in MKP-1 expression 24 h after DOX treatment. Data are plotted as mean \pm SEM; * represents $p \leq 0.05$. $n = 9$ for both groups. Each n represents an average of at least 4 cells that compose a single dish. Dishes were obtained from multiple animals.

The ability of a MEK inhibitor when applied to SNs during DOX treatment to prolong the decrease in MKP-1 protein (Fig. 11) (although the effect size was small) and simultaneously enhance the late phase of ERK activation (Fig. 9b) suggests early MEK activity (during DOX treatment) has long-term consequences on MKP-1 expression and may thereby contribute to the level of delayed ERK activity. The late phase of ERK activation (Fig. 4b) occurring when MKP-1 expression is at baseline (Fig. 8) also appears to rely on a delayed phase of MEK activity (Fig. 9c). Therefore, early and late MEK activity appear to influence the magnitude of the late phase of ERK activity, although in opposing directions.

To determine whether the early and late phases of DOX-induced ERK activation also occur in mammalian cells, pERK was measured immediately and 24 h after DOX treatment in cultured rat cortical neurons (Fig. 12a1 and Fig. 12b1). Cortical neuronal cultures were kindly provided by Dr. Andrey Tsvetkov and members of his laboratory. Dr. Jose Felix Moruno Manchon kindly performed the DOX treatments. All immunostaining, imaging using the automated EVOS microscopy system in Dr. Tsvetkov's laboratory, and analyses were performed by Dr. H. Lakshminarasimhan and myself as part of a collaborative effort. DOX exposure (0.25 μ M, 30 min) resulted in an increase in pERK immediately (Veh, 100.4 (95.8 to 103.8%)(median (interquartile range)), n = 4; DOX, 152.9 (136.9 to 206.1%), n = 5; Mann-Whitney U = 0.00; p = 0.016) and 24 h after treatment (Veh, 100.0 \pm 1.8%, n = 4; DOX, 142.7 \pm 7.1%, n = 4; $t_{(6)} = 5.82$; p = 0.001) (Fig. 12). A 30-min treatment was employed to mitigate neuronal damage as the cortical neurons appeared more sensitive to the toxic effects of DOX than *Aplysia* SNs (Liu et al. 2014). Previous work in the lab showed

that pERK levels are elevated 45 min after DOX in this same preparation, but analysis was performed with confocal microscopy (Liu et al. 2014). Here, additional time points were measured with the advantage of an automated microscopy system, which allowed for sampling of a greater number of cells. These findings suggest that biphasic activation of ERK in response to a brief exposure to DOX is not unique to *Aplysia*. In the conditions employed in this experiment, pERK levels did not return to baseline as we observed in *Aplysia* SNs. Therefore, it is possible that ERK activation may be sustained rather than biphasic in rat cortical neurons.

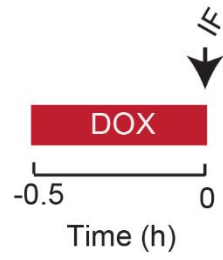
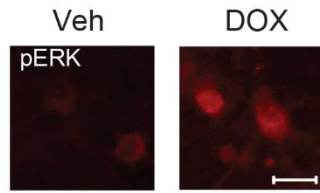
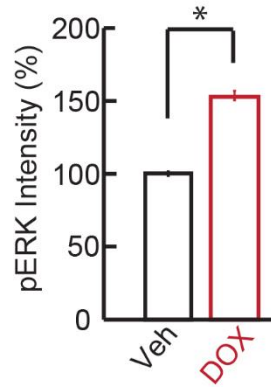
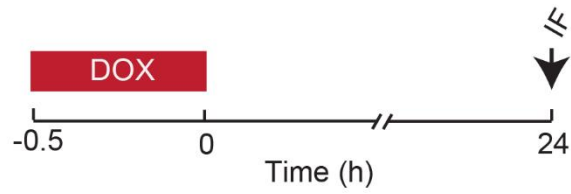
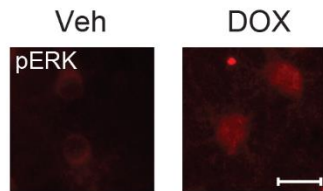
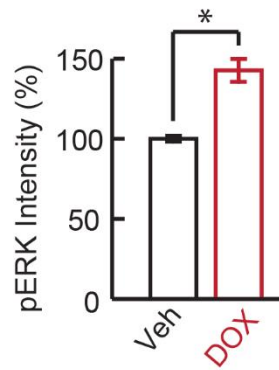
a1**a2****a3****b1****b2****b3**

Figure 12. ERK activation was enhanced in DOX-treated cortical neurons from rat both immediately and 24 h after treatment. (a1) Protocol for DOX or Veh application and immediate measurement of pERK levels in cortical neurons. Arrow represents fixation time and subsequent IF staining. (a2) Representative images of pERK staining in Veh- and DOX-treated cortical neurons immediately after treatment. Scale bar, 20 μ m. (a3) Summary data. Data are plotted as median (interquartile range); * represents $p \leq 0.05$. (b1) Protocol for DOX or Veh application and measurement of pERK levels in cortical neurons 24 h after treatment. Arrow represents fixation time and subsequent IF staining. (b2) Representative images of pERK staining in cortical neurons 24 h after the end of DOX or Veh treatment. Scale bar, 20 μ m. (b3) Summary data. DOX resulted in an increase in ERK activation immediately and 24 h after the end of treatment. Data are plotted as mean \pm SEM; * represents $p \leq 0.05$. $n = 4-5$. Each n value represents an average of 25-50 cells composing a well.

Collection of these data were a combined effort of Dr. H. Lakshminarasimhan and myself. Cortical neuron cultures were provided by Dr. Tsvetkov's lab, and Dr. Moruno Manchon performed the DOX treatments. Data and aspects of figure used with permission from Dr. H. Lakshminarasimhan.

Conclusion

DOX produced biphasic ERK activation in SNs (Fig. 4b), and enhanced ERK activation was observed immediately and 24 h after DOX treatment in rat cortical neurons (Fig. 12), suggesting that the effects of DOX on ERK activation are conserved across species. MKP-1 targets pERK and p-p38 MAPK (for review, see Jeffrey et al. 2007), and the initial increase in activation of the two kinases (Fig. 4) mirrors the transient decrease in MKP-1 expression (Fig. 8). The reduction in levels of MKP-1 may contribute to the increased levels of pERK and p-p38 MAPK immediately after DOX treatment. Indeed, a parallel experiment by Dr. H. Lakshminarasimhan suggests that the DOX-induced ERK activation observed immediately after treatment is MEK-independent (Fig. 9a), and given that MEK is thought to be the sole mediator of ERK phosphorylation (Shaul and Seger 2007), a phosphatase-dependent mechanism for the immediate ERK activation is plausible. In support of this model, MKP-1 levels returned to baseline by 2 h (Fig. 8), at which point neither pERK nor p-p38 MAPK was significantly different between DOX- and Veh-treated cells (Fig. 4).

A 2-h treatment with DOX has been shown to decrease levels of MKP-1 protein in breast cancer cell lines (Small et al. 2003), but this study only provided evidence for DOX-induced transcriptional repression of MKP-1 following longer treatment durations. If DOX represses MKP-1 transcription early, it is possible that this effect would manifest as a decrease in MKP-1 protein levels immediately after a 2-h DOX treatment due to the short half-lives of both MKP-1 mRNA and protein (1 to 2h and 40 min to 2h, respectively) (Boutros et al. 2008). The ability of MKP-1 protein levels to recover 2 h after DOX treatment may be due to the relief of transcriptional repression

once DOX is removed from solution, given that *mkp-1* is an immediate-early gene (Boutros et al. 2008). It is also possible that the decrease in MKP-1 protein observed immediately after DOX treatment is due to enhanced protein degradation through the ubiquitin proteasome pathway (Boutros et al. 2008; Ciftci et al. 2001). Interestingly, ERK $\frac{1}{2}$ can either enhance or reduce degradation of MKP-1 protein through phosphorylation of different serine residues, although it is not known which ERK isoforms contribute to these phosphorylation events (Boutros et al. 2008; Brondello et al. 1999; Lin, Chuang and Yang 2003; Lin and Yang 2006). Therefore, it is possible that ERK modulates MKP-1 protein levels through enhanced degradation, which may contribute to the initial decrease in MKP-1 protein and to the recovery of MKP-1 protein that coincides with reversal of levels of phosphorylated ERK to baseline. On the other hand, ERK-mediated stabilization of MKP-1 protein may contribute to the return of MKP-1 protein levels to baseline once DOX is removed. The mechanism by which DOX leads to an early decrease in MKP-1 protein and the mechanism by which MKP-1 protein levels recover fairly rapidly remain to be investigated.

24 h after DOX treatment, a time long after MKP-1 levels had returned to baseline (Fig. 8), a late phase of ERK activation was observed (Fig. 4b), suggesting that late activation of ERK occurs by some mechanism other than MKP-1 downregulation, possibly through a delayed phase of MEK activation (Fig. 9c). Together these findings suggest that the early and late phases of DOX-induced enhanced ERK activity are mechanistically distinct with the early phase being MEK-independent (at least when measured immediately after DOX treatment), and the late phase being, at least in part, MEK-dependent. Furthermore, inhibition of MEK during DOX treatment prolonged the

downregulation of MKP-1 (Fig. 11), which may, in combination with delayed or persistent MEK activation, contribute to potentiation of the late DOX-induced enhancement of ERK activation (Fig. 9b). The finding that application of the MEK inhibitor U0126 during DOX treatment modulated the late effects of DOX suggests that DOX does indeed induce MEK activity initially, possibly at the beginning of treatment, but that this MEK activity soon is repressed by putative inhibitory actions of p38 MAPK on MEK (Fioravante et al. 2006; Zhang et al. 2017). This may explain why U0126 application did not suppress the ERK activity measured immediately after treatment, but did modulate late effects of DOX, possibly through transcription-dependent events.

Chapter 4: Doxorubicin induces persistent changes in the biophysical properties of sensory neurons similar to serotonin and prevents serotonin-mediated long-term enhanced excitability.

Part of this chapter is based upon: Liu RY, Zhang Y, Coughlin BL, Cleary LJ, Byrne JH (2014). Doxorubicin attenuates serotonin-induced long-term synaptic facilitation by phosphorylation of p38 mitogen-activated protein kinase. *J. Neurosci.* 34: 13289-13300.

Permission policy of *The Journal of Neuroscience*: "If the request for permission is from an Original Author you DO NOT need to obtain permission for any non-commercial reuse of your own material."

Introduction

A single, 2-h exposure to DOX prevents LTF of the *Aplysia* sensorimotor synapse 24 h after treatment (Liu et al. 2014). In addition, the same treatment causes biphasic activation of ERK, consisting of an early (during and up to 1 h after the end of treatment) and a late phase of activation (24 h after the end of treatment) (Fig. 4b: Liu et al. 2014). Together, these findings suggest that DOX may produce other persistent and/or delayed effects in SNs. Given that DOX produces dynamic ERK activity (Fig. 4b) and that a large amount of evidence suggests a link between ERK and excitability (Adams and Sweatt 2002; Chin et al. 2006; Cohen-Matsliah et al. 2007; Rosenkranz et al. 2009; Sung et al. 2001), we hypothesized that DOX may affect the biophysical properties of neurons. Therefore, the effects of a 2-h DOX treatment on SN excitability, input resistance, firing threshold, and resting membrane potential were examined 24 and 48 h after treatment (see Fig. 6 for examples of biophysical measurements). The same phenomena were then measured after the standard 5-HT protocol (5, 5-min pulses of 5-HT separated by 20 min inter-stimulus intervals) in order to compare and contrast the effects of DOX treatment with changes associated with memory formation (i.e., 5-HT). In addition, the effect of DOX on 5-HT-induced LTEE was examined to determine if DOX blocks LTEE as it does LTF. While LTF and LTEE co-occur during LTS (Cleary et al. 1998) and are believed to both contribute to the memory trace (Mozzachiodi and Byrne 2010), these two phenomena are rarely studied together. Most *Aplysia* studies focus on LTF, but with the growing evidence for the importance of excitability in memory formation in both vertebrates and invertebrates (for reviews,

see Kim et al. 2016; Mozzachiodi and Byrne 2010), LTEE in *Aplysia* deserves closer inspection.

Results

The effects of DOX treatment on the biophysical properties of SNs over time

The effects of a single application of DOX (2 h, 2.5 μ M) on SN excitability, input resistance, firing threshold and resting membrane potential were examined 24 and 48 h after treatment (Fig. 13a). DOX produced a long-term increase in excitability that lasted for at least 48 h (Fig. 13b1 and Fig. 13b2). The excitability of DOX-treated SNs was $155.4 \pm 17.0\%$ ($n = 10$) of pretest levels at 24 h and $164.0 \pm 22.3\%$ ($n = 9$) of pretest levels at 48 h compared to $96.8 \pm 7.9\%$ ($n = 10$) and $112.9 \pm 8.4\%$ ($n = 9$) of pretest levels at 24 and 48 h, respectively, for Veh-treated SNs. The data were transformed with a log (base 10) function to achieve normality for parametric statistical analyses. A two-way ANOVA revealed a main effect of treatment ($F_{(1,34)} = 14.99$; $p < 0.001$) but not of time ($F_{(1,34)} = 1.04$; $p = 0.31$) and no interaction of treatment with time ($F_{(1,34)} = 0.42$; $p = 0.52$). Pairwise post-hoc comparisons revealed significant differences in excitability between Veh- and DOX-treated SNs 24 h ($p = 0.003$) and 48 h ($p = 0.033$) after treatment.

DOX caused an increase in input resistance (Fig. 13c). The input resistance of DOX-treated SNs was $123.1 \pm 9.1\%$ ($n = 10$) of pretest level at 24 h and $112.3 \pm 13.7\%$ ($n = 9$) of pretest level at 48 h compared to $95.8 \pm 6.0\%$ ($n = 10$) and $93.8 \pm 8.7\%$ ($n = 9$) of pretest levels at 24 and 48 h, respectively, for Veh-treated SNs. The data were transformed with a log (base 10) function to achieve normality as was performed for

the excitability data. A two-way ANOVA revealed a significant main effect of treatment ($F_{(1,34)} = 5.74$; $p = 0.022$) but no main effect of time ($F_{(1,34)} = 0.88$; $p = 0.36$) and no interaction of treatment with time ($F_{(1,34)} = 0.25$; $p = 0.62$). Pairwise post-hoc comparisons revealed a significant difference in input resistance between Veh- and DOX-treated SNs at 24 h ($p = 0.043$) but not at 48 h ($p = 0.20$).

DOX produced a persistent decrease in firing threshold (Fig. 13d). The firing threshold of DOX-treated SNs decreased by 0.058 ± 0.024 nA ($n = 10$) at 24 h and by 0.053 ± 0.027 nA ($n = 9$) at 48 h compared to increases of 0.046 ± 0.027 nA ($n = 10$) and 0.022 ± 0.023 nA ($n = 9$) at 24 and 48 h, respectively, in Veh-treated SNs. A two-way ANOVA revealed a main effect of treatment ($F_{(1,34)} = 12.41$; $p = 0.001$) but no main effect of time ($F_{(1,34)} = 0.13$; $p = 0.73$) and no interaction of treatment with time ($F_{(1,34)} = 0.33$; $p = 0.57$). Pairwise post-hoc comparisons revealed a significantly lower firing threshold in DOX-treated SNs compared to Veh-treated SNs at 24 h ($p = 0.005$) and at 48 h ($p = 0.05$).

Lastly, DOX appeared to promote a slightly more hyperpolarized resting membrane potential relative to Veh treatment (Fig. 13e). DOX treatment resulted in a slight depolarization of 1.00 ± 0.93 mV ($n = 10$) at 24 h and 0.57 ± 0.98 mV ($n = 9$) at 48 h compared to pre-test measures of resting membrane potential. Veh treatment resulted in a slightly greater depolarization of 2.82 ± 1.16 mV ($n = 10$) at 24 h and 2.53 ± 0.94 mV ($n = 9$) at 48 h compared to pre-test measures of resting membrane potential. A two-way ANOVA revealed a trend towards a main effect of treatment ($F_{(1,34)} = 3.45$; $p = 0.072$), but no apparent main effect of time ($F_{(1,34)} = 0.12$; $p = 0.73$) or interaction of treatment with time ($F_{(1,34)} = 0.0046$; $p = 0.95$).

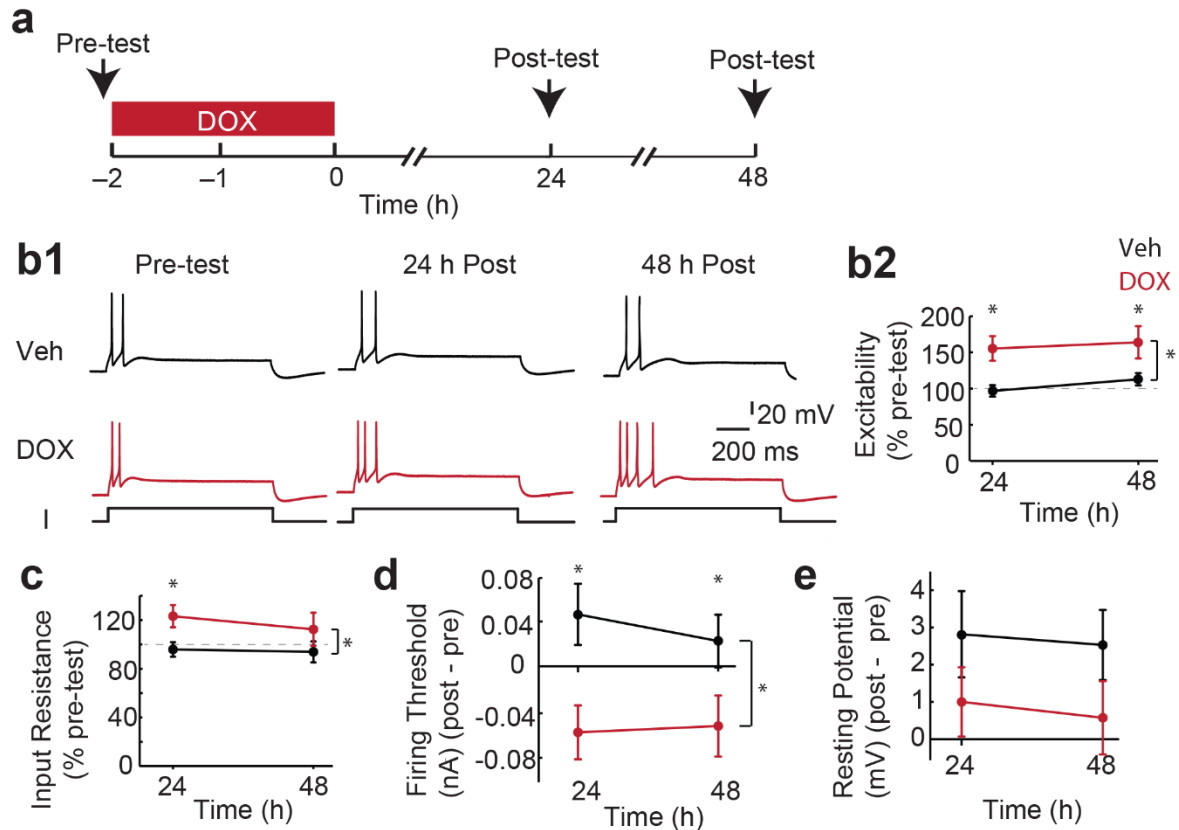


Figure 13. DOX produced persistent changes in the biophysical properties of SNs. (a) Protocol for application of DOX relative to the pre- and post-test measurements of biophysical properties. Arrows represent recording times. (b1) Representative action potentials elicited by a constant current injection (I) before (Pre-test) and after (24 h Post and 48 h Post) Veh or DOX treatment. (b2) Summary data for excitability. (c) Summary data for input resistance. (d) Summary data for firing threshold. (e) Summary data for resting membrane potential. Data are plotted as mean \pm SEM; * $p < 0.05$. * with brackets indicates main effects of treatment whereas * over specific time points indicate significant differences as determined by pairwise post-hoc comparisons. $n = 10$ at 24 h and $n = 9$ at 48 h for both treatment groups. Each n represents an average of 2 - 5 cells that compose a single dish. If multiple dishes from the same animal were given the same treatment, the averages responses from those

dishes were averaged to obtain a single n. Therefore, each n represents an average response from SNs from a single animal. DOX produced a persistent increase in excitability and decrease in firing threshold lasting at least 48 h. DOX also produced an increase in input resistance at 24 h.

For the groups of SNs shown in Fig. 13, there were no differences among the average pre-test measures of input resistance ($t_{(18)} = 0.24$; $p = 0.81$), firing threshold ($t_{(18)} = 0.92$; $p = 0.37$), or resting potential ($t_{(18)} = 1.90$; $p = 0.07$) (Table 1). While there was a trend towards a difference among the Veh- and DOX-treated SNs in pre-test measures of resting potential, the difference in means was less than 2 mV (Table 1) and likely has no physiological significance.

	Input Resistance (MΩ)	Firing Threshold (nA)	Resting Potential (mV)
Veh (n = 10)	93.8 \pm 38.6	0.42 \pm 0.07	-51.1 \pm 0.8
DOX (n = 10)	89.3 \pm 45.7	0.45 \pm 0.06	-49.3 \pm 0.6
p-value	0.81	0.37	0.07

Table 1. Pre-test (before treatment) measures of biophysical properties for groups in Fig. 13. There were no significant differences between the Veh and DOX groups in average measures of input resistance, firing threshold, and resting potential prior to treatment. Data are represented as mean \pm SEM. p-values are the result of unpaired, two-tailed t-tests.

In summary, a single 2-h application of DOX, a treatment that caused a deficit in synaptic plasticity (Liu et al. 2014), produced persistent increases in excitability, input resistance, and a long-lasting decrease in firing threshold of SNs.

The effects of 5-HT on the biophysical properties of SNs over time

The standard 5-HT protocol also increases SN excitability 24 h after treatment (Dale et al. 1987; Liu et al. 2011, 2014). We next asked how the biophysical changes induced by DOX (Fig. 13) compare to changes induced by 5-HT. The effects of the standard 5-HT (50 μ M) protocol on SN excitability, input resistance, firing threshold, and resting membrane potential were examined 24 and 48 h after treatment (Fig. 14a). The standard 5-HT protocol produced a long-term increase in excitability that lasted for at least 48 h (Fig. 14b1 and Fig. 14b2). The excitability of 5-HT-treated SNs was $225.7 \pm 24.2\%$ ($n = 6$) of pretest level at 24 h and $217.4 \pm 51.2\%$ ($n = 4$) of pretest level at 48 h compared to only $113.0 \pm 5.3\%$ ($n = 7$) and $118.7 \pm 19.9\%$ ($n = 5$) of pretest levels at 24 and 48 h, respectively, for Veh-treated SNs. A two-way ANOVA revealed a main effect of treatment ($F_{(1,18)} = 18.21$; $p < 0.001$) but not of time ($F_{(1,18)} = 0.0029$; $p = 0.96$) and no interaction of treatment with time ($F_{(1,18)} = 0.080$; $p = 0.78$). Pairwise post-hoc comparisons revealed significant differences in excitability between Veh- and 5-HT-treated SNs 24 h ($p = 0.002$) and 48 h ($p = 0.019$) after treatment.

The standard 5-HT protocol caused a trend towards increased input resistance (Fig. 14c). The input resistance of 5-HT treated SNs was $109.6 \pm 7.6\%$ ($n = 6$) of pretest level at 24 h but only $96.7 \pm 18.5\%$ ($n = 4$) of pretest level at 48 h compared to 88.1 ± 5.3 ($n = 7$) and $79.3 \pm 8.6\%$ ($n = 5$) of pretest levels at 24 and 48 h, respectively,

for Veh-treated SNs. A two-way ANOVA revealed a strong trend towards a main effect of treatment ($F_{(1,18)} = 4.20$; $p = 0.055$) but no main effect of time ($F_{(1,18)} = 1.31$; $p = 0.27$) and no interaction of treatment with time ($F_{(1,18)} = 0.048$; $p = 0.83$). An unpaired, two-tailed t-test revealed a significantly greater average input resistance in 5-HT-treated SNs compared to Veh-treated SNs at 24 h ($t_{(11)} = 2.37$; $p = 0.037$) in support of the trend observed with the two-way ANOVA.

The standard 5-HT protocol produced a persistent decrease in firing threshold (Fig. 14d). The firing threshold of 5-HT-treated SNs decreased by 0.11 ± 0.026 nA ($n = 6$) at 24 h and by 0.063 ± 0.055 nA ($n = 4$) at 48 h compared to increases of 0.0079 ± 0.016 nA ($n = 7$) and 0.053 ± 0.041 nA ($n = 5$) at 24 and 48 h, respectively, in Veh-treated SNs. A two-way ANOVA revealed a main effect of treatment ($F_{(1,18)} = 12.45$; $p = 0.002$) but no main effect of time ($F_{(1,18)} = 1.88$; $p = 0.19$) and no interaction of treatment with time ($F_{(1,18)} = 0.00011$; $p = 0.99$). Pairwise post-hoc comparisons revealed a significantly lower firing threshold in 5-HT-treated SNs compared to Veh-treated SNs at 24 h ($p = 0.013$) and 48 h ($p = 0.034$).

Lastly, the standard 5-HT protocol appeared to promote a slightly more hyperpolarized resting membrane potential relative to Veh treatment (Fig. 14e). 5-HT treatment resulted in a slight hyperpolarization of 0.19 ± 1.65 mV ($n = 6$) at 24 h and a slight depolarization of 1.79 ± 1.04 mV ($n = 4$) at 48 h compared to pretest measures of resting membrane potential. Veh treatment resulted in a depolarization of 2.95 ± 0.64 mV ($n = 7$) at 24 h and 4.12 ± 1.70 mV ($n = 5$) at 48 h compared to pretest measures of resting membrane potential. A two-way ANOVA revealed a strong trend towards a main effect of treatment ($F_{(1,18)} = 4.19$; $p = 0.056$), but no apparent main

effect of time ($F_{(1,18)} = 1.40$; $p = 0.25$) or interaction of treatment with time ($F_{(1,18)} = 0.092$; $p = 0.77$).

For the SNs examined in Fig. 14, there were no differences between the groups in average pre-test measures of input resistance ($t_{(11)} = 0.10$; $p = 0.34$), firing threshold ($U = 9.0$; $p = 0.10$), or resting potential ($t_{(11)} = 0.010$; $p = 0.92$) (Table 2).

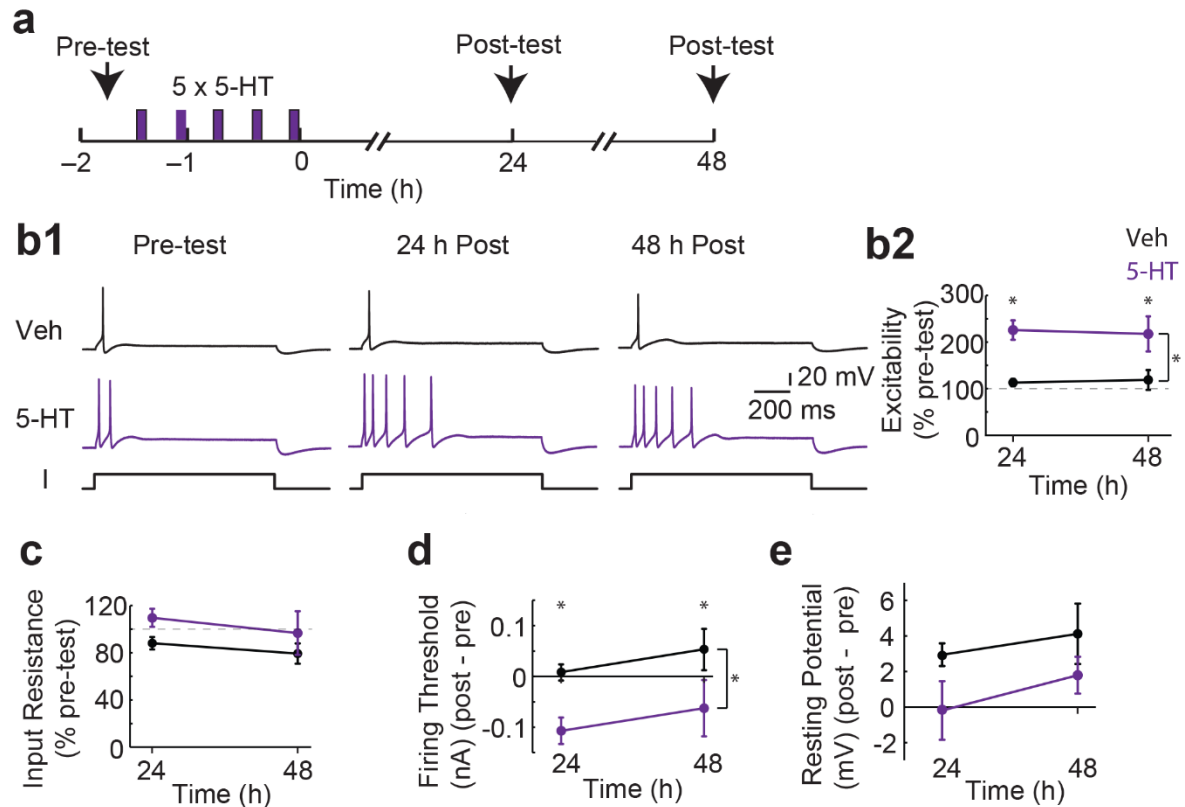


Figure 14. The standard 5-HT protocol produced persistent changes in the biophysical properties of SNs. (a) Protocol for application of 5-HT relative to the pre- and post-test measurements of biophysical properties. Arrows represent recording times. (b1) Representative action potentials elicited by a constant current injection (I) before (Pre-test) and after (24 h Post and 48 h Post) Veh or 5-HT treatment. (b2) Summary data for excitability. (c) Summary data for input resistance. (d) Summary data for firing threshold. (e) Summary data for resting membrane potential. The standard 5-HT protocol produced a long-term increase in excitability and long-term decrease in firing threshold lasting at least 48 h. Data are plotted as mean \pm SEM; * $p < 0.05$. * with brackets indicates main effects of treatment whereas * over specific time points indicates significant differences as determined by pairwise post-hoc comparisons. $n = 6 - 7$ at 24 h and $n = 4 - 5$ at 48 h. Each n represents an

average of 2 - 5 cells that compose a single dish. If multiple dishes from the same animal were given the same treatment, the averages responses from those dishes were averaged to obtain a single n. Therefore, each n represents an average response from SNs from a single animal.

	Input Resistance (MΩ)	Firing Threshold (nA)	Resting Potential (mV)
Veh (n = 7)	94.9 \pm 9.8	0.35 (0.30 - 0.40)	-48.3 \pm 1.0
5-HT (n = 6)	77.7 \pm 14.7	0.42 (0.38 - 0.46)	-48.2 \pm 1.1
p-value	0.34	0.10	0.92

Table 2. Pre-test (before treatment) measures of biophysical properties for groups in Fig. 14. There were no significant differences between the Veh and 5-HT groups in average measures of input resistance, firing threshold, and resting potential prior to treatment. Input resistance and resting potential data are represented as mean \pm SEM. Firing threshold average is represented as median (interquartile range). p-values are the result of unpaired, two-tailed t-tests for input resistance and resting potential. Because the firing threshold data do not pass normality, a Mann-Whitney rank sum test was administered.

In summary, the standard 5-HT protocol, an analog of LTS training, produced a persistent increase in excitability and decrease in firing threshold, as well as trends toward an increase in input resistance and hyperpolarization of the resting membrane potential relative to Veh treatment (Fig. 14). These changes were very similar to the changes that occurred after DOX treatment (Fig. 13). The finding that both DOX and 5-HT produce similar biophysical changes including excitability suggests that DOX may enhance 5-HT-induced LTEE. Alternatively, DOX may impair 5-HT-induced LTEE given that it prevents 5-HT-induced LTF (Liu et al. 2014).

The effects of DOX treatment on 5-HT-induced LTEE

We next determined whether DOX enhances or impairs 5-HT-induced LTEE. 1 μ M 5-HT was used to prevent saturation. In *Aplysia*, concentrations of 5-HT between 10 and 50 μ M appear saturating in regards to PKA activity (Müller and Carew 1998) and synaptic facilitation (Liu et al. 2014). 1 μ M 5-HT produces LTF, but the magnitude is approximately one-third the magnitude of LTF produced by 50 μ M 5-HT (Liu et al. 2014). Therefore, in order to determine whether the effects of DOX and 5-HT were additive, 1 μ M 5-HT was used. SN excitability was measured immediately prior to treatment (pre-test) and 24 after treatment (post-test) in 4 groups: 1) Veh, 2) 1 μ M 5-HT, 3) 2.5 μ M DOX alone, and 4) 5-HT + DOX (see Fig. 15a and Fig. 15b1 for protocol and representative traces). The excitability level produced by 5-HT alone was 170.9% (154.2 to 175%) (median (interquartile range)) (n = 6) of pre-test at 24 h. The excitability level of DOX-treated SNs was 122.9% (103.1 to 164.6%) (n = 6) of pretest level. The combination of 5-HT + DOX led to an excitability level of 143.8% (118.8 to

178.1%) ($n = 6$) compared to pre-test. Veh treatment led to no apparent change in excitability (100 to 109.4%) ($n = 6$) (Fig. 15b2). A Kruskal-Wallis one-way ANOVA on ranks revealed a significant difference among the four groups ($H = 9.16$, $df = 3$, $p = 0.027$). Post hoc comparisons revealed that DOX alone produced a significant increase in SN excitability 24 h after treatment compared to Veh treatment (DOX vs. Veh: difference of ranks = 37; $q = 4.189$, $p < 0.05$). 5-HT alone also significantly increased excitability 24 h after treatment compared to Veh treatment (5-HT vs. Veh: difference of ranks: 71; $q = 4.099$, $p < 0.05$). 5-HT-induced LTEE appeared attenuated by DOX but this effect was not statistically significant (5-HT + DOX vs. 5-HT: difference of ranks = 19; $q = 2.151$, $p > 0.05$).

For the groups of SNs examined in Fig. 15, there were no differences among the average pre-test measures of input resistance ($F_{(3,20)} = 0.25$; $p = 0.86$), firing threshold ($F_{(3,20)} = 0.37$; $p = 0.78$), or resting potential ($F_{(3,20)} = 1.46$; $p = 0.26$) (Table 3).

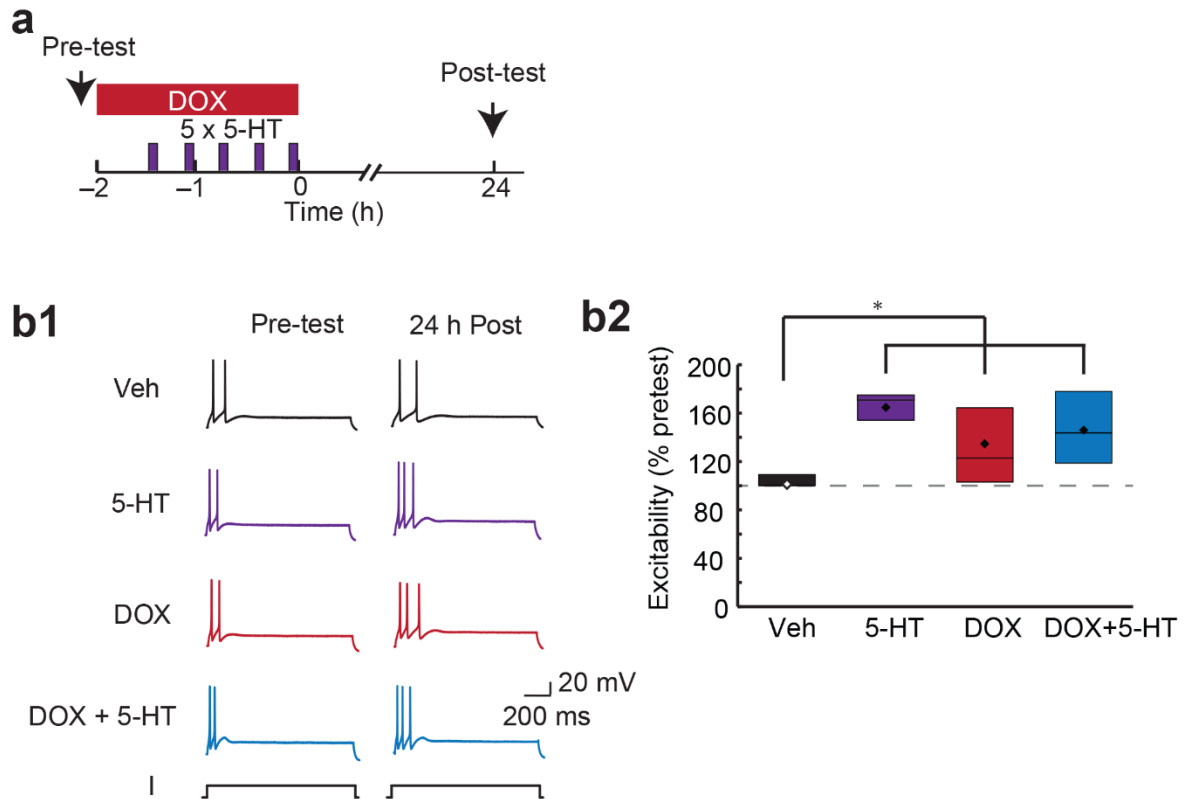


Figure 15. 5-HT does not potentiate the DOX-induced basal increase in excitability. (a) Protocol for DOX application with 5-HT or Veh. (b1) Examples of action potentials recorded immediately prior to (Pre-test) and 24 h after (24 h Post) treatment. (b2) Summary data. Data are represented as median (interquartile range). Significant differences from the Veh group are indicated by * for $p < 0.05$. Diamond markers represent means. $n = 6$. Each n represents an average of 2 - 5 cells that compose a single dish. If multiple dishes from the same animal were given the same treatment, the averages responses from those dishes were averaged to obtain a single n . Therefore, each n represents an average response from SNs from a single animal.

Figure adapted from: Liu RY, Zhang Y, Coughlin BL, Cleary LJ, Byrne JH (2014). Doxorubicin attenuates serotonin-induced long-term synaptic facilitation by

phosphorylation of p38 mitogen-activated protein kinase. *J. Neurosci.* 34: 13289-13300. I am an original author on this article, and therefore do not need to obtain permission from *The Journal of Neuroscience* for its noncommercial use, per *J. Neurosci.* policy.

	Input Resistance (MΩ)	Firing Threshold (nA)	Resting Potential (mV)
Veh (n = 6)	139.6 ± 19.0	0.47 ± 0.06	-50.8 ± 1.3
5-HT (n = 6)	128.4 ± 15.0	0.53 ± 0.06	-48.4 ± 0.9
DOX (n = 6)	122.4 ± 13.5	0.53 ± 0.04	-49.1 ± 0.6
DOX + 5-HT (n= 6)	133.2 ± 8.6	0.48 ± 0.03	-48.1 ± 1.1
p-value	0.86	0.78	0.26

Table 3. Pre-test (before treatment) measures of biophysical properties for groups in Fig. 15. There were no significant differences among the Veh, 5-HT, DOX, and DOX + 5-HT groups in average measures of input resistance, firing threshold, and resting potential prior to treatment. Data are represented as mean ± SEM. p-values are the result of a one-way ANOVA.

Conclusion

These results clearly indicate that an acute treatment with DOX has a powerful and persistent effect on neuronal excitability (Fig. 13b2) that extends beyond the period of elevated kinase phosphorylation (Fig. 4). Consistent with enhanced basal excitability, DOX also induced an increase in input resistance and a decrease in firing threshold of SNs (Fig. 13c and Fig. 13d). Together, these changes promote an increase in firing probability by cells upon stimulation. These biophysical alterations by DOX are similar to changes observed during memory formation (Moyer, Thompson and Disterhoft 1996; Mozzachiodi et al., 2008) and after the standard 5-HT protocol (Fig. 14; Dale et al. 1987; Liu et al. 2011, 2014), an analog of LTM training. Even the time courses were similar between the two treatments for each biophysical property, although only two time points were examined. Excitability and firing threshold endured for at least 48 h whereas the input resistance changes were shorter lived (Fig. 13 and Fig. 14). The investigation of more time points would help determine differences between the two treatments.

These findings led to the hypothesis that DOX would enhance 5-HT-induced LTEE, although DOX may impair LTEE as it did LTF (Liu et al. 2014). Indeed, DOX did not potentiate LTEE produced by 5-HT (Fig. 15). This experiment employed a lower concentration of 5-HT (1 μ M) than the earlier 5-HT experiment (50 μ M, Fig. 14), to avoid saturation of the underlying biochemical pathways by 5-HT. Indeed 1 μ M 5-HT increased excitability by approximately 70% compared to pre-test (Fig. 15) and 50 μ M 5-HT caused a 125% increase in excitability relative to pre-test (Fig. 14b2). This finding agrees qualitatively with the effects of 5-HT concentration on LTF (Liu et al.

2014), but the differences in changes in EPSP magnitude between the two concentrations of 5-HT are greater than for LTEE. 1 μ M 5-HT produces an average change in EPSP that is approximately one-third the magnitude of the average change in EPSP produced by 50 μ M 5-HT (Liu et al. 2014). For LTEE, 1 μ M 5-HT produced an average increase in excitability that is just over half the average increase produced by 50 μ M 5-HT (Fig. 14b2 and Fig. 15). This finding suggests that 5-HT-induced LTEE and LTF may not be interchangeable readouts of LTS.

In line with the idea of divergence between LTEE and LTF, DOX completely blocks 5-HT-induced LTF, as 5-HT treatment is no different from control (Veh) treatment (Liu et al. 2014). However, DOX produces a basal increase in excitability that appears to prevent any additional enhancement by 5-HT (Fig. 13b2 and Fig. 15). The basal increase in excitability by DOX may occlude any change in excitability promoted by 5-HT treatment. This finding is perplexing given that it is not due to a ceiling effect. Average excitability levels can increase by at least 125% (2.25 fold) compared to pre-test with a higher concentration of 5-HT (Fig. 14b2), and the increase in excitability produced by DOX in combination with the lower concentration of 5-HT is only about 44% (1.44 fold) compared to pre-test (Fig. 15).

Results presented here for 5-HT-treated SNs are comparable to results from previous studies. First, LTS training produces a doubling of the median number of spikes elicited by a test current injection (2 nA, 1 s) into SNs (Cleary et al. 1998) when a comparison is made between SNs from trained and untrained (control) sides of animals. While SNs from Cleary et al. (1998) were not isolated from their postsynaptic contacts and were exposed to the effects of LTS training which include the release of

endogenous 5-HT rather than exogenous application of 5-HT, the magnitude of the change in excitability falls between the average change produced by 1 μ M 5-HT (Fig. 15) and 50 μ M 5-HT (Fig. 14b2) in isolated SNs in culture. Furthermore, the magnitude of the change in excitability produced by 50 μ M 5-HT at 24 h reported here (125% increase compared to pre-test, Fig. 14b2) is comparable to the magnitude change reported by Liu et al. (2011) using the same concentration (170% increase compared to pre-test) in isolated SNs in culture. In addition, the change in excitability produced by 1 μ M 5-HT at 24 h (Fig. 15) is comparable to the change reported by Dale et al. (1987) at the same concentration using similar magnitudes of test current injections in isolated SNs. 5-HT produced a trend towards an increase in input resistance at 24 h (Fig. 14c) as was also reported by Dale et al. (1987). These comparisons highlight the reproducibility of the effects of 5-HT on isolated SNs and their similarity to *in vivo* changes in SN excitability implicated in memory formation.

However, the data presented here have one notable inconsistency with the Liu et al. (2011) LTEE study. Liu et al. (2011) found that 5-HT-induced LTEE is evident 24 h after treatment but only a trend towards increased excitability was reported at 48 h. My investigations have shown that 5-HT-induced LTEE can last for at least 48 h (Fig. 14b2). *In vivo* experiments would be necessary to determine the duration of LTEE produced by behavioral training. Furthermore, it suggests that electrophysiological data beyond 24 h in cultured isolated SNs may be too variable to perform detailed mechanistic studies. During the course of my studies, I observed much more variability in electrophysiological responses \geq 48 h after treatments than

at 24 h. Therefore, subsequent electrophysiological studies reported in this dissertation will focus on the 24-h time point.

**Chapter 5: Doxorubicin-induced persistent changes in basal excitability
depend on early ERK activity, but not p38 MAPK activity.**

Introduction

In addition to the role of ERK in modulating synaptic strength, ERK enhances neuronal excitability (Adams and Sweatt 2002; Chin et al. 2006; Cohen-Matsliah et al. 2007; Rosenkranz et al. 2009; Sung et al. 2001). Activation of ERK is sufficient to induce long-lasting changes in excitability of *Aplysia* SNs. Specifically, injection of active ERK into SNs results in enhanced excitability 24 h later (Sung et al. 2001). In addition, I have found that application of NSC 295642, a MAPK phosphatase-3 (MKP-3) inhibitor, induced an increase in excitability 24 h after treatment (Fig. 16) (Veh, $75.8 \pm 5.6\%$, $n = 7$; NSC, $102.9 \pm 6.3\%$, $n = 5$; $t_{(10)} = 3.2$, $p = 0.009$). MKP-3 dephosphorylates and inactivates MAPKs but has greater specificity for ERK than p38 MAPK (Camps et al. 2000). The particular concentration and duration of treatment chosen for this experiment ($0.01 \mu\text{M}$, 2 h) enhances phosphorylation of ERK in *Aplysia* SNs without affecting levels of phosphorylation of p38 MAPK (Liu et al. 2017). ERK activation is also required for enhanced long-term excitability mediated by application of transforming growth factor beta 1 (TGF- β 1) in SNs, as evidenced by the ability of the MEK inhibitor U0126 to block this form of excitability (Chin et al. 2006). In this study, transient activation of ERK (returned to basal levels before the removal of TGF- β 1) was sufficient to enhance excitability 24 h later (Chin et al. 2006). Based on these findings, it is possible that the basal increase in excitability depends on ERK activity during DOX treatment.

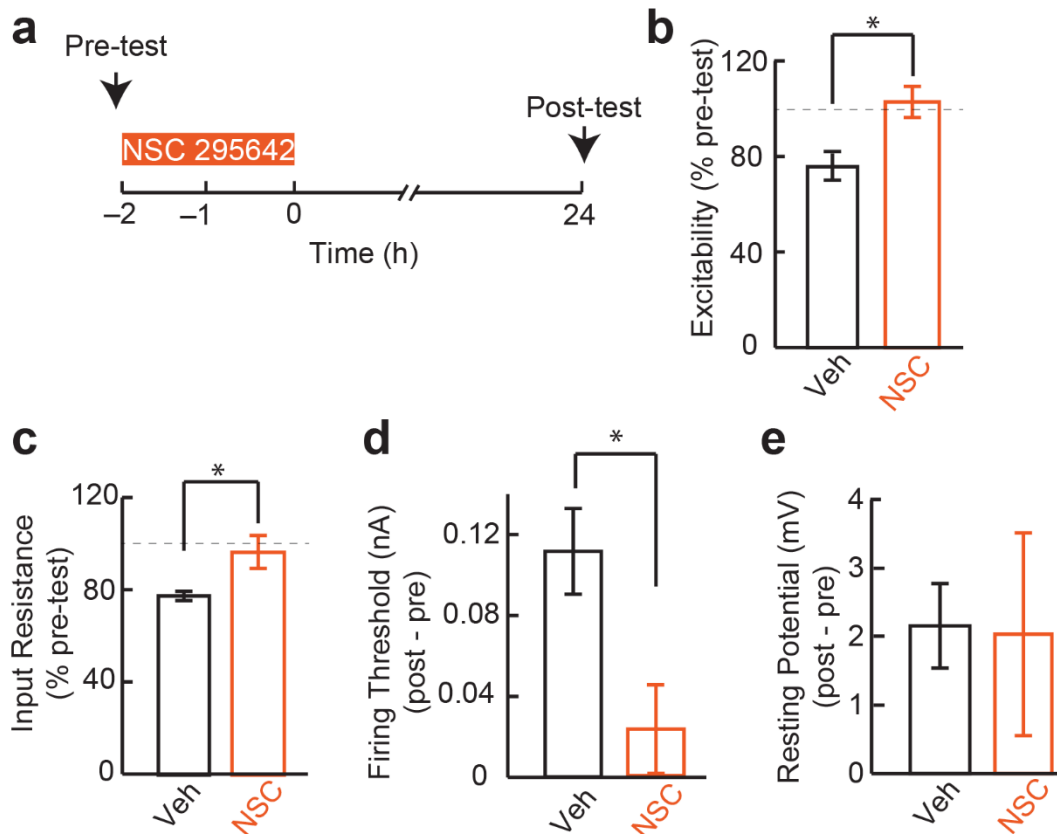


Figure 16. A single brief application of the MKP-3 inhibitor NSC 295642 induced a persistent increase in excitability of SNs. (a) Protocol for application of NSC 295642 (or Veh) and measurement of excitability before and 24 h after the end of treatment. Arrows represent recording times. (b) Summary data for excitability. (c) Summary data for input resistance. (d) Summary data for firing threshold. (e) Summary data for resting potential. NSC 295642 caused a persistent increase in excitability and input resistance, and a decrease in firing threshold, presumably due to its ability to enhance levels of pERK. Data are plotted as mean \pm SEM; * represents $p \leq 0.05$. $n = 5 - 7$. Each n represents an average of 2 - 5 cells that compose a single dish. If multiple dishes from the same animal were given the same treatment, the

averages responses from those dishes were averaged to obtain a single n . Therefore, each n represents an average response from SNs from a single animal.

The role of p38 MAPK in excitability is unclear. p38 MAPK has been implicated in suppression of excitability in CA1 pyramidal and cerebellar neurons (Poolos, Bullis & Roth 2006; Ster et al. 2007) but also in the hyperexcitability of CA1 pyramidal and dorsal root ganglion neurons under certain pathological conditions (Hudmon et al. 2008; Jin & Gereau 2006; Zhang et al. 2010). The role of p38 MAPK in *Aplysia* SN excitability has not been investigated. Because p38 MAPK is known to activate CREB2 (Guan et al. 2002, 2003), which represses CREB1-mediated transcription (Bartsch et al. 1995), it is predicted that activation of p38 MAPK would oppose any enhancement of excitability mediated by pathways that converge on CREB1, such as ERK or PKA. Given that DOX leads to enhanced levels of activated ERK and p38 MAPK during and briefly after treatment (Fig. 4; Liu et al. 2014), it is difficult to explain the enhanced basal excitability observed 24 h later (Fig. 13 and Fig. 15). It could be that the DOX-induced enhancement of basal excitability is actually a result of the late phase of ERK activity at 24 h, or it could be that the excitability is induced by the early ERK activation but that the increase would be even greater if DOX-induced p38 MAPK activity was reduced. Indeed, blockade of p38 MAPK activity with the inhibitor SB 203580 prevents DOX-induced deficits in LTF (Liu et al. 2014), suggesting that SB 203580 may enhance DOX-mediated excitability. A third possibility is that p38 MAPK mediates the enhancement of excitability by DOX. This possibility should not be overlooked due to the absence of data on the effect of p38 MAPK on SN excitability.

It is of particular interest to determine if the DOX-induced increase in basal neuronal excitability depends upon ERK and/or p38 MAPK activation. It is predicted that the basal increase in excitability observed 24 h after DOX depends upon ERK

activation and that inhibition of p38 MAPK would enhance DOX-mediated excitability. These experiments will also shed light on the role of p38 MAPK in SN excitability.

Results

To test the hypothesis that MEK inhibition during DOX treatment will block persistent excitability, four groups were employed: (1) Veh; (2) U0126; (3) DOX; and (4) U0126 + DOX (see Fig. 17a and Fig. 17b1 for protocol and representative traces for each group). DOX led to an excitability level of $165.5 \pm 14.7\%$ ($n = 7$) compared to pre-test level, but the combination of U0126 + DOX led to an excitability level of only $117.6 \pm 8.4\%$ ($n = 6$) compared to pre-test. The excitability of Veh- and U0126-treated SNs were $109.2 \pm 8.4\%$ ($n = 8$) and $124.2 \pm 11.2\%$ ($n = 7$), respectively (Fig. 17b2). A two-way ANOVA revealed a significant main effect of DOX ($F_{(1,24)} = 5.04$; $p = 0.034$), as well as no basal effect of U0126 ($F_{(1,24)} = 2.2$; $p = 0.15$). The DOX-induced increase in excitability was blocked by application of U0126 (Interaction: DOX x U0126; $F_{(1,24)} = 8.07$; $p = 0.009$). There were no differences among the groups in average pre-test measures of input resistance ($F_{(3,24)} = 0.65$; $p = 0.59$), firing threshold ($F_{(3,24)} = 0.15$; $p = 0.93$), or resting potential ($F_{(3,24)} = 0.16$; $p = 0.92$) (Table 4). These results indicate that the DOX-induced long-lasting increase in excitability depends on MEK activation during DOX treatment.

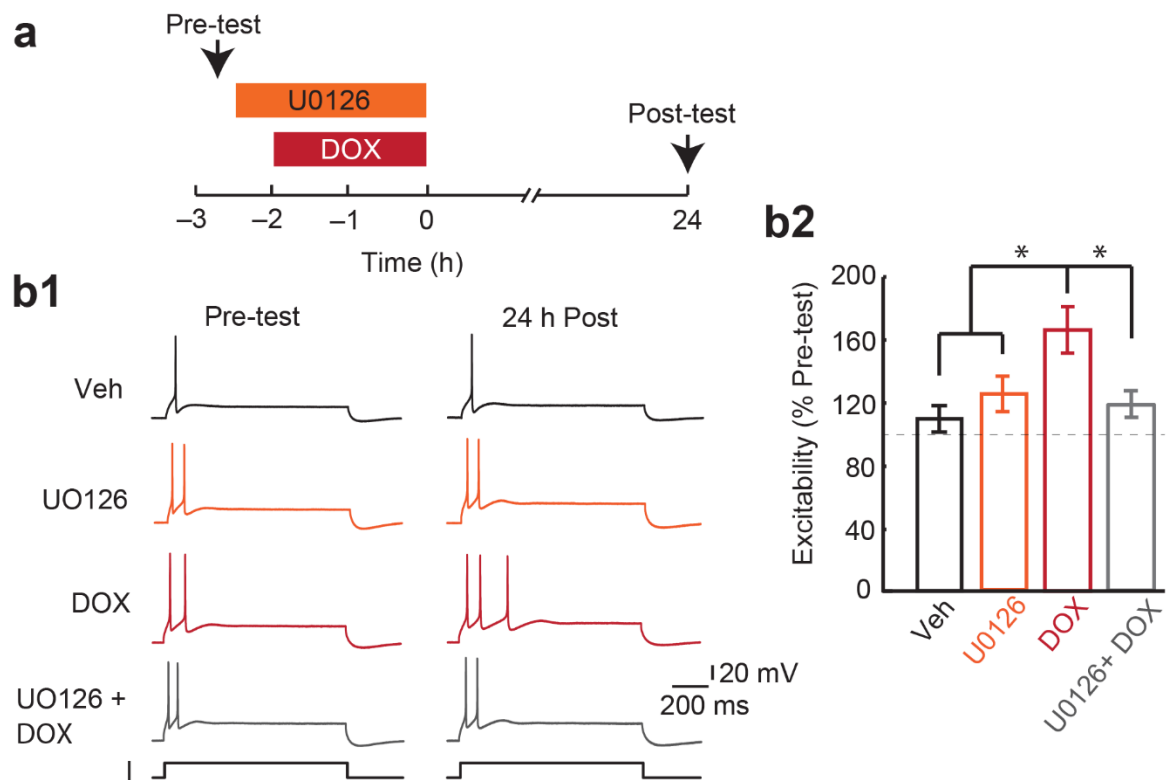


Figure 17. MEK inhibition during DOX treatment blocked the increase in basal excitability at 24 h. (a) Protocol for application of U0126 and DOX and measurement of excitability 24 h after the end of treatment. Arrows represent recording times. (b1) Examples of action potentials recorded prior to treatment (Pre-test) and 24 h after the end of treatment (24 h Post). (b2) Summary data. The DOX-induced persistent increase in excitability depended on MEK activation. Data are plotted as mean \pm SEM; * represents $p \leq 0.05$. $n = 6 - 8$. Each n represents an average of 2 - 5 cells that compose a single dish. If multiple dishes from the same animal were given the same treatment, the averages responses from those dishes were averaged to obtain a single n . Therefore, each n represents an average response from SNs from a single animal.

	Input Resistance (MΩ)	Firing Threshold (nA)	Resting Potential (mV)
Veh (n = 8)	153.2 \pm 17.1	0.45 \pm 0.03	-47.6 \pm 0.4
U0126 (n = 7)	144.1 \pm 12.4	0.47 \pm 0.03	-47.7 \pm 0.8
DOX (n = 7)	127.5 \pm 6.9	0.48 \pm 0.04	-48.2 \pm 1.2
U0126 + DOX (n= 6)	146.4 \pm 15.2	0.48 \pm 0.04	-47.4 \pm 0.8
p-value	0.59	0.93	0.92

Table 4. Pre-test (before treatment) measures of biophysical properties for groups in Fig. 17. There were no significant differences among the Veh, U0126, DOX, and U0126 + DOX groups in average measures of input resistance, firing threshold, and resting potential prior to treatment. Data are represented as mean \pm SEM. p-values are the result of a one-way ANOVA.

The effect of MEK inhibition during DOX treatment on other biophysical properties are presented in Table 5. As observed previously (Fig. 13c), DOX produced a significant increase in input resistance compared to Veh treatment at 24 h ($F_{(1,24)} = 7.0$; $p = 0.014$), but this effect was not reversed by application of U0126 (U0126 \times DOX, $F_{(1,24)} = 0.82$; $p = 0.37$). In agreement with previous experiments (Fig. 13d), DOX also decreased the firing threshold of SNs, although a two-way ANOVA only revealed a trend toward a main effect of DOX ($F_{(1,24)} = 3.48$; $p = 0.074$). However, an unpaired, two-tailed t-test revealed a significant difference in the change in firing threshold between DOX- and Veh-treated SNs ($t_{(13)} = 2.81$; $p = 0.015$). The DOX-induced decrease in firing threshold was reversed by application of U0126 (U0126 \times DOX, $F_{(1,24)} = 4.47$; $p = 0.045$). DOX did not affect resting membrane potential (DOX, $F_{(1,24)} = 0.31$; $p = 0.59$). No main effects of U0126 were observed for any of the measured biophysical properties (Input resistance, $F_{(1,24)} = 0.075$, $p = 0.79$); Firing threshold, $F_{(1,24)} = 1.06$, $p = 0.31$; Resting membrane potential, $F_{(1,24)} = 1.87$, $p = 0.18$), suggesting that basal MEK inhibition does not alter properties of SNs. In summary, application of U0126 during DOX treatment prevented the DOX-induced changes in excitability and firing threshold but not input resistance.

Treatment	n	Input Resistance (% pretest)	Firing Threshold (post - pretest) (nA)	Resting Potential (post - pretest) (mV)
Veh	8	88.3 ± 5.6	0.025 ± 0.02	0.73 ± 1.01
U0126	7	94.7 ± 3.4	0.007 ± 0.019	1.72 ± 0.80
DOX	7	107.6 ± 4.1	-0.042 ± 0.011	0.18 ± 0.34
U0126 + DOX	6	104.2 ± 8.2	0.011 ± 0.012*	1.38 ± 0.79

Table 5. Effects of the MEK inhibitor U0126 (20 μ M) on DOX-induced changes in biophysical properties of SNs. Application of U0126 during DOX treatment reversed the decrease in firing threshold but did not reverse the increase in input resistance observed 24 h after treatment. Data are represented as mean \pm SEM. *(p < 0.05) specifies a significant interaction of U0126 and DOX. In this case, this interaction indicates a reversal of a DOX-mediated change in the presence of U0126.

To determine whether p38 MAPK activation during DOX treatment influences excitability, four groups were employed: (1) Veh; (2) SB 203580; (3) DOX; and (4) SB 203580 + DOX (see Fig. 18a and Fig. 18b1 for protocol and representative traces for each group). DOX induced comparable levels of excitability regardless of the presence of SB 203580 (DOX: $141.7 \pm 8.3\%$, $n = 13$; SB 203580 + DOX: $141.4 \pm 12.6\%$, $n = 8$). The excitability of Veh- and SB 203580-treated SNs were $115.1 \pm 4.1\%$ ($n = 14$) and $111.6 \pm 10.1\%$ ($n = 8$), respectively (Fig. 18b2). A two-way ANOVA revealed a significant main effect of DOX ($F_{(1,39)} = 11.02$; $p = 0.002$), as well as no basal effect of SB 203580 ($F_{(1,39)} = 0.051$; $p = 0.82$). The DOX-induced increase in excitability was not affected by application of SB 203580 (DOX x SB 203580; $F_{(1,39)} = 0.033$; $p = 0.86$). There were no differences among groups in average pre-test measures of input resistance ($H = 0.83$, d.f. = 3; $p = 0.84$), firing threshold ($F_{(3,39)} = 0.19$; $p = 0.90$), or resting potential ($F_{(3,39)} = 0.35$; $p = 0.79$) (Table 6). These results show that the DOX-induced long-lasting increase in excitability does not rely on p38 MAPK activation during DOX treatment. These findings also suggest that p38 MAPK may not play a significant role in SN excitability in general.

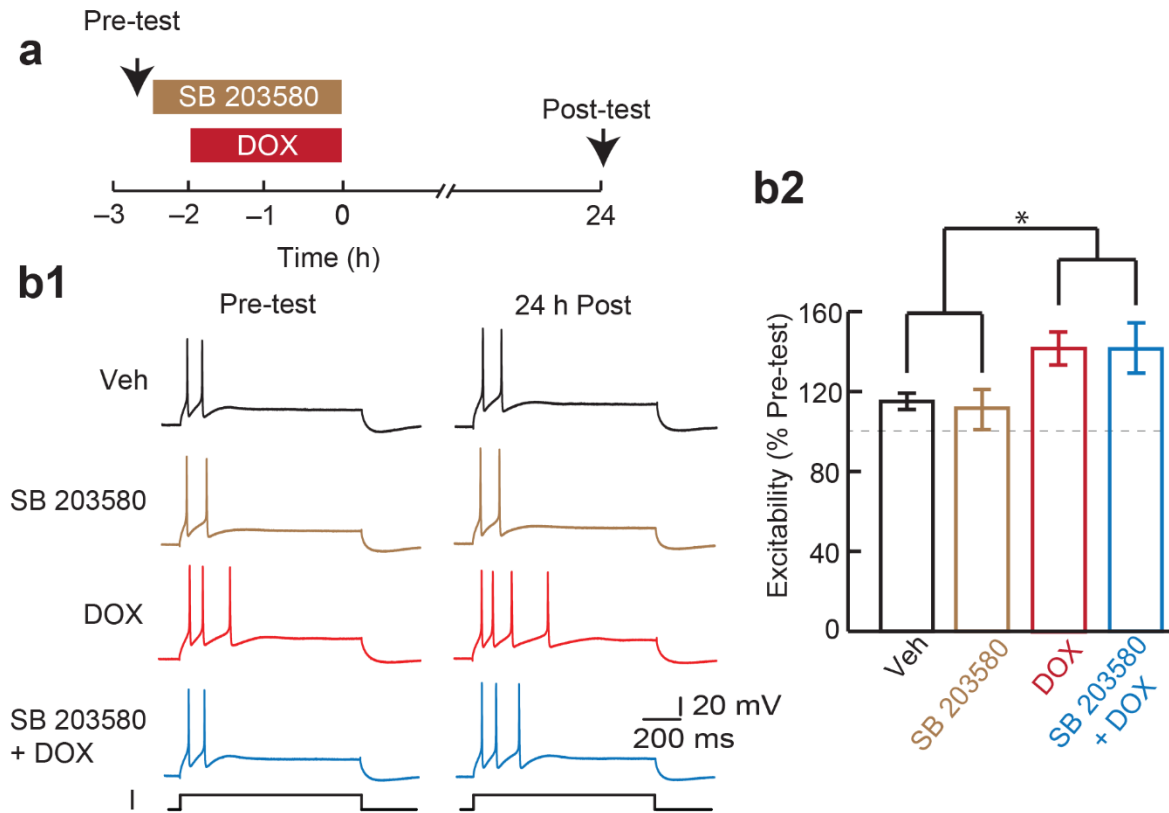


Figure 18. p38 MAPK inhibition during DOX treatment did not affect the persistent increase in basal excitability. (a) Protocol for application of SB 203580 and DOX and measurement of excitability 24 h after treatment. Arrows represent recording times. (b1) Examples of action potentials recorded prior to treatment (Pre-test) and 24 h after the end of treatment (24 h Post). (b2) Summary data. Data are plotted as mean \pm SEM; * represents $p \leq 0.05$. $n = 8 - 14$. Each n represents an average of 2 - 5 cells that compose a single dish. If multiple dishes from the same animal were given the same treatment, the averages responses from those dishes were averaged to obtain a single n . Therefore, each n represents an average response from SNs from a single animal.

	Input Resistance (MΩ)	Firing Threshold (nA)	Resting Potential (mV)
Veh (n = 14)	145.8 (118.8 – 167.8)	0.42 ± 0.02	-47.2 ± 0.7
SB 203580 (n = 8)	130.5 (107.5 – 156.2)	0.43 ± 0.03	-47.9 ± 0.6
DOX (n = 13)	135.7 (119.1 – 155.4)	0.44 ± 0.02	-47.9 ± 0.5
SB 203580 + DOX (n= 8)	131.4 (117.8 – 163.5)	0.42 ± 0.02	-47.3 ± 0.7
p-value	0.84	0.90	0.79

Table 6. Pre-test (before treatment) measures of biophysical properties for groups in Fig. 18. There were no significant differences among the Veh, SB 203580, DOX, and SB 203580 + DOX groups in average measures of input resistance, firing threshold, and resting potential prior to treatment. Data are represented as mean ± SEM for firing threshold and resting potential. Data for input resistance is represented as median (interquartile range). p-values for firing threshold and resting potential are the result of a one-way ANOVA. p-value for input resistance is from a Kruskal-Wallis one-way ANOVA on ranks.

Conclusion

The increase in excitability 24 h after DOX treatment depended on ERK but not p38 MAPK activation (Fig. 17 and Fig. 18). Therefore, in agreement with prior studies (Chin et al. 2006; Sung et al. 2001) as well as my own findings that the MKP-3 inhibitor NSC 295642 is sufficient to induce a long-term increase in excitability (Fig. 16), ERK activation was necessary to induce long-lasting changes in excitability of SNs by DOX. Similarly, MEK inhibition during DOX treatment reversed the decrease in firing threshold observed at 24 h (Table 5). MEK inhibition did not reverse the DOX-induced increase in input resistance (Table 5), suggesting an additional mechanism for the overall increase in excitability of the SNs. Another possibility is that the increase in input resistance 24 h after DOX treatment is produced by the MEK-independent enhanced ERK activation observed immediately after treatment (Fig. 9a). During this time, it appears that the enhanced ERK activity is mediated by a downregulation of MKP-1 (Fig. 8).

Unlike ERK, p38 MAPK activation was not necessary for the DOX-induced increase in basal excitability (Fig. 18). Thus, while p38 MAPK blocks 5-HT-induced LTF (Liu et al. 2014), p38 MAPK activation does not influence the basal presynaptic excitability (Fig. 18). It is possible that the p38 MAPK-mediated suppression of LTF depends on the postsynaptic MN. Indeed, several postsynaptic events are necessary for LTF induction (Glanzman 2008). Furthermore, some presynaptic changes associated with memory formation are thought to depend on retrograde signals from the postsynaptic MN (Glanzman 2008). Therefore, determining the effects of DOX on

the postsynaptic MN may be important for understanding the contrasting effects of p38 MAPK on SN excitability and synaptic facilitation.

Chapter 6: Doxorubicin-induced persistent changes in excitability and input resistance of sensory neurons are negatively correlated with late ERK activity.

Introduction

While the preceding chapter addressed the contribution of the early ERK and p38 MAPK activation by DOX to the persistent change in excitability, it did not address the late phase of ERK activation and its relation to the persistent excitability. Initially, it was thought that the late pERK and late excitability would be positively correlated when both measures are recorded from each SN, given the role of ERK in promoting excitability in these cells (Fig. 16 and Fig. 17; Chin et al. 2006; Sung et al. 2001). However, application of a MEK inhibitor during DOX treatment potentiated the late phase of ERK activation (Fig. 9b) and blocked the persistent increase in excitability (Fig. 17). From these findings, it is unclear what relation the late pERK will have with the late excitability in individual SNs. We therefore undertook the following series of experiments. Biophysical measurements from isolated SNs were made before and 24 h after DOX treatment, and then the SNs were fixed and pERK levels were measured. This allowed for correlation of biophysical properties with pERK level in the same SN at the same time point.

Results

Excitability vs. pERK

To understand the relation between late ERK activation and persistent excitability induced by DOX, correlations between these two phenomena were determined by measuring both excitability and pERK in individual SNs. For these experiments, I performed the electrophysiology and Dr. H. Lakshminarasimhan performed the immunostaining. We both contributed to the confocal imaging and analysis. Two

groups were included in this experiment: (1) Veh; and (2) DOX. SN excitability was measured before and 24 h after treatment, and cells were fixed immediately after the post-test to assess pERK levels (Fig. 19a). Veh-treated cells showed no correlation between excitability and pERK ($n = 32$; $r = 0.02$; $p = 0.9$), but DOX-treated cells exhibited a negative correlation between excitability and pERK ($n = 31$; $r = 0.41$; $p = 0.02$) (Fig. 19c). A negative correlation between excitability and pERK was not anticipated but highlights the inherent complexity of the relationship between the molecular and physiological events that arise from DOX exposure.

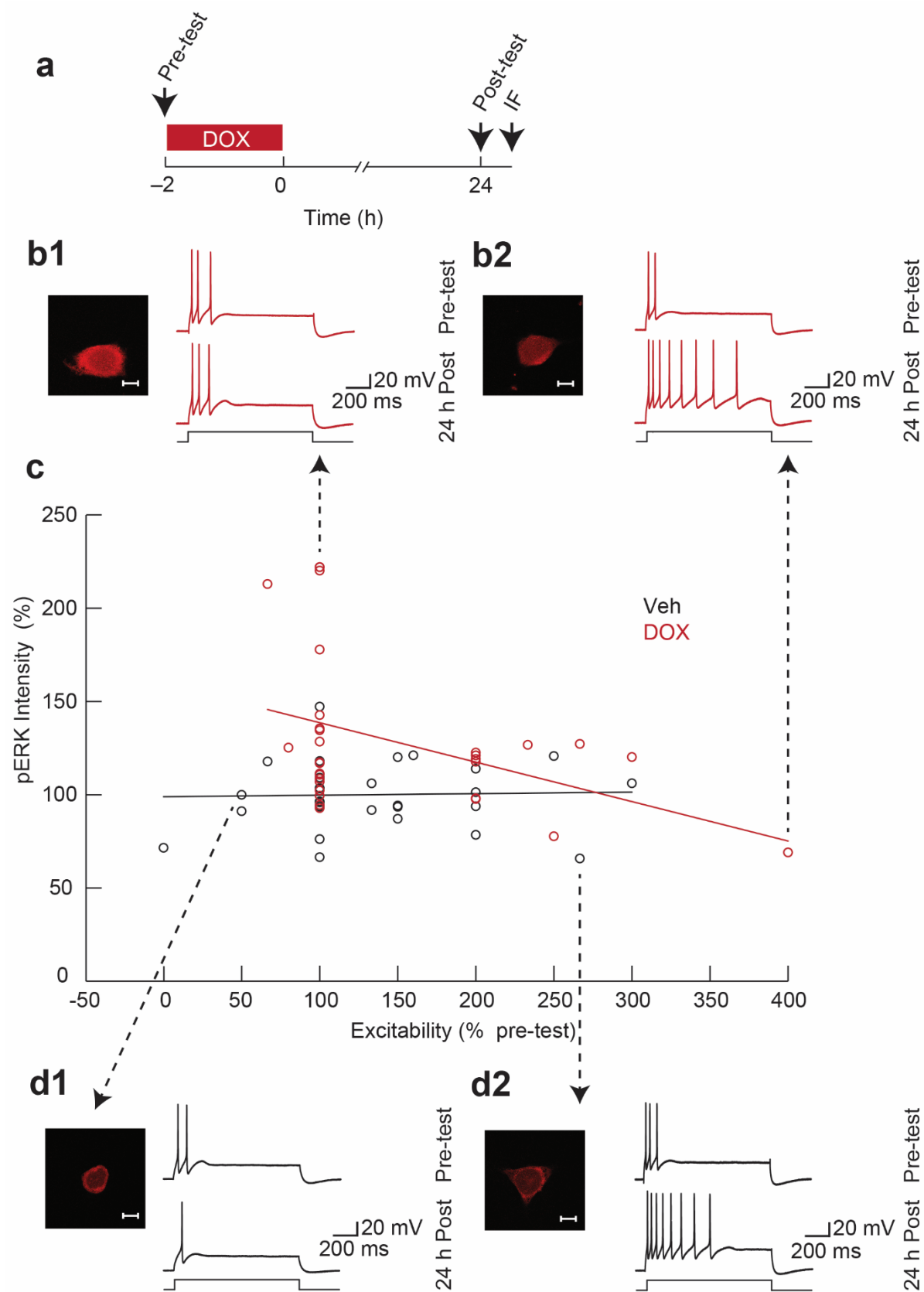


Figure 19. The DOX-induced increase in excitability and the late phase of ERK activation were negatively correlated.

(a) Protocol for application of DOX and measurement of excitability followed by fixation and IF staining as indicated by arrows. (b1) Representative confocal image of a DOX-treated SN (scale bar, 20 μ m) and the corresponding action potentials elicited prior to treatment (Pre-test) and 24 h after the end of treatment (24 h Post). This SN exhibited a relatively high level of pERK but no change in excitability. (b2) Representative confocal image of a DOX-treated SN (scale bar, 20 μ m) and corresponding action potentials. This SN exhibited a relatively low level of pERK but enhanced excitability. (c) Summary data. Open circles reflect the excitability (x-axis) and the level of pERK (y-axis, represented as percent of Veh) of individual SNs. (d1) Representative confocal image (scale bar, 20 μ m) and corresponding action potentials for a Veh-treated SN that exhibited a decrease in excitability. (d2) Representative confocal image (scale bar, 20 μ m) and the corresponding action potentials from a Veh-treated SN that exhibited an increase in excitability. pERK and excitability were negatively correlated in DOX-treated SNs but not in Veh-treated SNs. $n = 31 - 32$. Each n represents a single SN. SNs were obtained from numerous animals.

For this correlation experiment, I performed the electrophysiology and Dr. H. Lakshminarasimhan completed the immunostaining for pERK. We both contributed to the confocal imaging, analysis, and creation of the figure. pERK data and figure used with permission from Dr. H. Lakshminarasimhan.

Input resistance vs. pERK

DOX caused an increase in input resistance in SNs 24 h after treatment (Fig. 13c). Using the same population of SNs examined in Fig. 19, we determined whether the change in input resistance (represented as percent of pre-test input resistance) correlated with the pERK levels measured 24 h after DOX treatment. Two groups were included in this experiment: (1) Veh; and (2) DOX. SN input resistance was measured before and 24 h after treatment, and cells were fixed immediately after the post-test to assess pERK levels (Fig. 20a). The Veh-treated cells showed no correlation between input resistance and pERK ($n = 32$; $r = 0.14$; $p = 0.44$), but DOX-treated cells exhibited a negative correlation between input resistance and pERK levels ($n = 31$; $r = 0.37$; $p = 0.04$) (Fig. 20c). Both excitability and input resistance increased in response to DOX treatment (Fig. 13b2, Fig. 13c, and Fig. 15), and both of these properties were negatively correlated with pERK levels 24 h after the end of DOX treatment (Fig. 19 and Fig. 20).

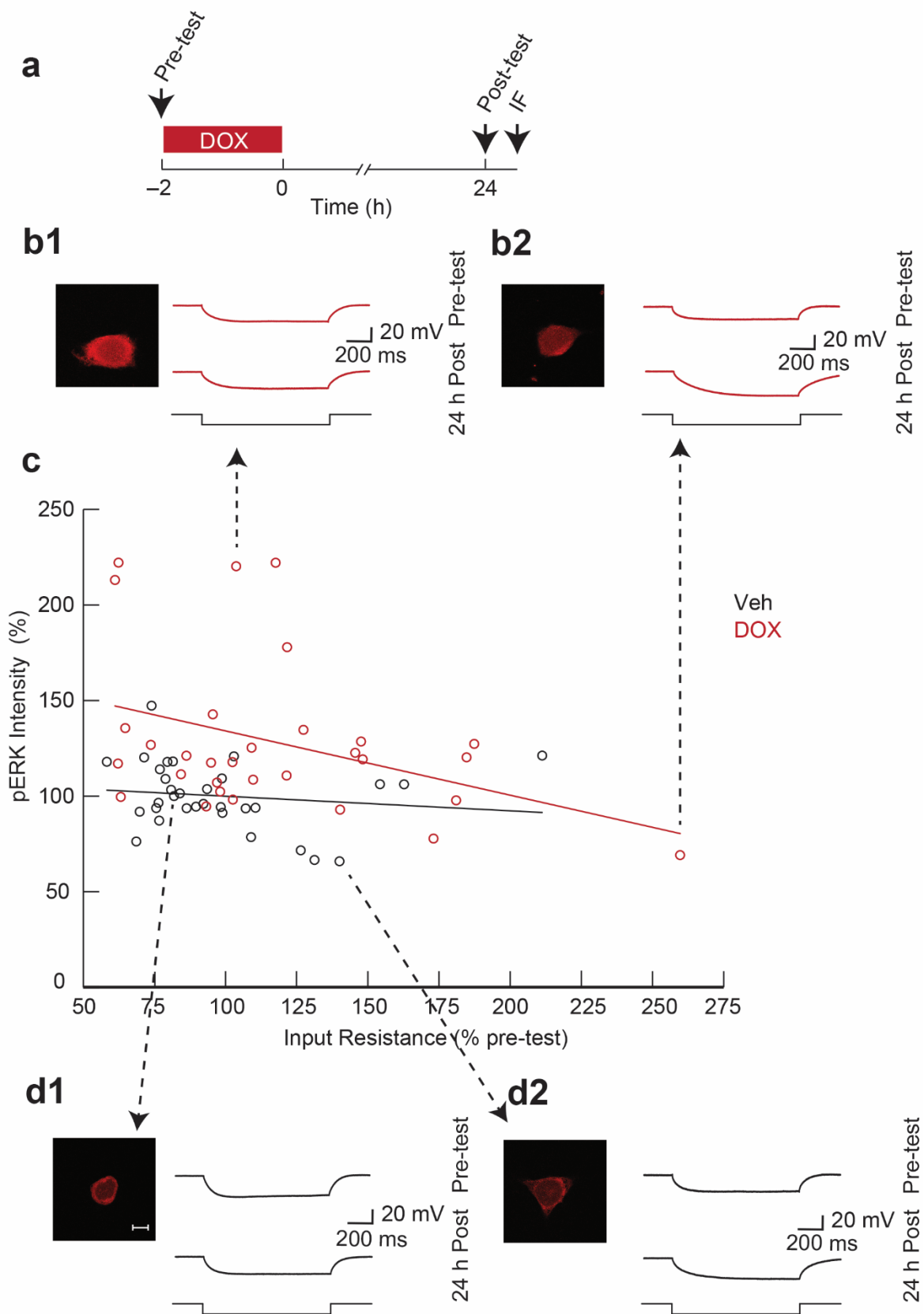


Figure 20. The DOX-induced increase in input resistance and the late phase of ERK activation were negatively correlated.

(a) Protocol for application of DOX and measurement of input resistance followed by fixation and IF staining as indicated by arrows. (b1) Representative confocal image of a DOX-treated SN (scale bar, 20 μ m) and the corresponding traces elicited by a hyperpolarizing current injection prior to treatment (Pre-test) and 24 h after the end of treatment (24 h Post). This SN exhibited a relatively high level of pERK but no change in input resistance. (b2) Representative confocal image of a DOX-treated SN (scale bar, 20 μ m) and corresponding traces. This SN exhibited a relatively low level of pERK but an increase in input resistance. (c) Summary data. Open circles represent input resistance (x-axis, represented as percent of pre-test) and level of pERK (y-axis, represented as percent of Veh) of individual SNs. Black open circles represent individual Veh-treated cells and red open circles represent individual Dox-treated cells. (d1) Representative confocal image (scale bar, 20 μ m) and corresponding traces for a Veh-treated SN that exhibited a decrease in input resistance. (d2) Representative confocal image (scale bar, 20 μ m) and the corresponding traces from a Veh-treated SN that exhibited an increase in input resistance. n = 31 – 32. Each n represents a single SN. SNs were obtained from numerous animals.

pERK data and aspects of figure used with permission from Dr. H. Lakshminarasimhan.

Firing threshold vs. pERK

DOX treatment caused a persistent decrease in firing threshold (Fig. 13d) which would promote enhanced responsiveness of SNs to stimuli. The same population of SNs examined in Fig. 19 and Fig. 20 was next examined to determine whether the change in firing threshold correlated with the pERK levels measured 24 h after DOX treatment. Two groups were included in this experiment: (1) Veh; and (2) DOX. SN firing threshold was measured before and 24 h after treatment, and cells were fixed immediately after the post-test to assess pERK levels (Fig. 21a). Both Veh- and DOX-treated SNs showed no correlation between firing threshold and pERK (Veh: $n = 32$; $r = 0.08$; $p = 0.65$; DOX: $n = 31$; $r = 0.23$; $p = 0.22$) (Fig. 21c). DOX induced a persistent decrease in firing threshold (Fig. 13d), but unlike excitability and input resistance (Fig. 19 and Fig. 20), this change did not significantly correlate with pERK levels in individual SNs.

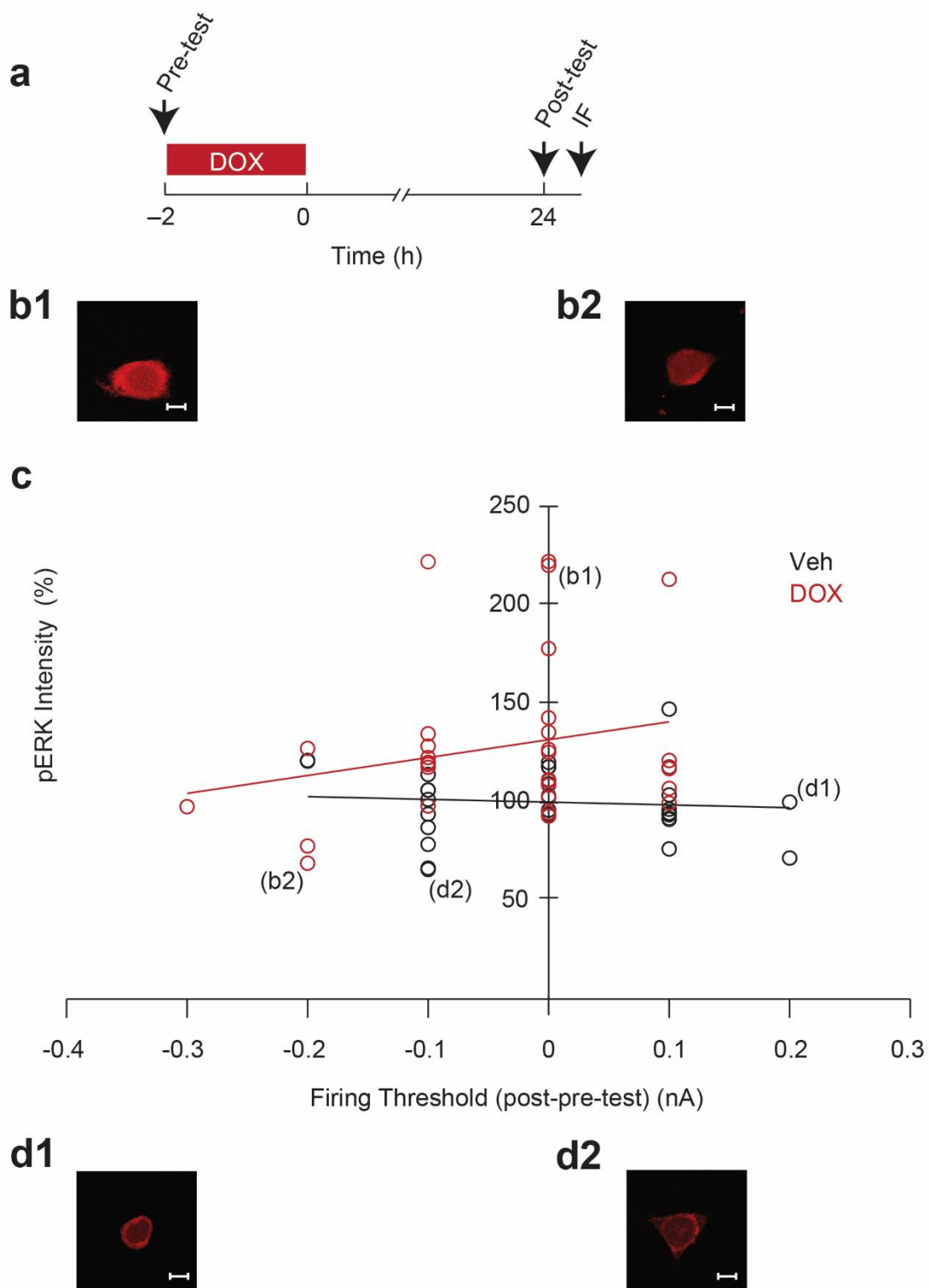


Figure 21. The DOX-induced decrease in firing threshold and the late phase of ERK activation were not correlated.

(a) Protocol for application of DOX and measurement of firing threshold followed by fixation and IF staining as indicated by arrows. (b1) Confocal image of a DOX-treated SN (scale bar, 20 μ m) that had a relatively high level of pERK but no change in firing threshold. (b2) Confocal image of a DOX-treated SN (scale bar, 20 μ m) that exhibited a relatively low level of pERK and a decrease in firing threshold. Circles labeled with identity of cell in this figure to avoid overlapping arrows. (c) Summary data. Open circles represent change in firing threshold (x-axis, represented as post-test minus pre-test) and level of pERK (y-axis, represented as percent of Veh) of individual SNs. Black open circles represent individual Veh-treated SNs and red open circles represent individual DOX-treated SNs. (d1) Confocal image (scale bar, 20 μ m) of a Veh-treated SN that exhibited an increase in firing threshold. (d2) Confocal image (scale bar, 20 μ m) of a Veh-treated SN that exhibited a slight decrease in firing threshold. Representative traces are not included as in Fig. 19 and Fig. 20, because firing threshold is represented by just one spike. Because the same four SNs are shown in Fig. 19, Fig. 20 and Fig. 21 to show how individual SNs fit in the correlation graphs, representative action potentials can be observed in the excitability correlation (Fig. 19). $n = 31 - 32$. Each n represents a single SN. SNs were obtained from numerous animals.

pERK data and aspects of figure used with permission from Dr. H. Lakshminarasimhan.

Conclusion

A negative correlation was discovered between the DOX-induced late ERK activation and both the basal excitability and input resistance (Fig. 19c and Fig. 20c). Furthermore, MEK inhibition both blocked the DOX-induced enhanced excitability and potentiated the late DOX-induced ERK activation (Fig. 17 and Fig. 9b). These results raise several intriguing questions: 1) Are the late activation of ERK and basal excitability causally linked, and if so, how? It is possible that late ERK activation is part of a homeostatic mechanism to reverse the DOX-induced enhanced excitability. A more excitable cell may lower its level of pERK to suppress aberrant changes in excitability. Such a mechanism may be advantageous given that deleterious side-effects of DOX can be reversed by reducing neuronal activity (Moruno Manchon et al. 2016). 2) Are the DOX-induced late ERK activation and enhanced excitability primarily a reflection of the early levels of ERK activation? Individual SNs containing higher levels of pERK during DOX treatment may go on to exhibit higher levels of excitability and higher levels of MKP-1 at later time points which would promote dephosphorylation of ERK. Conversely, SNs containing lower levels of pERK initially may show lower levels of excitability and MKP-1 protein later, and therefore relatively higher levels of pERK. Such an effect would explain the negative correlation between pERK and excitability 24 h after DOX treatment and would also suggest a lack of direct causality between the two phenomena. 3) Does the late ERK activation play a compensatory role in the context of reduced synaptic facilitation in response to DOX (Liu et al. 2014)? Late activation of ERK occurs when activated p38 MAPK levels are no longer elevated (Fig. 4) and thus may promote normal synaptic facilitation.

Investigations into these emerging hypotheses would contribute significantly to our understanding of how DOX affects neurons and mechanisms implicated in memory formation in addition to possibly uncovering protective mechanisms employed by neurons in response to chemotherapy that includes DOX.

Chapter 7: Discussion

An apparent paradox: DOX induces a basal increase in excitability but prevents 5-HT-induced LTEE and LTF

Both DOX and 5-HT produced long-term changes in excitability (Fig. 13b2 and Fig. 14b2; Dale et al. 1987; Liu et al. 2011, 2014), yet their effects on excitability were not additive (Fig. 15; Liu et al. 2014). It may be that in the presence of DOX, 5-HT is unable to induce LTEE. This interpretation agrees with the finding that DOX prevented another cellular analog of LTS, 5-HT-induced LTF (Liu et al. 2014). The difference between the effects of DOX on excitability and synaptic strength is that DOX alone enhanced basal excitability (Fig. 13b2 and Fig. 15; Liu et al. 2014) but not basal synaptic strength assessed 24 h after DOX exposure (Liu et al. 2014). Furthermore, the DOX-induced increase in basal excitability, while so far has only been measured in isolated SNs, is presumed to occur in the presynaptic SN when synapsed with the postsynaptic MN. One might predict that enhanced presynaptic excitability would promote the strengthening of the synapse upon 5-HT exposure through enhanced transmitter release. On the contrary, DOX completely prevents 5-HT-induced LTF despite the enhanced presynaptic excitability (Liu et al. 2014). Therefore, while the excitability changes induced by both DOX and 5-HT appear similar, they do not have the same consequence on the strengthening of the synapse.

There are numerous directions to pursue to gain an understanding of this apparent paradox. The most likely explanation based on the available data is that the inhibitory effect of p38 MAPK on 5-HT-induced LTF is dominant (Liu et al. 2014). Therefore, DOX-induced activation of ERK promotes the basal increase in excitability (Fig. 17), but competition between active ERK and p38 MAPK pathways interferes

with LTF induction. p38 MAPK suppresses LTF and promotes LTD through its activation of CREB2, a repressor of transcription by CREB1 (Bartsch et al. 1995), and DOX enhances p38 MAPK-induced phosphorylation of CREB2 (Liu et al. 2014). CREB1 activation is necessary for both 5-HT-induced LTF and LTEE (Bartsch et al. 1998; Dash et al. 1990; Liu et al. 2008, 2011; Zhou et al. 2015; for reviews, see Alberini 2009; Barco et al. 2006; Benito and Barco 2010; Kandel 2001, 2012). Therefore, the difference between DOX-mediated increases in excitability and 5-HT-mediated increases in excitability may be that CREB1 is not the primary mediator of the enhanced excitability in the case of DOX. Furthermore, this scenario may explain why 5-HT is unable to induce LTEE in the presence of DOX (Fig. 15). It is possible that p38 MAPK inhibits 5-HT-induced LTEE as it does LTF. Therefore, DOX may be promoting excitability through CREB1-independent processes.

Evidence for enhanced activity of neurons caused by DOX treatment was also observed in rat cortical neurons, and this effect was alleviated by administration of the anti-epileptic drug levetiracetam (Moruno Manchon et al. 2016). Therefore, DOX-induced enhancement of basal excitability may depend on mechanisms similar to those observed in epilepsy, such as abnormal modulation of sodium channels (for review, see Lin and Baines 2015). In support of this possibility, DOX was observed to cause a delay in the inactivation of a voltage-gated Na⁺ current in dorsal root ganglion neurons of rat (Wu et al. 2015), which would promote an increase in neuronal excitability.

An alternative, although not mutually exclusive possibility to explain why DOX increases basal SN excitability but does not promote 5-HT-induced LTF is that DOX

overrides any stimulatory effects from the presynaptic SN through its actions within the postsynaptic MN. The action of DOX on molecules in the MN essential to LTF induction have not been investigated yet, but such an investigation is essential to understanding how DOX may interfere with LTF induction and presumably LTM induction. Initial studies of the mechanisms of LTF and LTM in *Aplysia* focused on the presynaptic SN likely due to the knowledge that induction of STF requires presynaptic but not postsynaptic processes (Byrne and Kandel 1996; Glanzman 2008; Kandel 2001). From these studies, investigators naturally sought to understand presynaptic contributions to the long-term components of memory. Subsequent studies conducted by the Glanzman and Schacher laboratories have highlighted the need to consider postsynaptic contributions to LTM processes in *Aplysia*. For example, LTF requires elevated postsynaptic Ca^{2+} and postsynaptic protein synthesis (for review, see Glanzman 2008). Furthermore, postsynaptic CREB2 expression has been implicated in the modulation of a persistent form of LTF induced by two days of 5-HT application (Hu et al. 2015). In Liu et al. (2014), the p38 MAPK inhibitor that rescued the DOX-induced impairment of LTF was applied to the SN-MN co-cultures, therefore, it is not known whether the rescue was mediated by effects on the pre- and/or postsynaptic neurons. In summary, LTF impairment might represent postsynaptic events in addition to presynaptic changes induced by DOX. Such postsynaptic events would not be captured in the isolated SN culture system employed for DOX studies in *Aplysia* thus far.

Brief exposure to DOX induces a complex interconnected chain of events in neurons

The investigations described in this dissertation along with those of my collaborator, Dr. H. Lakshminarasimhan, reveal highly complex interactions of just a few elements of two MAPK pathways and their relation to SN excitability (Fig. 22). The rationale for a focus on ERK and p38 MAPK was their known roles in processes underlying LTM induction. Therefore, basal modulation of these kinases may impact processes implicated in memory. Due to the potential for crosstalk between these two MAPK pathways (Fioravante et al. 2006; Zhang et al. 2017) and their competing effects on downstream transcriptional events involved in memory formation (Bartsch et al. 1995; Guan et al. 2002, 2003; Michael et al. 1998), it is important to consider ERK and p38 MAPK in parallel to predict the physiological and potential behavioral consequences of their modulation.

A single 2-h exposure to DOX resulted in activation of ERK and p38 MAPK during treatment and for approximately 1 h after the end of treatment (Liu et al. 2014; Fig. 4 and Fig. 22, Pathways 1 and 2). Immediately after treatment, MKP-1 protein levels were depressed (Fig. 8; Fig. 22, Pathway 3) and the time course of recovery correlated temporally with the return of pERK and p-p38 MAPK to basal levels (Fig. 4 and Fig. 8). Because both ERK and p38 MAPK are substrates of MKP-1 (Camps et al. 2000), the decrease in MKP-1 may be contributing to the enhanced activity of ERK and p38 MAPK (Fig. 22, Pathways 4a and 4b). DOX also caused a late phase of ERK activation measured 24 h after the end of treatment that depended on late MEK activity (Fig. 4b, Fig. 9c, and Fig. 22, Pathway 5) and a simultaneous enhancement of basal excitability

(Fig. 13b2 and Fig. 15). Surprisingly, application of a MEK inhibitor during DOX treatment did not block the early ERK activation when measured immediately after treatment (Fig. 9a), but it did block the DOX-induced enhancement of basal excitability (Fig. 17), prolonged the decrease in MKP-1 protein levels (Fig. 11), and potentiated the late phase of ERK activation at 24 h (Fig. 9b). Therefore, it is possible that although the MEK inhibitor did not block the early phase of ERK activation when measured immediately after DOX treatment (Fig. 9a), there may be some MEK activation during the initial exposure to DOX that is sufficient to induce the late excitability (Fig. 22, Pathway 6). Furthermore, p38 MAPK can inhibit the MEK-ERK pathway (Fioravante et al. 2006; Zhang et al. 2017; Fig. 22, Pathway 7). Therefore, the MEK pathway may be suppressed with increased time of exposure to DOX due to the increase in p38 MAPK activity (Fig. 4c). Such crosstalk could explain the finding that the MEK inhibitor failed to block the early ERK activation but did exert latent effects on DOX-induced excitability, MKP-1 levels, and ERK phosphorylation that manifested 24 h later. In addition, it is possible that the MEK inhibitor prolongs the repression of MKP-1 expression by blocking a stimulatory effect of the MEK-ERK pathway on MKP-1 (Fig. 22, Pathway 8) transcription and protein stabilization known to exist in other systems (Brondello et al. 1997; Caunt and Keyse 2013; Cook et al. 1997; Li et al. 2001; Small et al. 2003, 2004). We conclude that the seemingly contradictory finding of early application of a MEK inhibitor potentiating the late ERK activity (Fig. 9b) is likely due to the prolonged decrease in MKP-1 (Fig. 11) resulting in a reduced rate of dephosphorylation of pERK.

It is apparent that molecular events initiated early during DOX treatment have prolonged effects in neurons and that cross-talk among MAPK pathways as well as complex kinase-phosphatase interactions, both direct and indirect, enhance the complexity of events that may affect neurons in their basal state. Such basal alterations may interact with the molecular events necessary for memory induction.

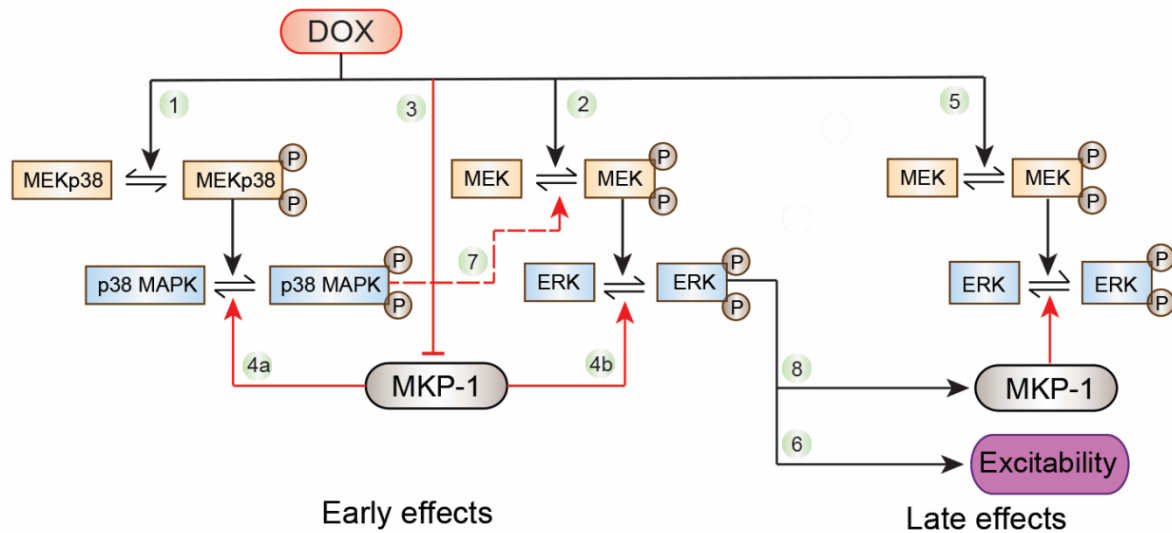


Figure 22. Summary diagram. DOX (2.5 μM, 2 h) produced early increases in activation of p38 MAPK and ERK as well as a late phase of MEK-dependent ERK activation and basal excitability. DOX also lead to an early suppression of MKP-1 protein. MEK inhibition during DOX treatment blocked the basal increase in excitability, enhanced the late phase of ERK activation, and prolonged the downregulation of MKP-1 protein. Black arrows indicate net stimulatory effects (i.e., phosphorylation (activation) and increased excitability). Red arrows indicate net inhibitory effects via dephosphorylation. Red bar indicates net inhibitory effects on protein levels. Red dashed line indicates a putative net inhibitory effect of activated p38 MAPK on activated MEK (Fioravante et al. 2006; Zhang et al. 2017). Numbered lines are for ease of reference in the Discussion.

This summary diagram was generated through the efforts of both Dr. H. Lakshminarasimhan and myself. I created the first draft of the pathway layout, Dr. H. Lakshminarasimhan created the digital version, and I made a revised version. Used with permission from Dr. H. Lakshminarasimhan.

Future Directions

As discussed previously, one important direction to pursue in the future is determining the effects of DOX on the postsynaptic MN given the known postsynaptic contributions to LTF and LTS (Glanzman 2008). It is important to compare the findings from isolated SNs presented here to findings in SNs co-cultured with MNs due to possible influence from retrograde signals originating from the MN (Glanzman 2008).

Another important question is whether the DOX-induced increase in excitability depends upon transcriptional events mediated by CREB1. 5-HT-induced LTEE depends upon protein synthesis (Dale et al. 1987) and CREB1 (Liu et al. 2011). The inability of 5-HT to produce LTEE in the presence of DOX despite the prevalence of a basal increase in excitability by DOX suggests divergence between the mechanisms of induction of the long-lasting forms of excitability by 5-HT vs. DOX. In our lab, CREB1 small interfering RNA has been used to knock down CREB1 levels (Liu et al. 2011; Zhou et al. 2015). This would be a viable method for determining whether the DOX-mediated increase in excitability depends on CREB1 similar to 5-HT. Use of inhibitors of protein synthesis or transcription would be also helpful in determining whether the DOX-induced increase in excitability depends upon modulation of transcriptional events in the nucleus.

Another important research direction is to determine the similarities and differences between the molecular pathways involved in the induction of LTF and LTEE. The inhibitory effect of p38 MAPK on LTF is well established, yet the influence of p38 MAPK on LTEE is unknown. p38 MAPK does not appear to contribute to DOX-induced increases in basal excitability (Fig. 18), but it is possible that 5-HT-induced

increases in excitability depend on p38 MAPK through activation of CREB2 and subsequent suppression of CREB1-mediated transcription. Therefore, it may be possible for 5-HT to produce LTEE in the presence of DOX through simultaneous application of a p38 MAPK inhibitor similar to how such an inhibitor rescued DOX-induced deficits in LTF (Liu et al. 2014).

Another important research direction is to determine how a more clinically relevant treatment protocol would affect the same molecules in neurons as well as physiological correlates of memory. It is recognized that the effects of DOX can vary within a cell type for acute vs. repeated exposure to DOX (Jung and Min 2016; Segredo et al. 2014). The studies described in this dissertation along with those in Liu et al. (2014) used a single, brief application of DOX. This treatment protocol was chosen to determine how initial DOX exposure may act on molecules and processes implicated in memory formation, while avoiding effects of cumulative toxicity. A caveat to these studies is that even at the low concentration and short duration of exposure used, DOX is capable of causing DNA damage, based on recent findings in rat cortical neurons from the Tsvetkov lab (Moruno Manchon et al. 2016). Despite the toxic effects that may be more apparent with repeated exposure to DOX, the effects of multiple rounds of treatment on 5-HT-induced LTF and LTEE as well as investigations into the concurrent molecular changes would be important to enhance the clinical relevance of these studies.

It will also be important to determine how DOX regulates the stress-activated MAPK JNK. DOX leads to increased JNK activity in other cell types (e.g., Rojo et al. 2009), but JNK activity has not been measured in *Aplysia* SNs following DOX

treatment. JNK has been implicated in learning and memory due to its requirement in LTM for inhibitory avoidance, its role in a brain-derived neurotrophic factor (BDNF) positive feedback loop in cortical neurons, and its enhanced activity as part of the activator protein 1 transcriptional complex following LTP (for review, see Mirasis et al. 2016). Assessment of JNK activity following DOX treatment is necessary for a more complete understanding of the modulation of MAPK pathways in neurons. Furthermore, the role of JNK in learning and memory in *Aplysia* remains to be explored.

Another essential research direction to pursue in order to assess the relevance of these findings to higher level organisms is to extend the findings in rat cortical neurons (Fig. 12; Liu et al. 2014). The initial activation of p38 MAPK and ERK as well as the late activation of ERK are conserved in rat cortical neurons (Fig. 12; Liu et al. 2014), but the rest of the findings including the detailed mechanistic investigations involving inhibitors have not been attempted in cortical neurons. Furthermore, *in vivo* investigations using rats or mice treated with DOX would also be critical for assessing the potential relevance to humans exposed to DOX.

Lastly, I will mention one more important extension of the studies described in this dissertation. It is unknown exactly how DOX modulates ERK, p38 MAPK and MKP-1 in SNs. It is possible that these changes are not a result of direct signaling by DOX. DOX induces oxidative stress, and this is one of the mechanisms by which DOX exerts antitumor effects (Aluise et al. 2010). It may be that DOX-induced modulation of MAPK pathways can be mitigated or lessened with concurrent administration of antioxidants. Such an approach was effective at mitigating deficits in memory for

passive avoidance associated with a combinatorial drug treatment that included DOX in rats (Konat et al. 2008).

There are many questions to address in order to fully understand the mechanisms underlying memory deficits associated with CICD. The investigations presented in this dissertation support the model that DOX may, in part, cause memory impairments through interference with the induction of physiological correlates of memory formation, and this may occur through basal modulation of related molecular pathways and biophysical properties of neurons.

Bibliography

- Adams JP, Sweatt JD (2002). Molecular psychology: roles for the ERK MAP kinase cascade in memory. *Annu. Rev. Pharmacol. Toxicol.* 42: 135-163.
- Ahles TA, Saykin AJ (2007). Candidate mechanisms for chemotherapy-induced cognitive changes. *Nature Rev. Can.* 7: 192-201.
- Alberini CM, Ghirardi M, Metz R, Kandel ER (1994). C/EBP is an immediate-early gene required for the consolidation of long-term facilitation in *Aplysia*. *Cell* 76: 1099-1114.
- Alberini CM (2009). Transcription factors in long-term memory and synaptic plasticity. *Physiol. Rev.* 89: 121-145.
- Alhowail AH, Suppiramaniam V, Arnold R. Doxorubicin alters mechanisms of memory formation in Ex vivo and In vivo models of Chemobrain. Program No. 838.05. 2016 Neuroscience Meeting Planner. San Diego, CA: Society for Neuroscience, 2016. Online.
- Alkon DL, Sakakibara M, Forman R, Harrigan J, Lederhendler I, Farley J (1985). Reduction of two voltage-dependent K⁺ currents mediates retention of a learned association. *Behav. Neural Biol.* 44: 278-300.
- Alkon DL, Shoukimas JJ, Heldman E (1982). Calcium-mediated decrease of a voltage-dependent potassium current. *Biophys. J.* 40: 245-250.
- Aluise CD, Sultana R, Tangpong J, Vore M, St Clair D, Moscow JA, Butterfield DA (2010). Chemo brain (chemo fog) as a potential side effect of doxorubicin administration: role of cytokine-induced, oxidative/nitrosative stress in cognitive dysfunction. *Adv. Exp. Med. Biol.* 678: 147-156.

- Angers A, Fioravante D, Chin J, Cleary LJ, Bean AJ, Byrne JH (2002). Serotonin stimulates phosphorylation of *Aplysia* synapsin and alters its subcellular distribution in sensory neurons. *J. Neurosci.* 22: 5412-5422.
- Bacskai BJ, Hochner B, Mahaut-Smith M, Adams SR, Kaang BK, Kandel ER, Tsien RY (1993). Spatially resolved dynamics of cAMP and protein kinase A subunits in *Aplysia* sensory neurons. *Science* 260: 222-226.
- Bailey CH, Kaang BK, Chen M, Martin KC, Lim CS, Casadio A, Kandel ER (1997). Mutation in the phosphorylation sites of MAP kinase blocks learning-related internalization of apCAM in *Aplysia* sensory neurons. *Neuron* 18: 913-924.
- Bain J, Plater L, Elliott M, Shpiro N, Hastie CJ, McLauchlan H, Klevernic I, Arthur JS, Alessi DR, Cohen P (2007). The selectivity of protein kinase inhibitors: a further update. *Biochem. J.* 408: 297-315.
- Barco A, Bailey CH, Kandel ER (2006). Common molecular mechanisms in explicit and implicit memory. *J. Neurochem.* 97: 1520-1533.
- Barry RL, Byun NE, Tantawy MN, Mackey CA, Wilson GH, Stark AJ, Flom MP, Gee LC, Quarles CC (2017). In vivo neuroimaging and behavioral correlates in a rat model of chemotherapy-induced cognitive dysfunction. *Brain Imaging Behav.* doi: 10.1007/s11682-017-9674-2. [Epub ahead of print]
- Bartsch D, Casadio A, Karl KA, Serodio P, Kandel ER (1998). CREB1 encodes a nuclear activator, a repressor, and a cytoplasmic modulator that form a regulatory unit critical for long-term facilitation. *Cell* 95: 211–223.
- Bartsch D, Ghirardi M, Skehel PA, Karl KA, Herder SP, Chen M, Bailey CH, Kandel ER (1995). *Aplysia* CREB2 represses long-term facilitation: relief of

- repression converts transient facilitation into long-term functional and structural change. *Cell* 83: 979-992.
- Baxter DA, Canavier CC, Clark JW Jr, Byrne JH (1999). Computational model of the serotonergic modulation of sensory neurons in *Aplysia*. *J. Neurophysiol.* 82: 2914-2935.
- Benito E, Barco A (2010). CREB's control of intrinsic and synaptic plasticity: implications for CREB-dependent memory models. *Trends Neurosci.* 33: 230-240.
- Boutros T, Chevet E, Metrakos P (2008). Mitogen-activated protein (MAP) kinase/MAP kinase phosphatase regulation: roles in cell growth, death, and cancer. *Pharmacol. Rev.* 60: 261-310.
- Brondello JM, Brunet A, Pouyssegur J, McKenzie FR (1997). The dual specificity mitogen-activated protein kinase phosphatase-1 and -2 are induced by the p42/p44MAPK cascade. *J. Biol. Chem.* 272: 1368-1376.
- Brondello JM, Pouyssegur J, and McKenzie FR (1999). Reduced MAP kinase phosphatase-1 degradation after p42/p44MAPK-dependent phosphorylation. *Science* 286: 2514–2517.
- Byrne JH, Hawkins RD (2015). Nonassociative learning in invertebrates. *Cold Spring Harbor Perspect. Biol.* 7: a021675.
- Byrne JH, Kandel ER (1996). Presynaptic facilitation revisited: state and time dependence. *J. Neurosci.* 16: 425-435.
- Camps M, Nichols A, Arkinstall S (2000). Dual specificity phosphatases: a gene family for control of MAP kinase function. *FASEB J.* 14: 6-16.

- Cargnello M, Roux PP (2011). Activation and function of the MAPKs and their substrates, the MAPK-activated protein kinases. *Microbiol. Mol. Biol. Rev.* 75: 50-83.
- Castellucci V, Pinsker H, Kupfermann I, Kandel ER (1970). Neuronal mechanisms of habituation and dishabituation of the gill-withdrawal reflex in *Aplysia*. *Science* 167:1745-1748.
- Caunt CJ, Keyse SM (2013). Dual-specificity MAP kinase phosphatases (MKPs): shaping the outcome of MAP kinase signalling. *FEBS J.* 280: 489-504.
- Chen A, Muzzio IA, Malleret G, Bartsch D, Verbitsky M, Pavlidis P, Yonan AL, Vronskaya S, Grody MB, Cepeda I, Gilliam TC, Kandel ER (2003). Inducible enhancement of memory storage and synaptic plasticity in transgenic mice expressing an inhibitor of ATF4 (CREB-2) and C/EBP proteins. *Neuron* 39: 655-669.
- Chin J, Angers A, Cleary LJ, Eskin A, Byrne JH (1999). TGF-beta1 in *Aplysia*: role in long-term changes in the excitability of sensory neurons and distribution of TbetaR-II-like immunoreactivity. *Learn. Mem.* 6: 317-330.
- Chin J, Angers A, Cleary LJ, Eskin A, Byrne JH (2002). Transforming growth factor beta1 alters synapsin distribution and modulates synaptic depression in *Aplysia*. *J. Neurosci.* 22: RC220.
- Chin J, Liu RY, Cleary LJ, Eskin A, Byrne JH (2006). TGF- β -induced long-term changes in neuronal excitability in *Aplysia* sensory neurons depend on MAPK. *J. Neurophysiol.* 95: 3286–3290.

- Choi J, Yip-Schneider M, Albertin F, Wiesenauer C, Wang Y, Schmidt CM (2008). The effect of doxorubicin on MEK-ERK signaling predicts its efficacy in HCC. *J. Surg. Res.* 150: 219-226.
- Christie LA, Acharya MM, Parihar VK, Nguyen A, Martirosian V, Limoli CL (2012). Impaired cognitive function and hippocampal neurogenesis following cancer chemotherapy. *Clin. Cancer Res.* 18: 1954-1965.
- Ciftci O, Ullrich O, Schmidt CA, Diestel A, Hass R (2001). Regulation of the nuclear proteasome activity in myelomonocytic human leukemia cells after adriamycin treatment. *Blood* 97: 2830–2838.
- Cleary LJ, Byrne JH, Frost WN (1995). Role of interneurons in defensive withdrawal reflexes in *Aplysia*. *Learn. Mem.* 2: 133-151.
- Cleary LJ, Lee WL, Byrne JH (1998). Cellular correlates of long-term sensitization in *Aplysia*. *J. Neurosci.* 18: 5988–5998.
- Cohen-Matsliah SI, Brosh I, Rosenblum K, Barkai E (2007). A novel role for extracellular signal-regulated kinase in maintaining long-term memory-relevant excitability changes. *J. Neurosci.* 27: 12584-12589.
- Cook SJ, Beltman J, Cadwallader KA, McMahon M, McCormick F (1997). Regulation of mitogen-activated protein kinase phosphatase-1 expression by extracellular signal-related kinase-dependent and Ca²⁺-dependent signal pathways in Rat-1 cells. *J. Biol. Chem.* 272: 13309–13319.
- Crow TJ, Alkon DL (1980). Associative behavioral modification in hermissenda: cellular correlates. *Science* 209: 412-414.

- Dale N, Kandel ER, Schacher S (1987). Serotonin produces long-term changes in the excitability of *Aplysia* sensory neurons in culture that depend on new protein synthesis. *J. Neurosci.* 7: 2232-2238.
- Dale N, Schacher S, Kandel ER (1988). Long-term facilitation in *Aplysia* involves increase in transmitter release. *Science* 239: 282-285.
- Dash PK, Hochner B, Kandel ER (1990). Injection of the cAMP-responsive element into the nucleus of *Aplysia* sensory neurons blocks long-term facilitation. *Nature* 345: 718-721.
- Dowdy S, Wearden S, Chilko D (2004). *Statistics for Research* (3rd ed.). Hoboken, NJ: John Wiley & Sons, Inc.
- Esdin J, Pearce K, Glanzman DL (2010). Long-term habituation of the gill-withdrawal reflex in *Aplysia* requires gene transcription, calcineurin and L-type voltage-gated calcium channels. *Front. Behav. Neurosci.* 4: 181.
- Ezzeddine Y, Glanzman DL (2003). Prolonged habituation of the gill-withdrawal reflex in *Aplysia* depends on protein synthesis, protein phosphatase activity, and postsynaptic glutamate receptors. *J. Neurosci.* 23: 9585-9594.
- Farley J (1988). Associative training results in persistent reductions in a calcium-activated potassium current in *Hermissenda* Type B photoreceptors. *Behav. Neurosci.* 102: 784-802.
- Favata MF, Horiuchi KY, Manos EJ, Daulerio AJ, Stradley DA, Feeser WS, Van Dyk DE, Pitts WJ, Earl RA, Hobbs F, Copeland RA, Magolda RL, Scherle PA, Trzaskos JM (1998). Identification of a novel inhibitor of mitogen-activated protein kinase kinase. *J. Biol. Chem.* 273: 18623-18632.

- Fioravante D, Smolen PD, Byrne JH (2006). The 5-HT- and FMRFa-activated signaling pathways interact at the level of the Erk MAPK cascade: potential inhibitory constraints on memory formation. *Neurosci. Lett.* 396: 235-240.
- Frost WN, Castellucci VF, Hawkins RD, Kandel ER (1985). Monosynaptic connections made by the sensory neurons of the gill- and siphon-withdrawal reflex in *Aplysia* participate in the storage of long-term memory for sensitization. *Proc. Natl. Acad. Sci. USA* 82: 8266-8269.
- Giese KP, Mizuno K (2013). The roles of protein kinases in learning and memory. *Learn. Mem.* 20: 540–552.
- Glanzman DL, Mackey SL, Hawkins RD, Dyke AM, Lloyd PE, Kandel ER (1989). Depletion of serotonin in the nervous system of *Aplysia* reduces the behavioral enhancement of gill withdrawal as well as the heterosynaptic facilitation produced by tail shock. *J. Neurosci.* 9: 4200-4213.
- Glanzman DL (2008). New tricks for an old slug: the critical role of postsynaptic mechanisms in learning and memory in *Aplysia*. *Prog. Brain Res.* 169: 277-292.
- Glanzman DL (2013). Synaptic mechanisms of induction and maintenance of long-term sensitization memory in *Aplysia*. In R. Menzel & P. R. Benjamin (Eds.), *Invertebrate Learning and Memory* (Vol. 22) (pp. 206-220). London, UK: Elsevier.
- Guan Z, Giustetto M, Lomvardas S, Kim JH, Miniaci MC, Schwartz JH, Thanos D, Kandel ER (2002). Integration of long-term-memory-related synaptic plasticity

involves bidirectional regulation of gene expression and chromatin structure.
Cell 111: 483-493.

Guan Z, Kim JH, Lomvardas S, Holick K, Xu S, Kandel ER, Schwartz JH (2003). p38 MAP kinase mediates both short-term and long-term synaptic depression in *Aplysia*. J. Neurosci. 23: 7317–7325.

Guise S, Braguer D, Carles G, Delacourte A, Briand C (2001). Hyperphosphorylation of tau is mediated by ERK activation during anticancer drug-induced apoptosis in neuroblastoma cells. J. Neurosci. Res. 63: 257–267.

Hawkins RD (1989). Localization of potential serotonergic facilitator neurons in *Aplysia* by glyoxylic acid histofluorescence combined with retrograde fluorescent labeling. J. Neurosci. 9: 4214-4226.

Hu JY, Glickman L, Wu F, Schacher S (2004). Serotonin regulates the secretion and autocrine action of a neuropeptide to activate MAPK required for long-term facilitation in *Aplysia*. Neuron 43: 373-385.

Hu JY, Levine A, Sung YJ, Schacher S (2015). cJun and CREB2 in the postsynaptic neuron contribute to persistent long-term facilitation at a behaviorally relevant synapse. J. Neurosci. 35: 386-395.

Hudmon A, Choi JS, Tyrrell L, Black JA, Rush AM, Waxman SG, Dib-Hajj SD (2008). Phosphorylation of Sodium Channel Nav1.8 by p38 Mitogen-Activated Protein Kinase Increases Current Density in Dorsal Root Ganglion Neurons. J. Neurosci. 28: 3190-3201.

- Jansen CE, Cooper BA, Dodd MJ, Miaskowski CA (2011). A prospective longitudinal study of chemotherapy-induced cognitive changes in breast cancer patients. *Support Care Cancer* 19: 1647-1656.
- Jeffrey KL, Camps M, Rommel C, Mackay CR (2007). Targeting dual-specificity phosphatases: manipulating MAP kinase signalling and immune responses. *Nat. Rev. Drug Discov.* 6: 391–403.
- Jin X, Gereau RW (2006). Acute p38-mediated modulation of tetrodotoxin-resistant sodium channels in mouse sensory neurons by tumor necrosis factor- α . *J. Neurosci.* 26: 246-255.
- Jung S, Min J. Cumulative effect of systemic chemotherapy on cognitive function. Program No. 39.08. 2016 Neuroscience Meeting Planner. San Diego, CA: Society for Neuroscience, 2016. Online.
- Kandel ER (2001). The molecular biology of memory storage: A dialogue between genes and synapses. *Science* 294: 1030-1038.
- Kandel ER (2012). The molecular biology of memory: cAMP, PKA, CRE, CREB-1, CREB-2, and CPEB. *Mol. Brain.* 5: 14.
- Kaang BK, Kandel ER, Grant SG (1993). Activation of cAMP-responsive genes by stimuli that produce long-term facilitation in *Aplysia* sensory neurons. *Neuron* 10: 427-435.
- Kassabov SR, Choi YB, Karl KA, Vishwasrao HD, Bailey CH, Kandel ER (2013). A single *Aplysia* neurotrophin mediates synaptic facilitation via differentially processed isoforms. *Cell Rep.* 3: 1213-1227.

- Kim JI, Cho HY, Han JH, Kaang BK (2016). Which Neurons Will Be the Engram - Activated Neurons and/or More Excitable Neurons? *Exp. Neurobiol.* 25 :55-63.
- Klein M, Hochner B, Kandel ER (1986). Facilitatory transmitters and cAMP can modulate accommodation as well as transmitter release in *Aplysia* sensory neurons: Evidence for parallel processing in a single cell. *Proc. Natl. Acad. Sci. USA* 83: 7994-7998.
- Konat GW, Kraszpulski M, James I, Zhang HT, Abraham J (2008). Cognitive dysfunction induced by chronic administration of common cancer chemotherapeutics in rats. *Metab. Brain Dis.* 23: 325-333.
- Kopec AM, Carew TJ (2013). Growth factor signaling and memory formation: temporal and spatial integration of a molecular network. *Learn. Mem.* 20: 531-539.
- Kopec AM, Philips GT, Carew TJ (2015). Distinct Growth Factor Families Are Recruited in Unique Spatiotemporal Domains during Long-Term Memory Formation in *Aplysia californica*. *Neuron* 86: 1228-1239.
- Lee YS, Choi SL, Jun H, Yim SJ, Lee JA, Kim HF, Lee SH, Shim J, Lee K, Jang DJ, Kaang BK (2012). AU-rich element-binding protein negatively regulates CCAAT enhancer-binding protein mRNA stability during long-term synaptic plasticity in *Aplysia*. *Proc. Natl. Acad. Sci. USA* 109: 15520-15525.
- Lee JA, Kim H, Lee YS, Kaang BK (2003). Overexpression and RNA interference of Ap-cyclic AMP-response element binding protein-2, a repressor of long-term facilitation, in *Aplysia kurodai* sensory-to-motor synapses. *Neurosci. Lett.* 337: 9-12.

- Lee SH, Lim CS, Park H, Lee JA, Han JH, Kim H, Cheang YH, Lee SH, Lee YS, Ko HG, Jang DH, Kim H, Miniaci MC, Bartsch D, Kim E, Bailey CH, Kandel ER, Kaang BK (2007). Nuclear translocation of CAM-associated protein activates transcription for long-term facilitation in *Aplysia*. *Cell* 129: 801-812.
- Lee SH, Park J, Che Y, Han PL, Lee JK (2000). Constitutive activity and differential localization of p38 alpha and p38 beta MAPKs in adult mouse brain. *J. Neurosci. Res.* 60: 623-631.
- Levenson J, Byrne JH, Eskin A (1999). Levels of serotonin in the hemolymph of *Aplysia* are modulated by light/dark cycles and sensitization training. *J. Neurosci.* 19: 8094-8103.
- Li J, Gorospe M, Hutter D, Barnes J, Keyse SM, Liu Y (2001). Transcriptional induction of MKP-1 in response to stress is associated with histone H3 phosphorylation–acetylation. *Mol. Cell Biol.* 21: 8213–8224.
- Liedke PE, Reolon GK, Kilpp B, Brunetto AL, Roesler R, Schwartzmann G (2009). Systemic administration of doxorubicin impairs aversively motivated memory in rats. *Pharmacol. Biochem. Behav.* 94: 239–243.
- Lin WH, Baines RA (2015). Regulation of membrane excitability: a convergence on voltage-gated sodium conductance. *Mol. Neurobiol.* 51: 57-67.
- Lin YW, Chuang SM, and Yang JL (2003). ERK1/2 achieves sustained activation by stimulating MAPK phosphatase-1 degradation via the ubiquitin-proteasome pathway. *J. Biol. Chem.* 278: 21534–21541.

- Lin YW and Yang JL (2006). Cooperation of ERK and SCF^{Skp2} for MKP-1 destruction provides a positive feedback regulation of proliferating signaling. *J. Biol. Chem.* 281: 915–926.
- Liu RY, Cleary LJ, Byrne JH (2011). The requirement for enhanced CREB1 expression in consolidation of long-term synaptic facilitation and long-term excitability in sensory neurons of *Aplysia*. *J. Neurosci.* 31: 6871-6879.
- Liu RY, Neveu CL, Smolen P, Cleary LJ, Byrne JH (2017). Superior long-term synaptic memory induced by combining dual pharmacological activation of PKA and ERK with an enhanced training protocol. *Learn. Mem.*, in press.
- Liu RY, Zhang Y, Coughlin BL, Cleary LJ, Byrne JH (2014). Doxorubicin attenuates serotonin-induced long-term synaptic facilitation by phosphorylation of p38 mitogen-activated protein kinase. *J. Neurosci.* 34: 13289-13300.
- Liu RY, Fioravante D, Shah S, Byrne JH (2008). cAMP response element-binding protein 1 feedback loop is necessary for consolidation of long-term synaptic facilitation in *Aplysia*. *J. Neurosci.* 28: 1970 -1976.
- Lorenzetti FD, Baxter DA, Byrne JH (2008). Molecular mechanisms underlying a cellular analog of operant reward learning. *Neuron* 59: 815-828.
- Mackey SL, Kandel ER, Hawkins RD (1989). Identified serotonergic neurons LCB1 and RCB1 in the cerebral ganglia of *Aplysia* produce presynaptic facilitation of siphon sensory neurons. *J. Neurosci.* 9: 4227-4235.
- Macleod JE, DeLeo JA, Hickey WF, Ahles TA, Saykin AJ, Bucci DJ (2007). Cancer chemotherapy impairs contextual but not cue-specific fear memory. *Behav. Brain Res.* 181: 168-172.

- Marinesco S, Carew TJ (2002). Serotonin release evoked by tail nerve stimulation in the CNS of *Aplysia*: characterization and relationship to heterosynaptic plasticity. *J. Neurosci.* 22: 2299-2312.
- Marinesco S, Kolkman KE, Carew TJ (2004). Serotonergic modulation in *Aplysia*. I. Distributed serotonergic network persistently activated by sensitizing stimuli. *J. Neurophysiol.* 92: 2468-2486.
- Martin KC, Michael D, Rose JC, Barad M, Casadio A, Zhu H, Kandel ER (1997). MAP kinase translocates into the nucleus of the presynaptic cell and is required for long-term facilitation in *Aplysia*. *Neuron* 18: 899–912.
- Michael D, Martin KC, Seger R, Ning MM, Baston R, Kandel ER (1998). Repeated pulses of serotonin required for long-term facilitation activate mitogen-activated protein kinase in sensory neurons of *Aplysia*. *Proc. Natl. Acad. Sci. USA* 95: 1864–1869.
- Michel M, Gardner JS, Green CL, Organ CL, Lyons LC (2013). Protein phosphatase-dependent circadian regulation of intermediate-term associative memory. *J. Neurosci.* 33: 4605-4613.
- Miris AA, Alexandrescu A, Carew TJ, Kopec AM (2016). The contribution of spatial and temporal molecular networks in the induction of long-term memory and its underlying synaptic plasticity. *AIMS Neurosci.* 3: 356-384.
- Mitra S, Tsvetkov AS, Finkbeiner S (2009). Single neuron ubiquitin-proteasome dynamics accompanying inclusion body formation in huntington disease. *J. Biol. Chem.* 284: 4398–4403.

- Montarolo PG, Goelet P, Castellucci VF, Morgan J, Kandel ER, Schacher S (1986). A critical period for macromolecular synthesis in long-term heterosynaptic facilitation in *Aplysia*. *Science* 234: 1249-1254.
- Moruno Manchon JF, Dabaghian Y, Uzor N-E, Kesler SR, Wefel JS, Tsvetkov AS (2016). Levetiracetam mitigates doxorubicin-induced DNA and synaptic damage in neurons. *Sci. Rep.* 6: 25705.
- Moruno Manchon JF, Uzor N-E, Dabaghian Y, Furr-Stimming EE, Finkbeiner S, Tsvetkov AS (2015). Cytoplasmic sphingosine-1-phosphate pathway modulates neuronal autophagy. *Sci. Rep.* 5: 15213.
- Moyer JR Jr, Thompson LT, Disterhoft JF (1996). Trace eyeblink conditioning increases CA1 excitability in a transient and learning-specific manner. *J. Neurosci.* 16: 5536-5546.
- Mozzachiodi R, Byrne JH (2010). More than synaptic plasticity: role of nonsynaptic plasticity in learning and memory. *Trends Neurosci.* 33: 17-26.
- Mozzachiodi R, Lorenzetti FD, Baxter DA, Byrne JH (2008). Changes in neuronal excitability serve as a mechanism of long-term memory for operant conditioning. *Nat. Neurosci.* 11: 1146-1148.
- Müller U, Carew TJ (1998). Serotonin induces temporally and mechanistically distinct phases of persistent PKA activity in *Aplysia* sensory neurons. *Neuron* 21: 1423-1434.
- Murphy LO, Blenis J (2006). MAPK signal specificity: the right place at the right time. *Trends Biochem. Sci.* 31: 268-275.

- Myers JS (2009). Chemotherapy-related cognitive impairment. Clin. J. Oncol. Nurs. 13: 413-421.
- O'Farrell E, MacKenzie J, Collins B (2013). Clearing the air: a review of our current understanding of "chemo fog". Curr. Oncol. Rep. 15: 260.
- Ormond J, Hislop J, Zhao Y, Webb N, Vaillaincourt F, Dyer JR, Ferraro G, Barker P, Martin KC, Sossin WS (2004). ApTrkl, a Trk-like receptor, mediates serotonin-dependent ERK activation and long-term facilitation in *Aplysia* sensory neurons. Neuron 44: 715-728.
- Philpot RM, Ficken M, Wecker L (2016). Doxorubicin and cyclophosphamide lead to long-lasting impairment of spatial memory in female, but not male mice. Behav. Brain Res. 307: 165-175.
- Pinsker HM, Hening WA, Carew TJ, Kandel ER (1973). Long-term sensitization of a defensive withdrawal reflex in *Aplysia*. Science 182: 1039-1042.
- Pinsker H, Kupfermann I, Castellucci V, Kandel E (1970). Habituation and dishabituation of the gill-withdrawal reflex in *Aplysia*. Science 167:1740-1742.
- Poizat C, Puri PL, Bai Y, Kedes L (2005). Phosphorylation-dependent degradation of p300 by doxorubicin-activated p38 mitogen-activated protein kinase in cardiac cells. Mol. Cell Biol. 25: 2673–2687.
- Pollak DD, Minh BQ, Cicvaric A, Monje FJ (2014). A novel fibroblast growth factor receptor family member promotes neuronal outgrowth and synaptic plasticity in *Aplysia*. Amino Acids 46: 2477-2488.

- Poolos NP, Bullis JB, Roth MK (2006). Modulation of h-Channels in hippocampal pyramidal neurons by p38 mitogen-activated protein kinase. *J. Neurosci.* 26: 7995-8003.
- Pu L, Kopec AM, Boyle HD, Carew TJ (2014). A novel cysteine-rich neurotrophic factor in *Aplysia* facilitates growth, MAPK activation, and long-term synaptic facilitation. *Learn. Mem.* 21: 215-222.
- Purcell AL, Sharma SK, Bagnall MW, Sutton MA, Carew TJ (2003). Activation of a tyrosine kinase-MAPK cascade enhances the induction of long-term synaptic facilitation and long-term memory in *Aplysia*. *Neuron* 37: 473-484.
- Rojo F, González-Navarrete I, Bragado R, Dalmases A, Menéndez S, Cortes-Sempere M, Suárez C, Oliva C, Servitja S, Rodríguez-Fanjul V, Sánchez-Pérez I, Campas C, Corominas JM, Tusquets I, Bellosillo B, Serrano S, Perona R, Rovira A, Albanell J (2009). Mitogen-activated protein kinase phosphatase-1 in human breast cancer independently predicts prognosis and is repressed by doxorubicin. *Clin. Cancer Res.* 15: 3530–3539.
- Ramalho M, Fontes F, Ruano L, Pereira S, Lunet N (2017). Cognitive impairment in the first year after breast cancer diagnosis: A prospective cohort study. *Breast* 32: 173-178.
- Rosenkranz JA, Frick A, Johnston D (2009). Kinase-dependent modification of dendritic excitability after long-term potentiation. *J. Physiol.* 587: 115-125.
- Roth TL, Sweatt JD (2008). Rhythms of memory. *Nat. Neurosci.* 11: 993-994.

- Salas-Ramirez KY, Bagnall C, Frias L, Abdali SA, Ahles TA, Hubbard K (2015). Doxorubicin and cyclophosphamide induce cognitive dysfunction and activate the ERK and AKT signaling pathways. *Beh. Brain Res.* 292: 133-141.
- Sardi I, la Marca G, Cardellicchio S, Giunti L, Malvagia S, Genitori L, Massimino M, de Martino M, Giovannini MG (2013). Pharmacological modulation of blood-brain barrier increases permeability of doxorubicin into the rat brain. *Am. J. Cancer Res.* 3: 424-432.
- Schacher S, Proshansky E (1983). Neurite regeneration by *Aplysia* neurons in dissociated cell culture: modulation by *Aplysia* hemolymph and the presence of the initial axonal segment. *J. Neurosci.* 3: 2403-2413.
- Scholz KP, Byrne JH (1987). Long-term sensitization in *Aplysia*: biophysical correlates in tail sensory neurons. *Science* 235: 685-687.
- Segredo MP, Salvadori DM, Rocha NS, Moretto FC, Correa CR, Camargo EA, de Almeida DC, Reis RA, Freire CM, Braz MG, Tang G, Matsubara LS, Matsubara BB, Yeum KJ, Ferreira AL (2014). Oxidative stress on cardiotoxicity after treatment with single and multiple doses of doxorubicin. *Hum. Exp. Toxicol.* 33: 748-760.
- Seigers R, Loos M, Van Tellingen O, Boogerd W, Smit AB, Schagen SB (2015). Cognitive impact of cytotoxic agents in mice. *Psychopharmacology* 232: 17-37.
- Sharma SK, Bagnall MW, Sutton MA, Carew TJ (2003). Inhibition of calcineurin facilitates the induction of memory for sensitization in *Aplysia*: requirement of mitogen-activated protein kinase. *Proc. Natl. Acad. Sci. USA* 100: 4861-4866.

- Sharma SK, Carew TJ (2004). The roles of MAPK cascades in synaptic plasticity and memory in *Aplysia*: Facilitatory effects and inhibitory constraints. *Learn. Mem.* 11: 373-378.
- Sharma SK, Sherff CM, Shobe J, Bagnall MW, Sutton MA, Carew TJ (2003). Differential role of mitogen-activated protein kinase in three distinct phases of memory for sensitization in *Aplysia*. *J. Neurosci.* 23: 3899 -3907.
- Sharma SK, Sherff CM, Stough S, Hsuan V, Carew TJ (2006). A tropomyosin-related kinase B ligand is required for ERK activation, long-term synaptic facilitation, and long-term memory in *Aplysia*. *Proc. Natl. Acad. Sci. USA* 103: 14206-14210.
- Shaul YD, Seger R (2007). The MEK/ERK cascade: From signaling specificity to diverse functions. *Biochim. Biophys. Acta* 1773: 1213-1226.
- Small GW, Shi YY, Edmund NA, Somasundaram S, Moore DT, Orlowski RZ (2004). Evidence that mitogen-activated protein kinase phosphatase-1 induction by proteasome inhibitors plays an antiapoptotic role. *Mol. Pharmacol.* 66: 1478-1490.
- Small GW, Somasundaram S, Moore DT, Shi YY, Orlowski RZ (2003). Repression of mitogen-activated protein kinase (MAPK) phosphatase-1 by anthracyclines contributes to their antiapoptotic activation of p44/42-MAPK. *J. Pharmacol. Exp. Ther.* 307: 861-869.
- Stambouliau S, Choi JS, Ahn HS, Chang YW, Tyrrell L, Black JA, Waxman SG and Dib-Hajj SD (2010). ERK1/2 mitogen-activated protein kinase phosphorylates

- sodium channel Nav1.7 and alters its gating properties. J. Neurosci. 30: 1637-1647.
- Ster J, De Bock F, Guérineau NC, Janossy A, Barrère-Lemaire S, Bos JL, Bockaert J, Fagni L (2007). Exchange protein activated by cAMP (Epac) mediates cAMP activation of p38 MAPK and modulation of Ca²⁺-dependent K⁺ channels in cerebellar neurons. Proc. Natl. Acad. Sci. USA 104: 2519-2524.
- Sung YJ, Povelones M, Ambron RT (2001). RISK-1: a novel MAPK homologue in axoplasm that is activated and retrogradely transported after nerve injury. J. Neurobiol. 47: 67-79.
- Sweatt JD (2001). The neuronal MAP kinase cascade: a biochemical signal integration system subserving synaptic plasticity and memory. J. Neurochem. 76: 1-10.
- Sweatt JD (2004). Mitogen-activated protein kinases in synaptic plasticity and memory. Curr. Opin. Neurobiol. 14: 311-317.
- Sweatt JD (2016). Neural plasticity and behavior – sixty years of conceptual advances. J. Neurochem. 139: 179-199.
- Sweatt JD, Kandel ER (1989). Persistent and transcriptionally-dependent increase in protein phosphorylation in long-term facilitation of *Aplysia* sensory neurons. 339: 51-54.
- Tannock IF, Ahles TA, Ganz PA, Van Dam FS (2004). Cognitive impairment associated with chemotherapy for cancer: report of a workshop. J. Clin. Oncol. 22: 2233-2239.

- Thomas GM, Huganir RL (2004). MAPK cascade signalling and synaptic plasticity. Nat. Rev. Neurosci. 5: 173-183.
- Tsvetkov AS, Ando DM, Finkbeiner S (2013). Longitudinal imaging and analysis of neurons expressing polyglutamine-expanded proteins. Methods Mol. Biol. 1017: 1–20.
- Tsvetkov AS, Arrasate M, Barmada S, Ando DM, Sharma P, Shaby BA, Finkbeiner S (2013). Proteostasis of polyglutamine varies among neurons and predicts neurodegeneration. Nat. Chem. Biol. 9: 586-592.
- Tsvetkov AS, Miller J, Arrasate M, Wong JS, Pleiss MA, Finkbeiner S (2010). A small-molecule scaffold induces autophagy in primary neurons and protects against toxicity in a Huntington disease model. Proc. Natl. Acad. Sci. USA 107: 16982–16987.
- Wainwright ML, Byrne JH, Cleary LJ (2004). Dissociation of morphological and physiological changes associated with long-term memory in *Aplysia*. J. Neurophysiol. 92: 2628-2632.
- Walters ET, Byrne JH, Carew TJ, Kandel ER (1983). Mechanoafferent neurons innervating tail of *Aplysia*. II. Modulation by sensitizing stimulation. J. Neurophysiol. 50: 1543-1559.
- Wang XM, Walitt B, Saligan L, Tiwari AF, Cheung CW, Zhang ZJ (2015). Chemobrain: a critical review and causal hypothesis of link between cytokines and epigenetic reprogramming associated with chemotherapy. Cytokine 72: 86-96.

- Wefel JS, Schagen SB (2012). Chemotherapy-related cognitive dysfunction. *Curr. Neurol. Neurosci. Rep.* 12: 267-75.
- Westermarck J, Li SP, Kallunki T, Han J, Kähäri VM (2001). p38 mitogen-activated protein kinase-dependent activation of protein phosphatases 1 and 2A inhibits MEK1 and MEK2 activity and collagenase 1 (MMP-1) gene expression. *Mol. Cell Biol.* 21: 2373-2383.
- Wu SN, So EC, Liao YK, Huang YM (2015). Reversal by ranolazine of doxorubicin-induced prolongation in the inactivation of late sodium current in rat dorsal root ganglion neurons. *Pain Medicine* 16: 1032-1034.
- Yamamoto N, Hegde AN, Chain DG, Schwartz JH (1999). Activation and degradation of the transcription factor C/EBP during long-term facilitation in *Aplysia*. *J. Neurochem.* 73: 2415-2423.
- Zhang F, Endo S, Cleary LJ, Eskin A, Byrne JH (1997). Role of transforming growth factor- β in long-term synaptic facilitation in *Aplysia*. *Science* 275: 1318-1320.
- Zhang H, Wainwright M, Byrne JH, Cleary LJ (2003). Quantitation of contacts among sensory, motor, and serotonergic neurons in the pedal ganglion of *Aplysia*. *Learn. Mem.* 10: 387-393.
- Zhang R, Sun L, Hayashi Y, Liu X, Koyama S, Wu Z, Nakanishi H (2010). Acute p38-mediated inhibition of NMDA-induced outward currents in hippocampal CA1 neurons by interleukin-1 β . *Neurobiol. Dis.* 38: 68-77.
- Zhang Y, Liu RY, Heberton GA, Smolen P, Baxter DA, Cleary LJ, Byrne JH (2012). Computational design of enhanced learning protocols. *Nat. Neurosci.* 15: 294-297.

- Zhang Y, Smolen P, Baxter DA, Byrne JH (2017). Biphasic regulation of p38 MAPK by serotonin contributes to the efficacy of stimulus protocols that induce long-term synaptic facilitation. *eNeuro* 4.
- Zhou B, Wang ZX, Zhao Y, Brautigan DL, Zhang ZY (2002). The specificity of extracellular signal-regulated kinase 2 dephosphorylation by protein phosphatases. *J. Biol. Chem.* 277: 31818–31825.
- Zhou L, Zhang Y, Liu RY, Smolen P, Cleary LJ, Byrne JH (2015). Rescue of impaired long-term facilitation at sensorimotor synapses of *Aplysia* following siRNA knockdown of CREB1. *J. Neurosci.* 35: 1617-1626.

Vita

Brittany Coughlin was born in Sellersville, Pennsylvania on September 9, 1984, daughter of Sandra and Robert Fredericks. She graduated 2nd in her class from Upper Perkiomen High School, Pennsburg, Pennsylvania, in 2003. She graduated summa cum laude with a Bachelor of Science degree and a major in chemistry-biology from West Chester University of Pennsylvania in May, 2007. The following year, she worked as a teaching assistant and graduate student in the Biology Department at West Virginia University and then completed a Masters of Arts in Teaching degree at the University of Pittsburgh in June, 2009. Brittany entered the University of Texas Health Science Center at Houston Graduate School of Biomedical Sciences in the Spring of 2010 and the lab of Dr. Jack Byrne in the Fall of 2011. She currently resides in Kingwood, Texas with her husband and two children.

Permanent address:

1206 Castle Hill Trail

Kingwood, Texas 77339